

Andrews University

Digital Commons @ Andrews University

Master's Theses

Graduate Research

2019

Synthesis and Screening of Novel Hybrid Benzothiazoles in U-87 MG Glioblastoma Cell Line

Priscilla Kyi

Andrews University, priscillak@andrews.edu

Follow this and additional works at: <https://digitalcommons.andrews.edu/theses>

 Part of the [Biology Commons](#)

Recommended Citation

Kyi, Priscilla, "Synthesis and Screening of Novel Hybrid Benzothiazoles in U-87 MG Glioblastoma Cell Line" (2019). *Master's Theses*. 138.

<https://dx.doi.org/10.32597/theses/138/>

<https://digitalcommons.andrews.edu/theses/138>

This Thesis is brought to you for free and open access by the Graduate Research at Digital Commons @ Andrews University. It has been accepted for inclusion in Master's Theses by an authorized administrator of Digital Commons @ Andrews University. For more information, please contact repository@andrews.edu.

ABSTRACT

SYNTHESIS AND SCREENING OF NOVEL HYBRID BENZOTHAZOLES
IN U-87MG GLIOBLASTOMA CELL LINE

By

Priscilla Kyi

Co-chairs: Denise L. Smith and Desmond H. Murray

ABSTRACT TO GRADUATE STUDENT RESEARCH

Thesis

Andrews University

College of Arts and Sciences

Title: SYNTHESIS AND SCREENING OF NOVEL HYBRID BENZOTHAZOLES
IN U-87MG GLIOBLASTOMA CELL LINE

Name of researcher: Priscilla Kyi

Name and degree of faculty co-chairs: Denise L. Smith, Ph.D. and Desmond H. Murray,
Ph.D.

Date completed: July 2019

Benzothiazole is a heteroaromatic compound known for its wide range of bioactivities including anti-cancer, anti-viral, anti-microbial, anti-inflammatory, anti-convulsant, anti-diabetic, anti-helminthic, and anti-tubercular activities. Research has shown that derivatives of benzothiazole exhibit inhibition of proliferation via apoptosis in various human cancer cell lines, such as liver cancer (Wang, et. al., 2011). In this study, a series of novel hybrid benzothiazole α -cyanostilbene derivatives and styrylbenzothiazole derivatives containing boronic acid and non-boronic acid pharmacophores were

synthesized. The anti-cancer and anti-invasive properties of selected benzothiazole α -cyanostilbene derivatives on U-87MG glioblastoma cells were investigated *in vitro*.

U-87MG cells were incubated with synthesized novel hybrid compounds at varying concentration to determine the lethal concentration 50 (LC₅₀) of the compounds. All hybrid compounds displayed inhibitory effects on cell growth and the LC₅₀ of the compounds varied depending on the nature of the pharmacophores. Moreover, compounds containing both boronic acid substituent and fluoro substituent exhibit lower LC₅₀ than those that contain only one of the substituents. Cell motility has been investigated and we have found that there was no difference in motility between the treated and untreated cells. Results indicate anti-invasive properties in boronic acid and fluoro substituents at *ortho* position and boronic acid substituent at *para* position.

Andrews University
College of Arts and Sciences

SYNTHESIS AND SCREENING OF NOVEL HYBRID BENZOTHAZOLES
IN U-87MG GLIOBLASTOMA CELL LINE

A Thesis
Presented in Partial Fulfillment
of the Requirements for the Degree
Master of Science

By
Priscilla Kyi

2019

© Copyright by Priscilla Kyi 2019
All Rights Reserved

SYNTHESIS AND SCREENING OF NOVEL HYBRID BENZOTHAZOLES
IN U-87MG GLIOBLASTOMA CELL LINE

A Thesis
Presented in Partial Fulfillment
of the Requirements for the Degree
Master of Science

By
Priscilla Kyi

APPROVAL BY THE COMMITTEE:

Denise L. Smith, Ph.D., Co-chair

Desmond H. Murray, Ph.D., Co-chair

Robert Zdor, Ph.D.

7/18/2019
Date approved

For Papa, Nanu, Mg Lay, and Isaac

TABLE OF CONTENTS

ACKNOWLEDGEMENTS.....	xi
CHAPTER	
1. INTRODUCTION	
Overview of Research Project.....	1
Cancer.....	2
Brain Cancer.....	5
Glioblastoma Multiforme (GBM).....	6
History of Drug Discovery.....	8
Novel Hybrid Benzothiazoles.....	12
Predicted Bioavailability and Blood-brain barrier Permeability of Novel Hybrid Benzothiazoles.....	14
Lipophilicity.....	14
Oral Bioavailability.....	14
Blood-Brain Barrier Penetration.....	15
2. METHODOLOGY	
Candidate Novel Hybrid Benzothiazole Structures and Calculation of their Molecular Properties.....	17
Chemistry.....	17
Materials.....	17
Experimental Procedures.....	18
Benzothiazole α -cyanostilbenes.....	18
Styrylbenzothiazole.....	19
Diagnostic IR and NMR Peaks.....	20
Styrylbenzothiazole.....	20
Benzothiazole α -cyanostilbenes.....	21
Biology.....	21
Maintaining U-87MG Glioblastoma Cell Line.....	21
Compound Preparation.....	22
Treatment of U-87MG Glioblastoma Cell Line.....	23
Cell Viability Assay.....	23

	Confirmation of Lethal Concentration (LC ₅₀).....	24
	Wound Healing Scratch Assay.....	25
	Neurosphere Assay.....	26
	Invasion Assay.....	27
	Statistical Analysis.....	28
3. RESULT		
	Predicted Bioavailability and Blood-brain Barrier Permeability of Novel Hybrid Compounds.....	29
	Chemistry.....	30
	Biology.....	38
	Cell Viability Assay.....	38
	Confirmation of Lethal Concentration (LC ₅₀).....	42
	Wound healing Scratch Assay.....	44
	Neurosphere Assay.....	44
	Invasion Assay.....	47
4. DISCUSSION		
	Predicted Bioavailability and Blood-brain Barrier Permeability of Novel Hybrid Compounds.....	48
	Lipophilicity.....	48
	Oral Bioavailability.....	49
	Blood-Brain Penetration.....	49
	Chemistry.....	51
	Biological Evaluation.....	55
5. CONCLUSION		58
REFERENCES		60
APPENDIX		
	I. Spectral Data of Synthesized Compounds	66
	II. p-values of Test Compounds	109

ACKNOWLEDGEMENTS

I would first like to thank God for guiding me throughout my graduate studies. Despite my doubts, He has been faithful and provided me with guidance in time of need.

I thank my biology thesis advisor Dr. Denise Smith of Department of Biology. Dr. Smith was always available whenever I ran into trouble in the lab or when I had questions about my research or writing. I appreciate her support, guidance, patience and many wonderful experiences she has provided me during my graduate study.

My sincere thank also goes to my chemistry thesis advisor Dr. Desmond Murray of Department of Chemistry and Biochemistry at Andrews University. I appreciate his patience in teaching me organic chemistry and his very approachable demeanor. He taught me the importance of organic chemistry and the value of research.

I want to thank Dr. Zdor as well for serving as a member of my thesis committee. I value his insightful questions and recommendations for my thesis. His feedback and hard questions incentivized me to widen my research from various perspectives.

I would also like to acknowledge all the faculty and staff at Andrews University that have encouraged me in one way or another. I thank Dr. Marlene Murray, Dr. Tom Goodwin, and Mrs. Kathleen Demsky for their continuous support throughout my studies at Andrews University. I thank Angela for going above and beyond to assist me whenever I am in need. I am grateful to Dr. Peter Lyons for his guidance during my graduate studies. I also want to express my gratitude to the School of Graduate Studies and Research for their financial support.

I would also like to mention my friends that have supported me in one way or another. I thank my fellow graduate students for all the adventures we had. I thank Tendai Hunyenyiwa for being a wonderful labmate. I appreciate her for the stimulating discussions, for the coffee driven sleepless nights we spent completing assignments, and for the fun we had in the past two years. I thank Christina Rosette for her encouragement through words, company, and food.

Finally, I would like to express my profound gratitude to my brother, parents and Isaac for providing me with unfailing support and continuous encouragement throughout my years of study and through the process of writing.

CHAPTER 1

INTRODUCTION

Overview of Research Project

Cancer is one of the leading causes of death in the United States. Although glioblastoma multiforme (GBM) is not common in the overall cancer population it is one of the most lethal cancers, with a median survival of 12-15 months (Wen and Kesari, 2008). GBM is a malignant brain tumor that arises from astrocytes characterized by invasive growth and proliferation. Unfortunately, it is also one of the most common type of brain tumors in adults.

Glioblastoma is incurable due to its aggressive, rapid, invasive growth, and proliferation. At present, surgical removal of the malignant tumor, followed by systemic temozolomide chemotherapy and radiation therapy are used to treat GBM (Verhoeff et al., 2009). Despite the aggressive therapies, less than 5% of treated GBM patients survive 5 years after treatment due to recurrence of GBM after surgical removal of the tumor; the recurrence of GBM is often within the marginal tissues of the surgical removal site (Gaspar et al., 1992). Furthermore, maximizing the treatment effects of chemotherapy, surgery, and radiation therapy on a widely dispersed disease such as GBM could lead to neurological impairment as well as a reduced quality of the patient's life (Giese et al., 2003).

However, with the increase in understanding of GBM on a molecular level, new therapeutic approaches have emerged. One possible novel therapeutic agent is benzothiazole, a heterocyclic compound known for its wide range of biological properties including anti-cancer activities, specifically anti-invasive properties (Ali and Siddiqui, 2013; Hiyoshi et al., 2014). In this project, I have synthesized and determined whether novel hybrid benzothiazole derivatives can be used as anti-cancer and anti-invasion drugs for glioblastoma cells.

Cancer

Cancer is among the leading causes of death worldwide and it has a major impact on society. Humanity has been fighting cancer for centuries and while advancements are made, there is still no cure for most cancers. The American Cancer Society (2019) predicts that there will be 1,762,450 new cancer cases and about 606,880 Americans are expected to die of cancer in 2019.

Cancer is a collection of diseases characterized by uncontrolled growth and the spread of abnormal cells which results from atypical gene expression and/or regulation, favoring cell proliferation. Hanahan and Weinberg (2000) established six traits,

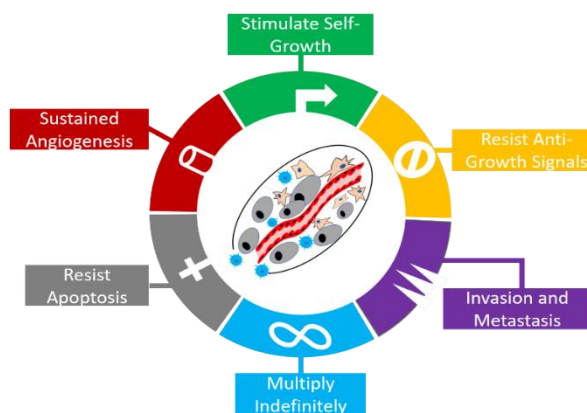


Figure 1 Hallmarks of Cancer. Six traits shared by all forms of cancers as established by Hanahan and Weinberg

known as the hallmarks of cancer, shared by all forms of cancers. These include the stimulation of self-growth, resistance to anti-growth signals, the ability to multiply

indefinitely, resistance to apoptosis, the ability to sustain angiogenesis and the ability to invade and metastasize (Fig 1).

While all of these traits play a role in cancer progression, invasion and metastasis constitute a vital role in the progression of cancer. Invasion occurs when the malignant cells migrate from the primary tumor mass to the local surrounding cells. The process of invasion begins with the detachment of the cancer cells from the original tumor mass. Subsequently, the tumor then secretes proteases which degrade the extracellular matrix. The cancer cells go through morphological changes where protrusions such as pseudopodia, lamellipodia, invadopodia and filopodia began to extend from the leading edge of the cell. These protrusions begin forming membrane anchors, contracting the cytoskeleton and allowing the cells to move forward (Nakada et al., 2007) (Fig. 2).

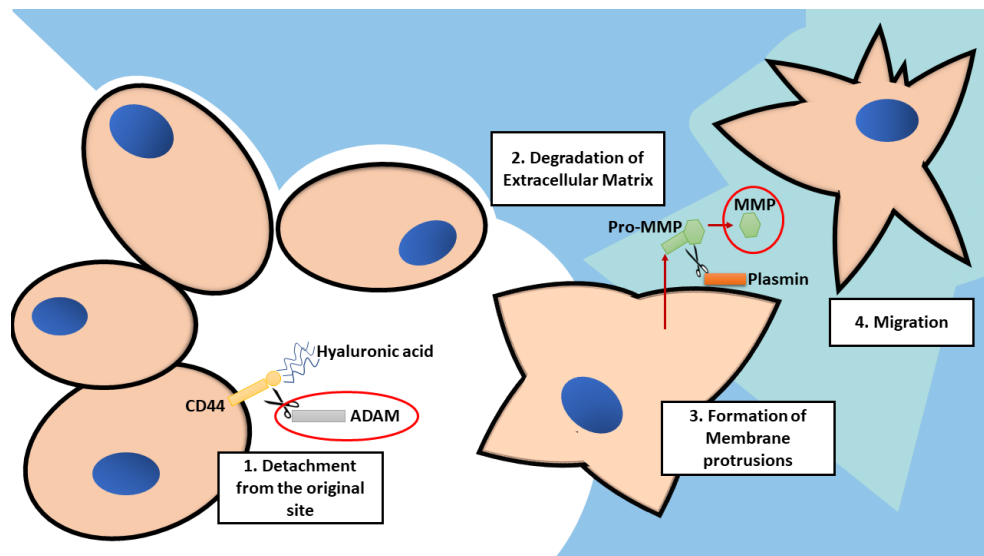


Figure 2 Invasion Cascade. Invasion occurs when the cancer cells moves from the initial tumor mass and spread to local normal cells. The process of invasion involves four main steps: detachment from the original, degradation of extracellular matrix, formation of membrane protrusions, and migration.

Metastasis is the dissemination of tumor cells from the primary site to a distant secondary site (Fig 3). In metastasis, after penetrating through the extracellular matrix, the migrating cell must arrive at the lymphatic or vascular system. Subsequently, the migrating cell travels through the vascular/lymphatic system while evading the immune system. The migrating cell then exits from the circulation, colonizes and proliferates at a secondary site (Chan & Giaccia, 2007) (Fig. 3).

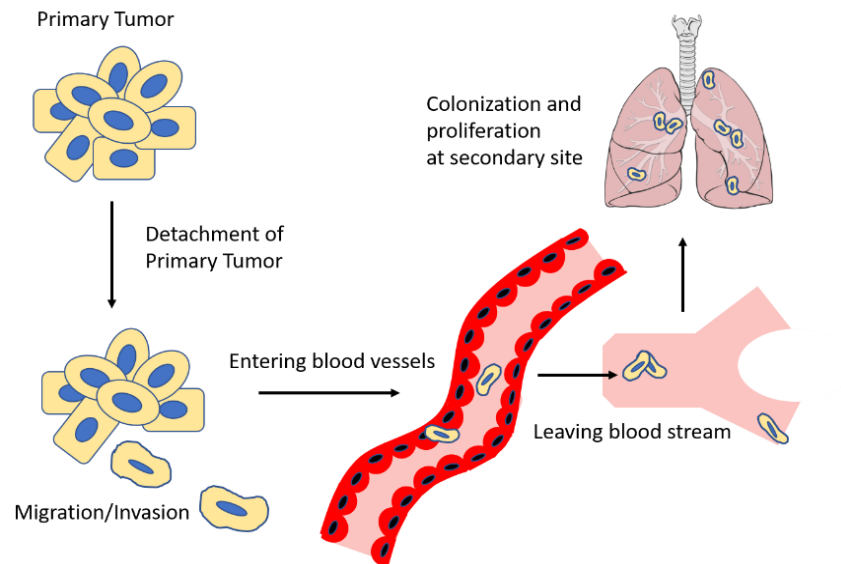


Figure 3 Metastatic Cascade. Metastasis occurs when the tumor cells from the primary site spread to a secondary site.

Brain Cancer

Brain cancer refers to the abnormal growth of cells in the brain. Although brain cancer is relatively rare, it is among the leading causes of cancer death. Common primary brain tumors include: glioma (tumor of the glial cells), meningiomas (tumor of the meninges), medulloblastoma (tumor of the neuroectodermal cells in the cerebellum), gangliogliomas (tumors of neurons and glial cells), and schwannomas (tumor of the Schwann cells).

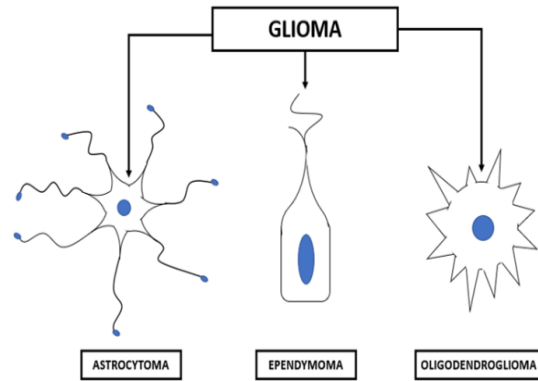


Figure 4 Classification of gliomas. Gliomas are classified by their structural appearances.

Gliomas refers to all tumors that begin in the glial cells and are classified by their structural appearances into three main groups: astrocytomas, oligodendrogliomas, and ependymomas (Fig. 4). While relatively rare, constituting only about 5% of all cancers, gliomas are the most proliferative. (American Cancer Society, 2016).

Astrocytomas are tumors that begin in the astrocytes. Astrocytes are star-shaped glial cells that play a vital role in a variety of tasks, such as synaptic support, axon guidance, maintenance of blood-brain barrier (Blackburn et al., 2009), maintenance of ionic homeostasis in glia (Simard & Nedergaard, 2004), and maintenance of synaptic homeostasis (Barbour et al., 1988). The interaction of astrocytes with neurons is essential for the growth of the dendritic cells, effective synapse formation, and the removal of unwanted synapses (Garwood et al., 2001). Astrocytomas make up about 80% of all malignant brain tumors (American Cancer Society, 2016). The World Health

Organization has classified astrocytomas into four grades based on their malignancy and proliferation (Fig. 5).

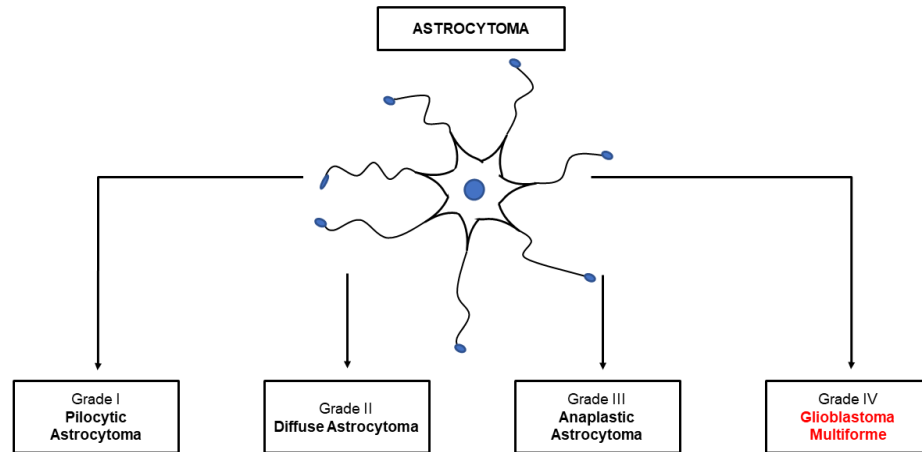


Figure 5 Classification of Astrocytoma: Astrocytomas are classified into four grades based on their proliferation and malignancy.

Glioblastoma Multiforme (GBM)

Glioblastoma multiforme (GBM) is the most common type of glioma. It is extremely lethal due to its invasive growth and proliferative nature. The median survival period for GBM is 12-15 months (Wen and Kesari, 2008).

Glioblastoma is incurable due to its aggressive and invasive growth, proliferative nature, and destructive malignancy. Currently, GBM is treated through surgical removal, followed by systemic temozolomide chemotherapy, and radiation therapy (Verhoeff et al., 2009). However, fewer than 5% of the patients survive GBM after the treatment due to recurrence of the tumor within the removal site. GBM also has poor prognosis as a result of its aggressive nature. Although GBM does not metastasize outside the brain, it is

extremely successful in the invasion of surrounding normal brain cells. Understanding the mechanism of invasion and key players involved in invasion can lead to development of novel therapies for glioblastoma.

One of the key players of glioblastoma invasion is the gene family of matrix-metalloproteinases (MMPs) which degrade the extracellular matrix proteins, creating a path for glioblastoma cells to invade surrounding normal brain tissues (Nakada et al., 2003). Several MMPs have been shown to play an important role in cell migration not only in central nervous system (CNS) but also in cell types outside the CNS. Ogier et al. (2006) have shown that the constitutive expression of MMP-2 was observed in astrocyte migration while MMP-9 expression was nearly undetectable. However, these two MMPs (MMP-2 and MMP-9) have been shown to be highly upregulated in glioblastoma cells and were correlated with increased invasion (Sawaya et al., 1996; Rao et al., 1996).

Another key player is the ADAM (a disintegrin and metalloproteinases) gene family, a family of multidomain membrane-anchored proteins that also play an important role in the invasion of glioblastoma cells. In normal cells, the members of the ADAM family play an important role in cell adhesion and cell fusion events and are often highly expressed in the brain, sperm and testis (Novak, 2004). Two ADAM members (ADAM-12 and ADAM-17) aid glioblastoma cells to invade neighboring tissues. ADAM-17 cleaves CD44, an adhesion molecule which binds to an extracellular matrix component (hyaluronic acid) and maintains cellular functions such as apoptosis, cell migration and proliferation (Takamune et al., 2007; Ponta et al., 2003). ADAM 12 has been directly correlated with proliferative activity and have been shown to be selectively expressed in glioblastoma cells (Kodama et al., 2004). At present, there is no cure for glioblastoma.

However, a better understanding of molecular mechanisms underlying the invasion of glioblastoma offers the hope of developing novel therapies.

History of Drug Discovery

In the past, drug discovery has depended heavily on random screening. In addition, the designing of novel drugs was based on the notion of a disease involving one target (Gediya and Njar, 2009). While this has led to the discovery of numerous novel drugs, the rate of drug discovery has decreased in recent years because new treatment regimens are increasingly difficult to identify (Bolognesi and Cavalli, 2016). In recent years, however, there is a growing interest in drugs that could impact multiple targets simultaneously. Multi-targeted drugs can be more effective and less vulnerable to resistance by the diseased cells through attack on multiple fronts (Zimmerman et al., 2007).

One common multi-target drug therapy currently used in designing novel drugs is the combination drug approach. Combination drugs, also known as drug cocktails, are when two or more active pharmaceutical drugs are combined physically into a single dosage form (Gautam and Saha, 2008). Compared to the single-target drugs, combination drugs are less prone to drug resistance and have been used to control numerous complex disease systems such as cancer. In combination chemotherapy, drugs that work through different mechanisms of actions are used to decrease the possibility of resistance by cancer cells to the treatment.

However, while combination drug therapy is highly effective, it also has multiple limitations. For example, in combination chemotherapy there is an increased likelihood

of side effects due to the increased number of drugs in the combination therapy. In addition, due to the number of drugs involved, it is often difficult to know which drug caused a specific side effect. Moreover, some side effects result not from a single drug, but due to the drug interactions between the drugs involved in the therapy.

In recent years, there is an increasing interest in the development of multi-component drugs where two or more pharmacophores are covalently linked into one single drug. The notion of pharmacophore was first introduced by Ehrlich in 1909 as a “molecular framework that carries the essential features responsible for a drug’s biological activity” (Ehrlich, 1909). However, in 1998, IUPAC further elaborated pharmacophores as “the ensemble of steric and electronic features that is necessary to ensure the optimal supramolecular interactions with a specific biological target structure and to trigger its biological response” (Langer and Hoffmann, 2006).

The concept of hybrid molecules was initially developed for the treatment of malaria. However, this strategy has been applied to the treatment of multiple complex disease systems such as cancer. One of the first hybrid anti-malarial drugs was reported by Dechy-Cabaret et al. (2000), where artemisinin and chloroquine moieties were covalently linked into one single molecule, trioxaquine. Trioxaquine has the properties of both artemisinin (alkylating heme) and of chloroquine (blocking polymerization). In 2009, Cavalli and Bolognesi designed a novel compound for combating *Trypanosoma* and *Leishmania* (Cavalli and Bolognesi, 2009).

Perhaps, the first hybrid drug and the only anti-cancer hybrid drug that's been used clinically is estramustine (Gediya and Njar, 2009). Estramustine was initially developed for the treatment of advanced prostate carcinoma (Jonsson et al., 1977) in

1977. However, over the years, it has been combined with other chemotherapeutic drugs to treat other forms of cancer such as glioblastoma multiforme (Piepmeier et al., 1993).

Hybrid drugs can be classified according to the type of linkage between the pharmacophores (Fig 6). Directly linked hybrid drugs are attached by the functional group of each pharmacophore which often results in an ester, a carbamate or an amide that can be hydrolyzed enzymatically (e.g. lactandrate).

Spacer linked hybrid drugs are classified as either cleavable or non-cleavable. Cleavable spacer linked hybrid drugs often contain ester linkages that can be cleaved by the plasma esterases (e.g. NO-aspirin). This releases the two pharmacophores which act independently. Non-cleavable spacer linked hybrid drugs contain a stable (in terms of chemical and enzymatic) linkage that cannot be hydrolyzed (e.g. estradiol-anilin mustard).

Merged/overlapped hybrid drugs contain pharmacophores that are overlapped structurally and may retain the functional properties of both or either of the overlapped drugs (e.g. azatoxin). Hybrid drugs are often synthesized from drugs that have already been developed. This is known as a *post hoc* approach. Another design of hybrids is

known as the *ad hoc* approach where scaffolds with liabilities such as instability *in vivo* are used for the synthesis of the hybrid drugs (Gediya and Njar 2009).

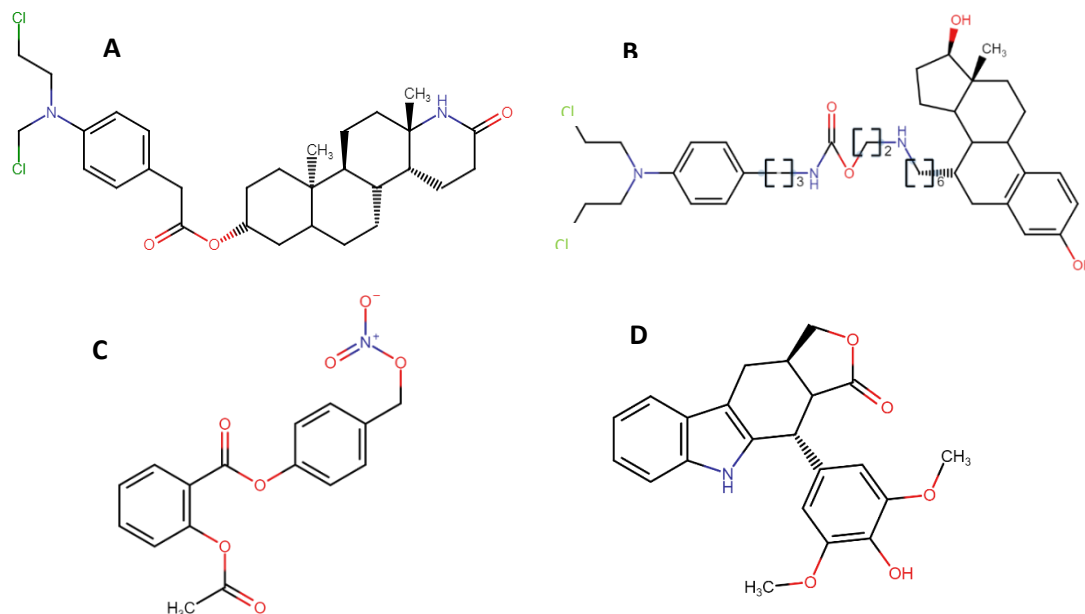


Figure 6 Example of types of hybrid drugs. A) Azatoxin B) Estradiol-Aniline Mustard C) NO-Aspirin D) Lactandrate

The hybrid compounds synthesized in this project can be classified as the merged/overlapped hybrids. This classification was due to the fact that all synthesized hybrid compounds contain a stilbene pharmacophore upon which other pharmacophores are directly attached, merged or embedded (Fig 7).

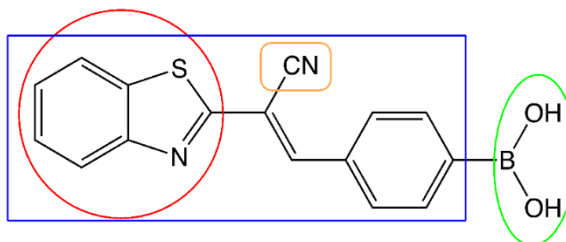


Figure 7 Example of synthesized compound. Blue: stilbene component, Red: Benzothiazole component, Yellow: cyano/nitrile component, Green: Boronic acid component

Novel Hybrid Benzothiazoles

In recent years, heterocyclic compound analogs and derivatives have been studied extensively due to their potential as new therapeutic agents against cancer. Heterocyclic compounds are cyclic rings with one or more different elements and they contain either nitrogen, oxygen, or sulfur within the ring. Heterocyclic compounds have been reported to display biological activities such as anti-fungal, anti-inflammatory, anti-convulsant, herbicidal and anti-cancer (Saini et al., 2013). Due to their wide range of biological activities, heterocyclic compounds can be found in a majority of medical and pharmaceutical drugs. An example of one heterocyclic compound that is currently used as a treatment for glioblastoma is temozolomide, . Heterocyclic compounds exist in two forms: aromatic and non-aromatic (Fig. 8). Heteroaromatic compounds are flat molecules that contain alternating double and single bonds and obey Hückel's rule ($4n + 2 \pi$ electrons). Hetero non-aromatic compounds are those that do not contain double bonds.

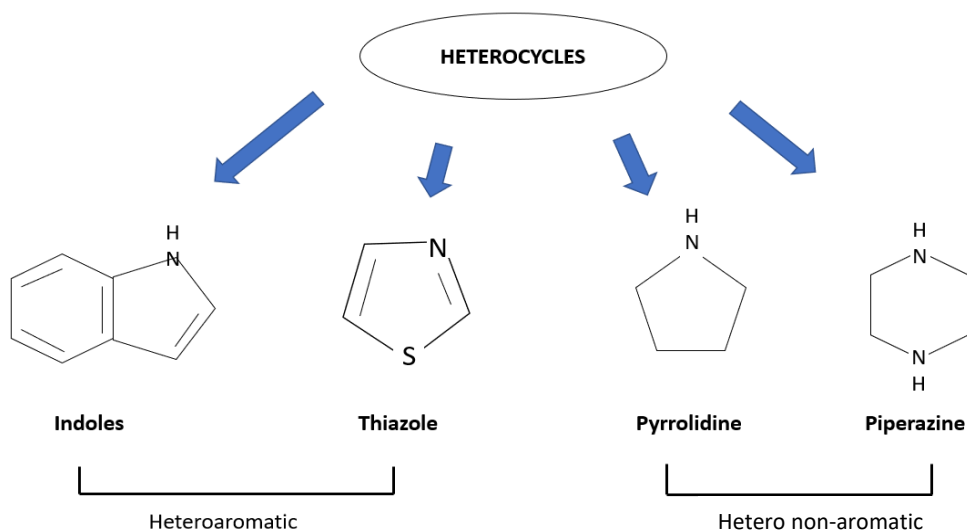


Figure 8 Example of heteroaromatic (left) compounds and hetero non-aromatic (right) compounds. Heteroaromatic compounds contain double bounds while hetero non-aromatic compounds do not contain any double bounds.

Benzothiazole is among these heterocyclic compounds, specifically heteroaromatic compounds, and has a wide range of biological activities including anti-

tumor, anti-helminthic, analgesic, anti-diabetic, anti-malarial, anti-tubercular, anti-inflammatory, anti-convulsant, and diuretic (Singh and Singh, 2014). Due to its aromaticity which makes the compound extremely stable, benzothiazole has been used as a scaffold to synthesize a large number of therapeutic agents (Ali and Siddiqui, 2013). Studies have shown the ability of benzothiazole derivatives to inhibit proliferation and invasiveness in breast cancer, colon cancer, and lung cancer (Hiyoshi et al., 2014; Mortimer et al., 2005; Wang et al., 2011); but to my knowledge, no published studies have investigated the therapeutic use of benzothiazole derivatives on glioblastoma.

One of the goals for this study is to synthesize novel hybrid benzothiazole compounds. One specific functional group of interest to hybridize with the benzothiazole is boronic acid. Boronic acids are compounds containing boron and two hydroxyl (-OH) groups and they have been shown to display bioactivities such as anti-cancer, anti-microbial, and anti-viral (Trippier and McGuigan, 2010). Due to their unique structural features, boronic acids have been used to develop potent enzyme inhibitors, as antibody mimics that recognize biologically important saccharides, and boron neutron capture agents for cancer therapy (Yang et al., 2003). Consequently, there is a growing interest in boronic acid containing drugs. Currently, there are only two FDA approved boronic acid containing drugs. Among them is bortezomib (Velcade®), used for the treatment of relapsed multiple myeloma and mantle cell lymphoma (Trippier and McGuigan, 2010).

Predicted Bioavailability and Blood-brain barrier Permeability of Novel Hybrid

Benzothiazoles

Lipophilicity

Lipophilicity plays an important role in the design and discovery of novel drugs. Lipophilic properties of a compound can be described using the octanol-water partition coefficient (LogP) which is the ratio of the concentration of the unionized molecule at equilibrium between aqueous and organic phases. Lipophilic compounds have the ability to dissolve in fats, oils, lipids and non-polar solvents. Lipophilicity is not synonymous with hydrophobicity. While hydrophobic compounds describe the interaction between the compound and water, lipophilic compounds interact with lipids. Lipophilicity of a compound affects its solubility, permeability, potency, selectivity, absorption, metabolism, and toxicity (Gao et al., 2017).

Oral Bioavailability

Oral bioavailability of novel hybrid benzothiazoles can be measured using Lipinski's rule of five. This method of measurement is commonly used when new drugs are designed and developed, and the oral bioavailability of the potential drug molecule is unknown. According to Lipinski's rule, the molecules would be orally active if: 1) the number of hydrogen-bond donors is less than five, 2) the molecular mass is less than 500, 3) calculated octanol-water partition coefficient (Log P) is less than five, and 4) the number of hydrogen acceptors is less than ten. Drugs that are orally active generally do not violate any of the above rules. In addition to Lipinski's rule of five, Veber et al.

(2002) added two more rules to improve the predictions of drug-likeness. They are as follows: 1) 10 or fewer rotatable bonds and 2) polar surface no greater than 140 Å.

Blood-Brain Barrier Penetration

Because the human brain is a highly sensitive and fragile neuronal organ system that requires high maintenance and regular supply of nutrients, fuels, and gases, the blood-brain barrier acts as a protective barrier that imposes various obstacles for foreign substances. The blood-brain barrier inhibits delivery of various therapeutic drugs and imposes an

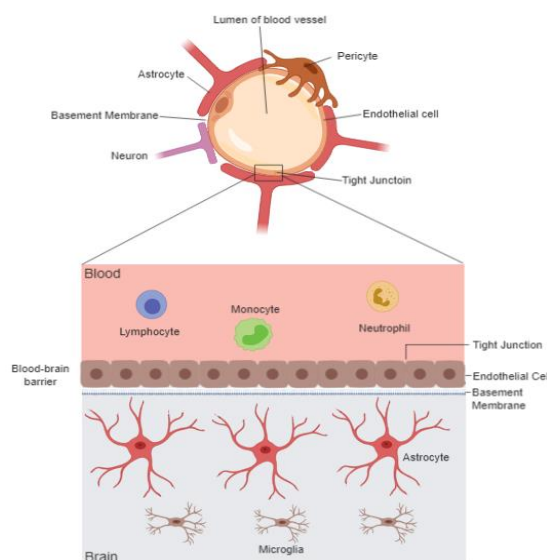


Figure 9 Blood-brain barrier acts as a protective barrier that prevents the entry of various foreign substances.

obstruction for delivery of a large number of drugs (Updahyay, 2014). The endothelial cells that make up the tight junction and their lack of fenestration preclude paracellular diffusion (Fig. 9). Therefore, the majority of drug blood-brain barrier penetration occurs through the passive diffusion through the cellular membrane (Pajouhesh and Lenz 2005).

Here, I have investigated the potential therapeutic role of novel benzothiazole derivatives. In this study I have 1) predicted the bioavailability and the blood-brain barrier permeability of designed novel hybrid benzothiazoles, 2) synthesized novel hybrid benzothiazoles, and 3) determined the anti-cancer and/or anti-invasive properties of the novel compounds by treating U-87MG glioblastoma cells with these compounds. I

hypothesize that benzothiazole containing compounds will inhibit the growth of U-87MG glioblastoma cells and exhibit anti-cancer/anti-invasive properties.

CHAPTER 2

METHODOLOGY

Candidate Novel Hybrid Benzothiazole Structures and Calculation of their Molecular Properties

The ChemSketch tool and Marvin JS by ChemAxon were used to draw all the hybrid molecules. Online server such as Molinspiration was employed to predict the biological properties of the tested hybrid molecules. . Percent of absorption was calculated using the modified equation $\% \text{ absorption} = 109 - 0.345 \times \text{TPSA}$ from Zhao et al. (2002). All figures were drawn using softwares such as ChemDoodle and BioRender.

Chemistry

Materials

The reagents and solvents used throughout the synthesis and analysis were commercially purchased from Sigma-Aldrich. The experiments were conducted under a conventional fume hood using a magnetic stirrer. IR spectra was obtained using Thermo Scientific Nicolet iS50 ATR Infrared Spectroscopy. NMR spectra was obtained using JEOL JNM-ECP400 FT NMR system, Eclipse400 FT NMR spectrometer, and Delta software.

Experimental Procedures

Benzothiazole α -cyanostilbenes

32 ml of water and 8 ml of ethanol was added into a clean and oven dried 50 ml round bottom flask containing a magnetic stir bar. After clamping the flask in place on a magnetic hot plate stirrer, the reagents

were added in the following order: 1) 2.5 mmol aromatic aldehyde containing or not containing boronic acid, 2) 2.5 mmol benzothiazole-2-acetonitrile, 3) 10 mmol of calcium oxide (CaO). This mixture was

refluxed for three hours in a conventional fume hood (Fig 10). After the reflux reaction was completed, the mixture was

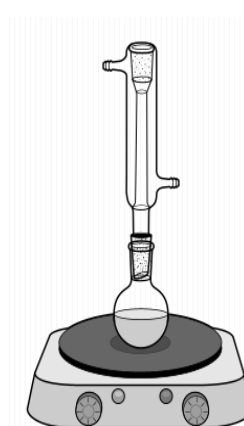


Figure 10 Reflux setup was used to synthesize novel hybrid benzothiazole α -cyanostilbenes



Figure 11 Vacuum filter setup was used to separate the solid product from the mixture.

placed into a beaker containing ice and 30 ml of saturated ammonium chloride (NH_4Cl) and stirred on a magnetic stirrer until neutralization had taken place. Neutralization was established by measuring pH using litmus pH test strips. The neutralized mixture was vacuum-filtered and air-dried for up to 48 h (Fig 11). The resulting products were weighted and characterized by obtaining their IR and NMR spectra and comparing with the IR and NMR spectra of the organic starting materials.

After analyzing the products, they were further purified using extraction methods. The product was extracted three times. The resulting product was further

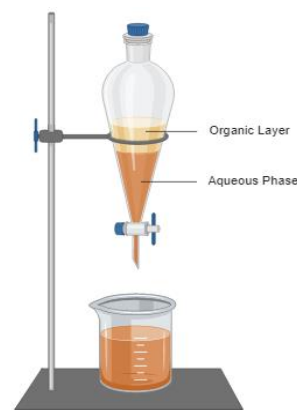


Figure 12 Extraction and washing setup were used to purify the products to prevent the presence of CaO

purified by washing. Deionized water and saturated sodium chloride were used as inorganic solvents and ethyl acetate was used as the organic solvent (Fig 12). Ethyl acetate was then evaporated using the rotary evaporator (Fig 13) and the product was air dried overnight and analyzed using IR and NMR spectroscopy.

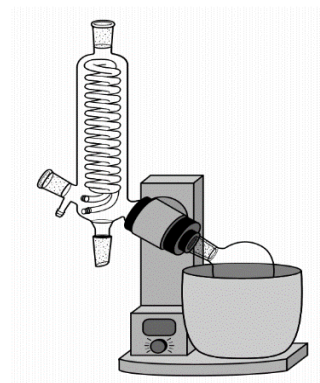


Figure 13 Rotary evaporator was used to remove the organic solvent

Styrylbenzothiazole

Preliminary tests were conducted to optimize synthesis of styrylbenzothiazoles. 15 ml of fresh dry dimethylformamide (DMF) was syringed into an oven-dried 50 ml round bottom flask containing a magnetic stir bar. A CaCl₂ drying tube was attached to the round bottom flask and the whole apparatus was clamped in place on a magnetic stirrer (Fig 14). The reagents were measured out and added to the flask in the following order: 1) 12.5 mmol lithium hydride, 2) 7.5 mmol potassium t-butoxide (KTB), 3) 2.5

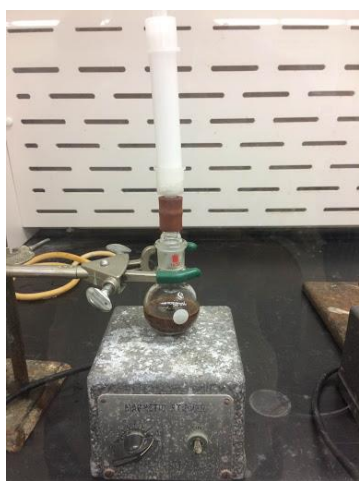


Figure 14 Synthesis of styrylbenzothiazole was achieved by stirring the starting materials at room temperature

mmol aromatic aldehyde with subunits containing/not containing boronic acid. The mixture was stirred at room temperature for four hours in a conventional fume hood. At the completion of the reaction, the mixture was poured into a beaker containing ice and 30 ml of saturated NH₄Cl. The mixture was stirred for 10 mins on a magnetic stirrer until neutralization had taken place. Neutralization was established by measuring pH using litmus pH test strips. After

neutralization, the mixture was vacuum filtered and air dried overnight. The resulting products were weighted and characterized by obtaining their IR and NMR spectra and comparing with the IR and NMR spectra of the organic starting materials.

Diagnostic IR and NMR Peaks

IR spectroscopy was used to identify the novel hybrid compound and determined the presence and absence of the functional group in the mixture. NMR was used to further determine the molecular structure and the purity of the synthesized compounds. The following are the diagnostic IR and ^1H NMR peaks expected to be observed in the synthesized compounds.

Styrylbenzothiazole:

Starting Materials: *Methylbenzothiazole*. The diagnostic IR peaks (cm^{-3}) for methylbenzothiazole include: 1250-1020 (C-N), 1500-1400 (C-C aromatic), 3000-3100 (C-H aromatic), 2850-3000 (C-H alkane). Diagnostic ^1H NMR peaks for (δ) for methylbenzothiazole include: 3.0 (CH₃), 7.5-8 (aromatic H), ~2.5 (H-C-N).

Formylphenylboronic acid: The diagnostic IR peaks for formylphenylboronic acid include: 1710 (C=O aldehyde), 1300-1400 (B-O), 3200-3500 (O-H). For the ^1H NMR spectrum, we should see peaks at 9.7-10 (C=O aldehyde), 7-8 (aromatic H), 2-5 (O-H).

The disappearance of the methyl peak at 2850-3000 (C-H alkane) and of the aldehyde peak at 1710 (C=O aldehyde) from the IR spectrum and methyl peak at 3.0 (CH₃) and aldehyde peak at 9.7-10 (C=O aldehyde) from ^1H NMR spectrum would indicate the formation of the desired product. In addition, we should see the formation of

C=C in the product which would be indicated by the peak at 1680-1640 from IR spectrum and ~7.0 from ^1H NMR spectrum.

Benzothiazole α -cyanostilbenes

Starting Materials: *Benzothiazoleacetonitrile*. The diagnostic IR peaks of (cm^{-3}) for benzothiazoleacetonitrile include: 2210-2260 (CN stretch), 1500-1400 (C-C aromatic), 3000-3100 (C-H aromatic), 2300-2000 (nitrile). Diagnostic ^1H NMR (δ) peaks include: 2.0-3.0 (nitrile), 7.5-8.0 (aromatic H). *Formylphenylboronic acid*: The diagnostic IR peaks for formylphenylboronic acid include: 1710 (C=O aldehyde), 1300-1400 (B-O), 3200-3500 (O-H). For the ^1H NMR spectrum, we should see peaks at 9.7-10 (C=O aldehyde), 7-8 (aromatic H), 2-5 (O-H).

The aldehyde peak should disappear from both IR and ^1H NMR if the desired product is formed. We should still see the nitrile peak at 2300-2000 for IR spectrum and at 2.0-3.0 for ^1H NMR spectrum. In addition, the formation of C=C bond should be seen on both ^1H NMR (~7.0) and IR (1680-160) spectrum if the product is present.

Biology

Maintaining U-87MG Glioblastoma Cell Line

U-87MG glioblastoma cells (ATCC) were grown and maintained in MEM (Minimum Essential Medium) supplemented with 10% fetal bovine serum (Gibco), and 100U/ml penicillin/streptomycin solution (Gibco). The cells were kept in a humidified 37°C , 5% CO_2 incubator. Every 48 h I observed the density of the cells in the plate, using a light microscope. When the density was low, the media was removed and replaced with

new media. However, when the density reached approximately 80%, the cell density was reduced by removing the old media and placing 2 *ml* of trypsin/EDTA (Gibco) on the cells for detachment, then removing half of the cells in the trypsin/EDTA solution, and lastly, adding 8 *ml* of new media to the plate.

Compound Preparation

Stock samples were prepared to evaluate the cell viability after they were treated with novel hybrid benzothiazoles. This preparation was completed at least 24 *h* prior to the experiment. To prepare the samples, 0.02 *g* of novel compounds were dissolved in 1 *ml* of dimethyl sulfoxide (DMSO). Previous studies in our lab have shown that 1% DMSO or less had no effect on cell viability.

Eight of the synthesized novel hybrid benzothiazole α -cyanostilbenes were selected for screening for their anti-cancer properties. These compounds were selected based on the heterocyclic subunit in the hybrid molecule containing boronic acid, non-boronic acid (fluoro), or both (fluoro and boronic acid) at *ortho*, *meta*, and *para* positions. Focusing on these compounds will allow us to compare the effects of position on the aromatic ring, as well as the effects of boronic versus nonboronic acid compounds. These compounds were also compared to selected starting materials.

Treatment of U-87MG Glioblastoma Cells

Novel hybrid compounds at varying concentration diluted in media (2.0 mg/ml, 1.0 mg/ml, 0.5 mg/ml, 0.25 mg/ml, 0.125 mg/ml, 0.0625 mg/ml, 0.03125 mg/ml, 0.015625 mg/ml, 0.0078125 mg/ml, 0.003906 mg/ml, 0.001953 mg/ml) were placed in eleven wells of a Corning™ Costar™ flat bottom 12-well cell culture plate. The control well contained untreated cells that were only exposed to the cell culture media (Fig 15).

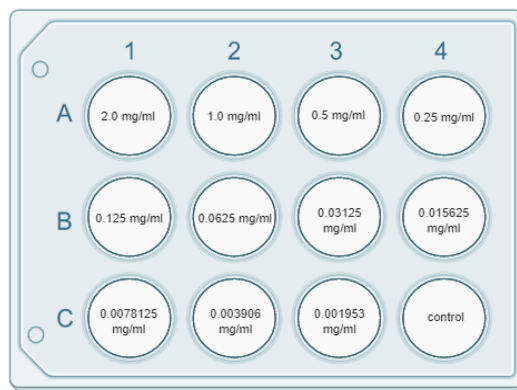


Figure 15 12-Well Plate Setup

Cell Viability Assay

Preliminary tests were conducted to determine a suitable cell viability assay which accurately reflected the lethal concentration (LC₅₀) of the novel hybrid compounds. A modified NIH cell viability assay was used to determine the effect of the novel hybrid compounds on U-87MG glioblastoma cell viability. The viability of U-87MG cells was determined after the cells were treated with varying concentrations of novel hybrid compounds. U-87MG cells were introduced into a Corning™ Costar™ flat bottom 12-well cell culture plate at the concentration of 10,000 cells/well. The cell count was estimated using the trypan blue exclusion method (Gibco) and a hemocytometer.

After the cells were introduced, they were placed into a humidified, 37°C and 5% CO₂ incubator for 24 h. Once the incubation period had elapsed, the cells were treated at varying concentration (2.0 mg/ml, 1.0 mg/ml, 0.5 mg/ml, 0.25 mg/ml, 0.125 mg/ml,

0.0625 mg/ml, 0.03125 mg/ml, 0.015625 mg/ml, 0.0078125 mg/ml, 0.003906 mg/ml, 0.001953 mg/ml) of novel hybrid benzothiazoles and incubated for 24 h under the conditions mentioned above.

At the end of the treatment period, the drug was removed, 1 ml of methanol was added to each of the wells and the cells were fixed for 5 mins. Methanol was removed at the end of the fixation, and crystal violet was added to the wells to stain the cells. The cells were then stained for 5 mins, washed and air-dried overnight. The stained cells were quantified using an inverted light microscope at 400x, with three individual fields per well counted and averaged (Fig 16). Each compound cell viability assay was repeated three times. The LC₅₀ for each compound was determined using linear regression.

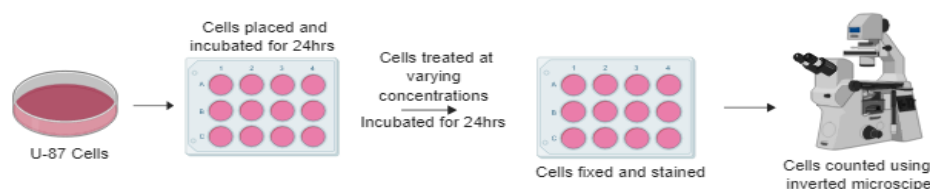


Figure 16 Cell Viability Assay Setup. Cells from the stock plate were introduced to the plate and was incubated. Cells were treated with compounds for 24hrs and were stained and counted.

Confirmation of Lethal Concentration (LC₅₀)

To confirm that the LC₅₀ values obtained from the cell viability assay were accurate, each calculated compound LC₅₀ concentration was tested an additional nine times. The cells for each trial were obtained from new stock cultures. 50,000 cells were introduced in each of the 24 wells of a CorningTM CostarTM flat bottom culture plates and incubated for 24 h in a humidified, 37°C, and 5% CO₂ incubator. The cells were then treated with the LC₅₀ of the novel hybrid benzothiazoles and incubated as above for 24 h.

At the end of the treatment, the cells were fixed and stained under the conditions mentioned above.

Wound Healing Scratch Assay

A modified wound healing scratch assay was performed to determine the effect of the novel hybrid benzothiazoles on motility of the U-87MG glioblastoma cells. 200,000 cells were introduced into 60 mm Thermo Scientific™ Nunc™ Cell Culture dishes and grown in MEM supplemented with 10% FBS and 100U/ml penicillin/streptomycin. The cells were allowed to grow in a 5% CO₂ humidified environment at 37°C until they reached 100% confluency as a monolayer (approximately 3 days). When the cells reached 100% confluency, a sterile 200 μ l pipette tip was used to scratch the monolayer across the center of the dish (Fig 17). After creating the scratch, the media was gently removed via vacuum suction to remove the detached cells. The dish was then replenished with fresh medium in the control plate and test compounds at the lowest tested concentration (LTC) and the highest concentration that resembles the control (HCRC) plate (Table 1). Migration

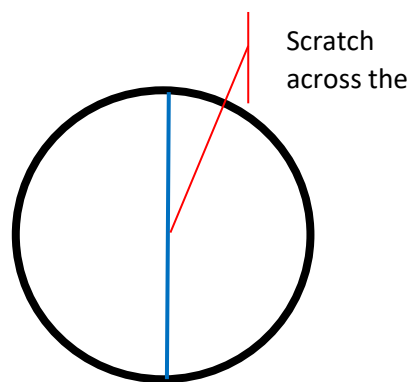


Figure 17 Scratch assay on 60mm dish. A scratch was made across the 100% confluent cell layer and were treated up to 24hrs.

process was documented by taking sequential digital photographs of the ‘wound’ using the inverted light microscope. Digital photographs were taken every 24 h for two days. Each concentration was evaluated in triplicate.

Table 1 Concentrations Used for Wound Healing Scratch Assay

Novel Hybrid Benzothiazole (mg/ml)								
	PKP2	PKP3	PKP4	PKP5	PKP6	PKP7	3F- 2BA	4F- 3BA
LTC	0.00195	0.00195	0.00195	0.00195	0.00195	0.00195	0.00195	0.00195
HCRC	0.00195	0.00195	0.00195	0.00781	0.00781	0.00781	0.00195	0.00195

*LTC = Lowest tested concentration; HCRC = Highest concentration that resembles the control

Neurosphere Assay

The effect of the novel hybrid benzothiazoles on the site of tumor initiation (neurospheres) was determined by performing the neurosphere assay. In this assay, the cells were seeded in 24 wells Corning™ Costar™ flat bottom culture plates at a concentration of 50,000 cells per 500 μ l, estimated by the trypan blue exclusion method.

After introduction of the cells, the plates were incubated for 24 h in a 5% CO₂ humidified incubator at 37°C to allow for cell attachment. Once the 24 h had passed, the media was removed and replaced with the LC₅₀ and the LTC of the tested compounds.

The cells were treated with novel hybrid compounds for a total of six days at the conditions mentioned above (Fig 18). After 24 h of treatment, the media from day one cells of both treated and untreated wells were removed and the cells were fixed and stained under the aforementioned conditions. The plates were returned to the incubator until the next assay day. Fixing and staining methods were repeated at day 3 and day 6 of the treatment. Neurospheres were assessed by determining their number and size.

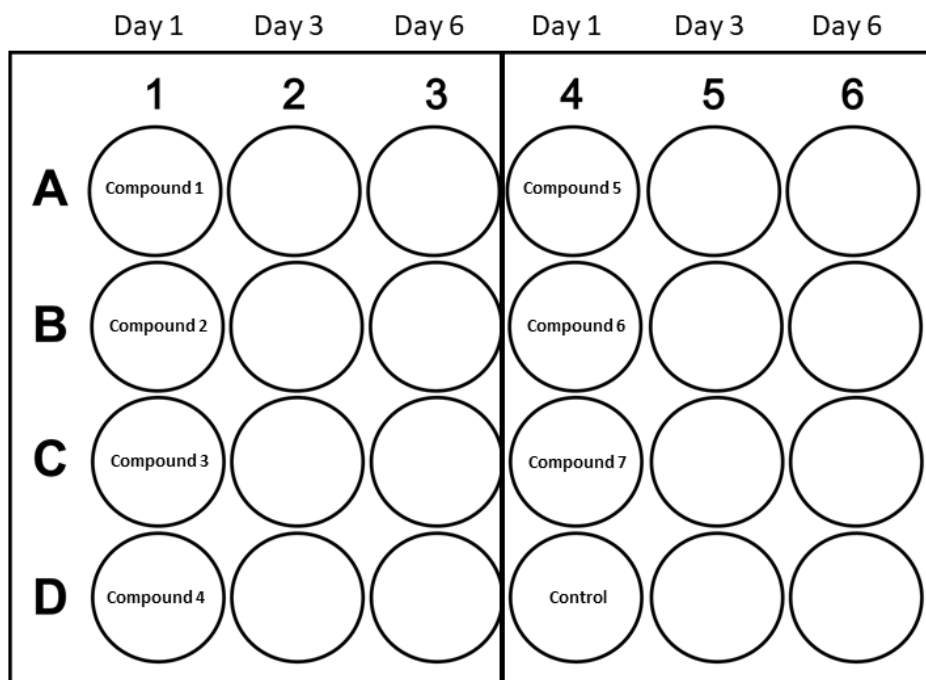


Figure 18 Neurosphere Assay Setup. Cells were introduced and were treated at LC₅₀ and HCRC of the tested compounds. Neurosphere formation was observed at the indicated time points.

Invasion Assay

Following the instructions from the CytoSelect™ Cell Invasion Assay Kit, U-87MG cells were suspended in serum free media. Novel hybrid benzothiazoles at HCRC were added directly to the cell suspension. The cell suspension with the novel compounds were kept for 24 hours at 37°C 5% CO₂ in a humidified incubator to allow the invasive cells to pass through the basement membrane and cling to the bottom of the insert while the non-invasive cells stay in the upper chamber. After the incubation period, the non-invasive cells were removed, and the invasive cells were stained. Stained invasive cells were quantified using the light microscope. The effect of the novel hybrid benzothiazoles on the invasiveness of GBM cells was analyzed by comparing the results of treated and untreated cells (Fig 19).

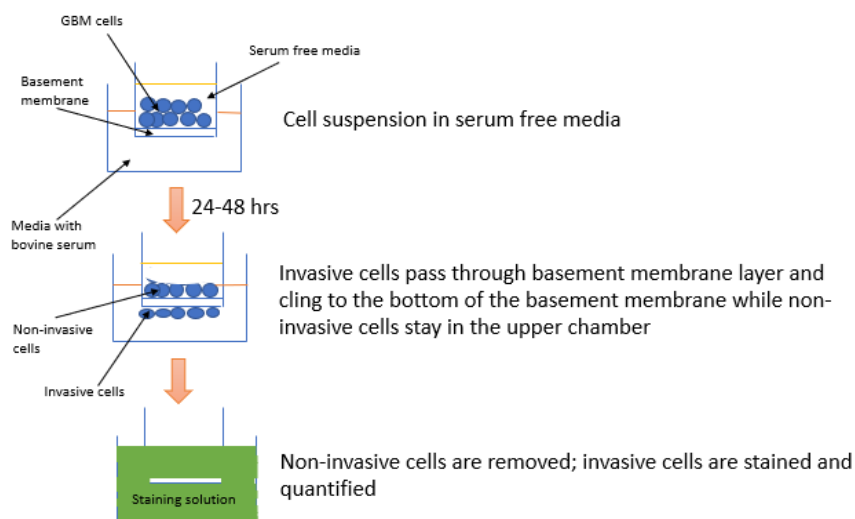


Figure 19 Invasion assay principle based on CytoSelect™ Cell Invasion Assay Kit. Cells were suspended in the serum free media containing/lacking test compounds. The cells were incubated for 24hrs and invasive cells were quantified.

Statistical Analysis

The significant difference between the concentrations and the control of each test compounds were calculated via one-way ANOVA with Dunette-adjusted post hoc test on IBM SPSS software. The significant difference of the invasion assay was determined via one-way ANOVA with Bonferroni-adjusted post hoc test on IBM SPSS software.

CHAPTER 3

RESULTS

Predicted Bioavailability and Blood-brain barrier Permeability of Novel Hybrid Compounds

Molecular properties for novel hybrid benzothiazoles were calculated using an online software, Molinspiration (<http://www.molinspiration.com/cgi-bin/properties>) and the values are given in Table 2.

Table 2 Predicted Molecular Properties of Novel Hybrid Benzothiazole Derivatives

Compound	LogP ¹	TPSA ²	nAtoms ³	nON ⁴	nOHNH ⁵	MW ⁶	nRotB ⁷	% ABS ⁸	R5 ⁹
PKP2	3.00	77.14	22	4	2	306.15	3	82.38	Pass
PKP3	2.77	77.14	22	4	2	306.15	3	82.38	Pass
PKP4	2.97	77.14	22	4	2	306.15	3	82.38	Pass
PKP5	3.89	36.68	20	2	0	280.33	2	96.34	Pass
PKP6	4.11	36.68	20	2	0	280.33	2	96.34	Pass
PKP7	4.09	36.68	20	2	0	280.33	2	96.34	Pass
4F-3BA	2.91	77.14	23	4	2	324.14	3	82.38	Pass
3F-4BA	2.88	77.14	23	4	2	324.14	3	82.38	Pass

1. Octanol-water partition coefficient
2. Topological polar surface area
3. Number of atoms
4. Number of hydrogen-bond acceptor
5. Number of hydrogen-bond donor
6. Molecular weight
7. Number of rotatable bonds
8. Percent absorption
9. Lipinski's rule of five violation

Chemistry

All benzothiazole α -cyanostilbenes products and styrylbenzothiazoles products were weighed and characterized by ^1H NMR and IR spectroscopy. Data for the novel hybrid compounds are shown below.

4-boronic acid- α -cyanobenzothiazolestilbene (PKP2)

Yield: 115.6%; IR (ATR, cm^{-1}): 2227 ($\text{C}\equiv\text{N}$ stretch), 3364 (O-H), 1429 (B-O); ^1H NMR (400 MHz, Methanol- d_3) δ : 2.0 (1H, s, OH), 7.4-8.0 (4H, m, Ar-H), 7.8 (2H, d, Ar-H), 8.2 (1H, s, CH)

3-boronic acid- α -cyanobenzothiazolestilbene (PKP4)

Yield: 108.8%; IR (ATR, cm^{-1}): 2223 ($\text{C}\equiv\text{N}$ stretch), 3120 (O-H), 1397 (B-O); ^1H NMR (400 MHz, Methanol- d_3) δ : 2.0 (1H, s, OH), 7.4-8.0 (4H, m, Ar-H), 7.5-8.0 (1H, m, Ar-H), 8.2 (1H, s, CH)

2-boronic acid- α -cyanobenzothiazolestilbene (PKP3)

Yield: 73.03%; IR (ATR, cm^{-1}): 2215 ($\text{C}\equiv\text{N}$ stretch), 3134 (O-H), 1404 (B-O); ^1H NMR (400 MHz, Methanol- d_3) δ : 2.0 (1H, s, OH), 7.5-8.0 (4H, m, Ar-H), 7.2-7.8 (1H, m, Ar-H), 8.2 (1H, s, CH)

2-fluoro- α -cyanobenzothiazolestilbene (PKP5)

Yield: 87.9%; IR (ATR, cm^{-1}): 3054 ($=\text{C-H}$), 2227 ($\text{C}\equiv\text{N}$ stretch), 1241 (C-F); ^1H NMR (400 MHz, Methanol- d_3) δ : 7.4-7.9 (4H, m, Ar-H), 7.3-7.8 (1H, m, Ar-H), 8.0 (1H, s, CH)

3-fluoro- α -cyanobenzothiazolestilbene (PKP7)

Yield: 101.6%; IR (ATR, cm^{-1}): 3057 ($=\text{C-H}$), 2218 ($\text{C}\equiv\text{N}$ stretch), 1193 (C-F); ^1H NMR (400 MHz, Methanol- d_3) δ : 7.4-7.9 (4H, m, Ar-H), 7.1-7.3 (1H, m, Ar-H), 8.2 (1H, s, CH)

4-fluoro- α -cyanobenzothiazolestilbene (PKP6)

Yield: 98.28%; IR (ATR, cm^{-1}): 3054 ($=\text{C-H}$), 2227 ($\text{C}\equiv\text{N}$ stretch), 1241 (C-F); ^1H NMR (400 MHz, Methanol- d_3) δ : 7.4-7.9 (4H, m, Ar-H), 7.4-7.5 (2H, d, Ar-H), 8.1 (1H, s, CH)

3-(trifluoromethyl)- α -cyanobenzothiazolestilbene (PKP8)

Yield: 98.20%; IR (ATR, cm^{-1}): ($=\text{C-H}$), 2234 ($\text{C}\equiv\text{N}$ stretch), 1203 (C-F); ^1H NMR (400 MHz, Methanol- d_3) δ : 7.4-7.9 (4H, m, Ar-H), 7.5-7.8 (2H, d, Ar-H), 8.2 (1H, s, CH)

4-(trifluoromethyl)- α -cyanobenzothiazolestilbene (PKP9)

Yield: 98.40%; IR (ATR, cm^{-1}): 3061 ($=\text{C-H}$), 2234 ($\text{C}\equiv\text{N}$ stretch), 1322 (C-F); ^1H NMR (400 MHz, Methanol- d_3) δ : 7.4-7.9 (4H, m, Ar-H), 7.7-7.8 (2H, d, Ar-H), 8.1 (1H, s, CH)

2-chloro- α -cyanobenzothiazolestilbene (PKP10)

Yield: 114.80%; IR (ATR, cm^{-1}): 3042 ($=\text{C-H}$), 2226 ($\text{C}\equiv\text{N}$ stretch), 751 (C-Cl); ^1H NMR (400 MHz, Methanol- d_3) δ : 7.4-7.9 (4H, m, Ar-H), 7.3-7.8 (1H, d, Ar-H), 8.0 (1H, s, CH)

3-chloro- α -cyanobenzothiazolestilbene (PKP11)

Yield: 89.90%; IR (ATR, cm^{-1}): 3032 ($=\text{C-H}$), 2236 ($\text{C}\equiv\text{N}$ stretch), 724 (C-Cl); ^1H NMR (400 MHz, Methanol- d_3) δ : 7.4-7.9 (4H, m, Ar-H), 7.5-8.1 (1H, d, Ar-H), 8.2 (1H, s, CH)

4-chloro- α -cyanobenzothiazolestilbene (PKP12)

Yield: 108.6%; IR (ATR, cm^{-1}): 3032 ($=\text{C-H}$), 2221 ($\text{C}\equiv\text{N}$ stretch), 758 (C-Cl); ^1H NMR (400 MHz, Methanol- d_3) δ : 7.4-7.8 (4H, m, Ar-H), 7.5-7.6 (2H, d, Ar-H), 8.1 (1H, s, CH)

α -cyanobenzothiazole-2-thiophene-stilbene (PKP13)

Yield: 108.60%; IR (ATR, cm^{-1}): 3057 ($=\text{C-H}$), 2212 (C-S); ^1H NMR (400 MHz, Methanol- d_3) δ : 7.4-8.0 (4H, m, Ar-H), 7.3 (1H, d, Ar-H), 7.4 (1H, d, CH)

5-methyl- α -cyanobenzothiazole-2-thiophenestilbene (PKP14)

Yield: 92.45%; IR (ATR, cm^{-1}): 3059 (=C-H), 2225 (C-S); ^1H NMR (400 MHz, Methanol- d_3) δ : 7.4-8.0 (4H, m, Ar-H), 7.0-7.1 (1H, d, Ar-H), 7.4 (1H, d, CH), 2.3 (3H, s, CH)

2-fluoro-5-boronic acid- α -cyanobenzothiazolestilbene (PKP15)

Yield: 108.58%; IR (ATR, cm^{-1}): 3032 (=C-H), 2221 ($\text{C}\equiv\text{N}$ stretch), 1404 (B-O); ^1H NMR (400 MHz, Methanol- d_3) δ : 2.0 (1H, s, OH), 7.4-8.0 (4H, m, Ar-H), 7.5-7.6 (1H, d, Ar-H), 8.2 (1H, s, CH)

2-fluoro-4-boronic acid- α -cyanobenzothiazolestilbene (PKP16)

Yield: 101.58%; IR (ATR, cm^{-1}): 3058 (O-H), 2218 ($\text{C}\equiv\text{N}$ stretch), 1422 (B-O); ^1H NMR (400 MHz, Methanol- d_3) δ : 2.0 (1H, s, OH), 7.4-7.9 (4H, m, Ar-H), 7.4-7.7 (1H, d, Ar-H), 8.3 (1H, s, CH)

4-fluoro-3-boronic acid- α -cyanobenzothiazolestilbene (4F-3BA)

Yield: 116.60%; IR (ATR, cm^{-1}): 3350 (O-H), 3058 (=C-H), 2218 ($\text{C}\equiv\text{N}$ stretch), 1422 (B-O); ^1H NMR (400 MHz, Methanol- d_3) δ : 2.0 (1H, s, OH), 7.4-8.0 (4H, m, Ar-H), 7.6-7.7 (1H, d, Ar-H), 8.1 (1H, s, CH)

3-fluoro-2-boronic acid- α -cyanobenzothiazolestilbene (3F-2BA)

Yield: 49.78%; IR (ATR, cm^{-1}): 3350 (O-H), 1411 (B-O), 1234 (C-F); ^1H NMR (400 MHz, Methanol- d_3) δ : 2.0 (1H, s, OH), 7.4-8.0 (4H, m, Ar-H), 7.2-7.5 (1H, d, Ar-H), 8.2 (1H, s, CH)

4-chloro-styrylbenzothiazole (PKP17)

Yield: 94.45%; IR (ATR, cm^{-1}): 3054 (=C-H), 752 (C-Cl); ^1H NMR (400 MHz, Methanol- d_3) δ : 7.4-8.0 (4H, m, Ar-H), 7.2-7.7 (1H, d, Ar-H), 7.3-7.5 (1H, d, CH)

3-chloro-styrylbenzothiazole (PKP18)

Yield: 97.80%; IR (ATR, cm^{-1}): 3052 (=C-H), 755 (C-Cl); ^1H NMR (400 MHz, Methanol- d_3) δ : 7.4-7.9 (4H, m, Ar-H), 7.3-7.5 (1H, d, Ar-H), 7.3-7.5 (1H, d, CH)

2-chloro-styrylbenzothiazole (PKP19)

Yield: 89.90%; IR (ATR, cm^{-1}): 3054 (=C-H), 752 (C-Cl); ^1H NMR (400 MHz, Methanol- d_3) δ : 7.4-8.0 (4H, m, Ar-H), 7.2-7.7 (1H, d, Ar-H), 7.3-7.5 (1H, d, CH)

2-fluoro-styrylbenzothiazole (PKP20)

Yield: 72.90%; IR (ATR, cm^{-1}): 3057 (=C-H), 1234 (C-F); ^1H NMR (400 MHz, Methanol- d_3) δ : 7.4-8.0 (4H, m, Ar-H), 7.2-7.7 (1H, d, Ar-H), 7.3-7.5 (1H, d, CH)

3-fluoro-styrylbenzothiazole (PKP21)

Yield: 97.60%; IR (ATR, cm^{-1}): 3052 (=C-H), 1246 (C-F); ^1H NMR (400 MHz, Methanol- d_3) δ : 7.4-8.0 (4H, m, Ar-H), 7.0-7.4 (1H, d, Ar-H), 7.3-7.5 (1H, d, CH)

4-fluoro-styrylbenzothiazole (PKP22)

Yield: 97.80%; IR (ATR, cm^{-1}): 3039 (=C-H), 1223 (C-F); ^1H NMR (400 MHz, Methanol- d_3) δ : 7.4-8.0 (4H, m, Ar-H), 7.2-7.6 (2H, d, Ar-H), 7.3-7.4 (1H, d, CH)

2-(trifluoromethyl)-styrylbenzothiazole (PKP23)

Yield: 82.77%; IR (ATR, cm^{-1}): 3053 (=C-H), 1102 (C-F); ^1H NMR (400 MHz, Methanol- d_3) δ : 7.4-8.0 (4H, m, Ar-H), 7.2-7.7 (1H, d, Ar-H), 7.3-7.6 (1H, d, CH)

3-(trifluoromethyl)-styrylbenzothiazole (PKP23)

Yield: 91.1%; IR (ATR, cm^{-1}): 3059 (=C-H), 1117 (C-F); ^1H NMR (400 MHz, Methanol- d_3) δ : 7.4-8.0 (4H, m, Ar-H), 7.7 (2H, d, Ar-H), 7.3-7.5 (1H, d, CH)

4-(trifluoromethyl)-styrylbenzothiazole (PKP24)

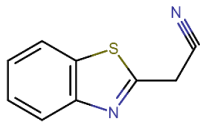
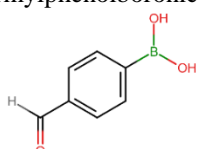
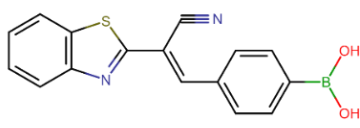
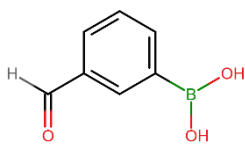
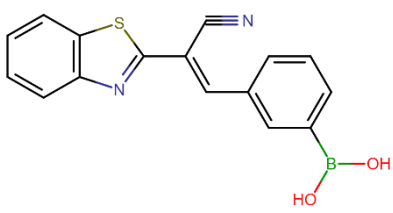
Yield: 81.00%; IR (ATR, cm^{-1}): 3060 (=C-H), 1322 (C-F); ^1H NMR (400 MHz, Methanol- d_3) δ : 7.4-8.0 (4H, m, Ar-H), 7.4-8.0 (1H, d, Ar-H), 7.3-7.4 (1H, d, CH)

Table 3 shows the structures of the reactants and the products in details.

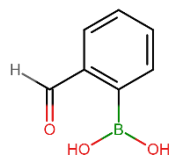
Benzothiazole α -cyanostilbenes were obtained in yields ranging from 49.78% to 116.60%, with the substituent 3-fluoro-2-formylphenylboronic acid having the lowest yield and the substituent 4-fluoro-3-formylphenylboronic acid having the highest yield. Overall, functional groups that are *ortho*-substituted have lower percent yield compared to those that are *meta*- and *para*-substituted, with the exception of the chlorobenzaldehyde substituents.

Styrylbenzothiazoles were obtained in yields ranging from 72.90% to 97.80%, with the substituent 2-fluorobenzaldehyde having the lowest yield and substituents 2-chlorobenzaldehyde and 4-fluorobenzaldehyde having the highest yield. In this family, there seems to be no relationship between the substituents' positions and the products' yield.

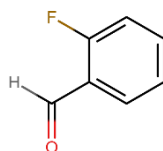
Table 3 Reactants and product structures

2-Benzothiazole Reactant	Aldehyde Reactant	2-Benzothiazole Product	Percent Yield (%)
-Acetonitrile		α -Cyanostilbenes	
	4-formylphenylboronic acid 	PKP2 	115.6
	3-formylphenylboronic acid 	PKP4 	108.8

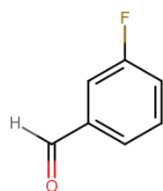
2-formylphenolboronic acid



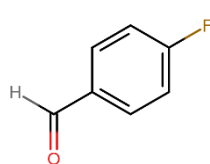
2-fluorobenzaldehyde



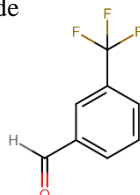
3-fluorobenzaldehyde



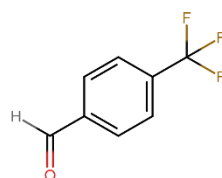
4-fluorobenzaldehyde



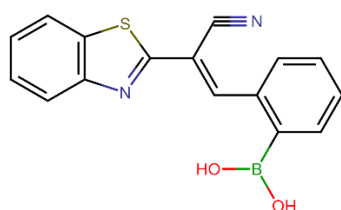
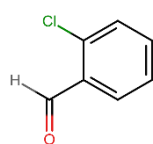
3-(trifluoromethyl) benzaldehyde



4-(trifluoromethyl) benzaldehyde

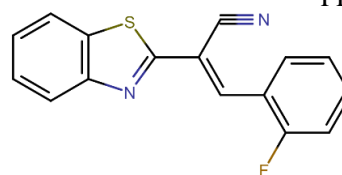


2-chlorobenzaldehyde



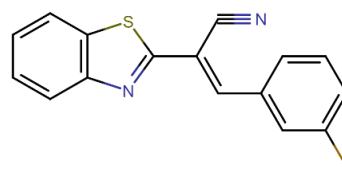
PKP3

73.03



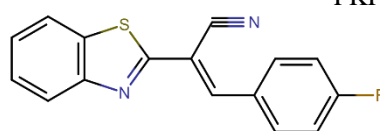
PKP5

87.9



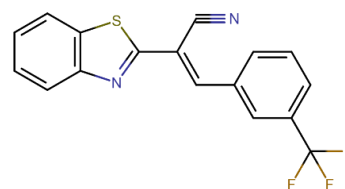
PKP7

101.6



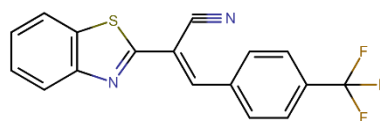
PKP6

98.28



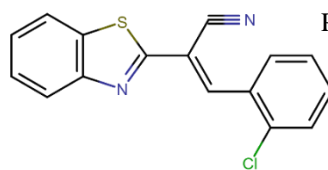
PKP8

98.2



PKP9

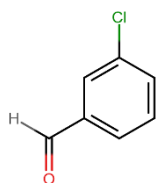
98.40



PKP10

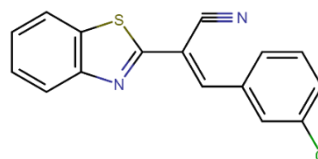
114.80

3-chlorobenzaldehyde

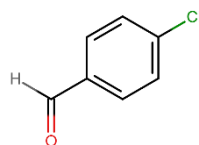


PKP11

102.80

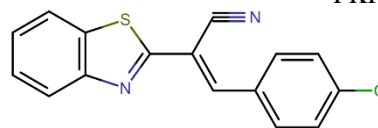
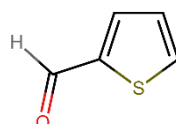


4-chlorobenzaldehyde



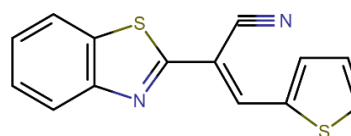
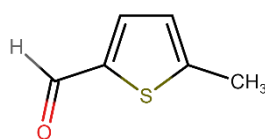
PKP12

108.60

2-thiophene-
carboxaldehyde

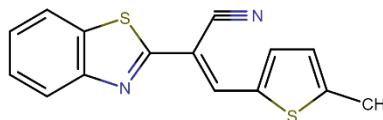
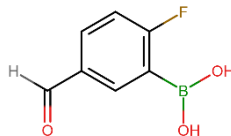
PKP13

108.60

5-methyl-2-thiophene-
carboxaldehyde

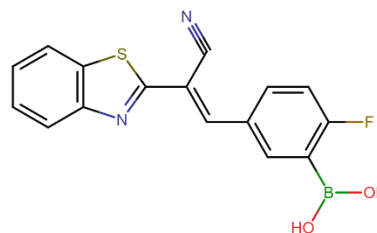
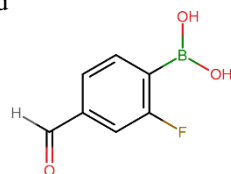
PKP14

92.45

2-fluoro-5-
formylphenylboronic
acid

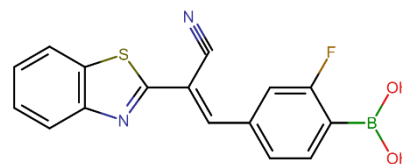
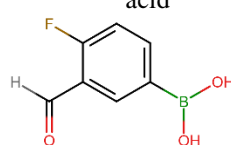
PKP15

108.58

2-fluoro-4-
formylphenylboronic
acid

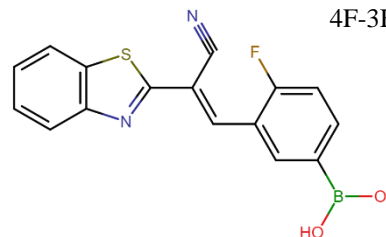
PKP16

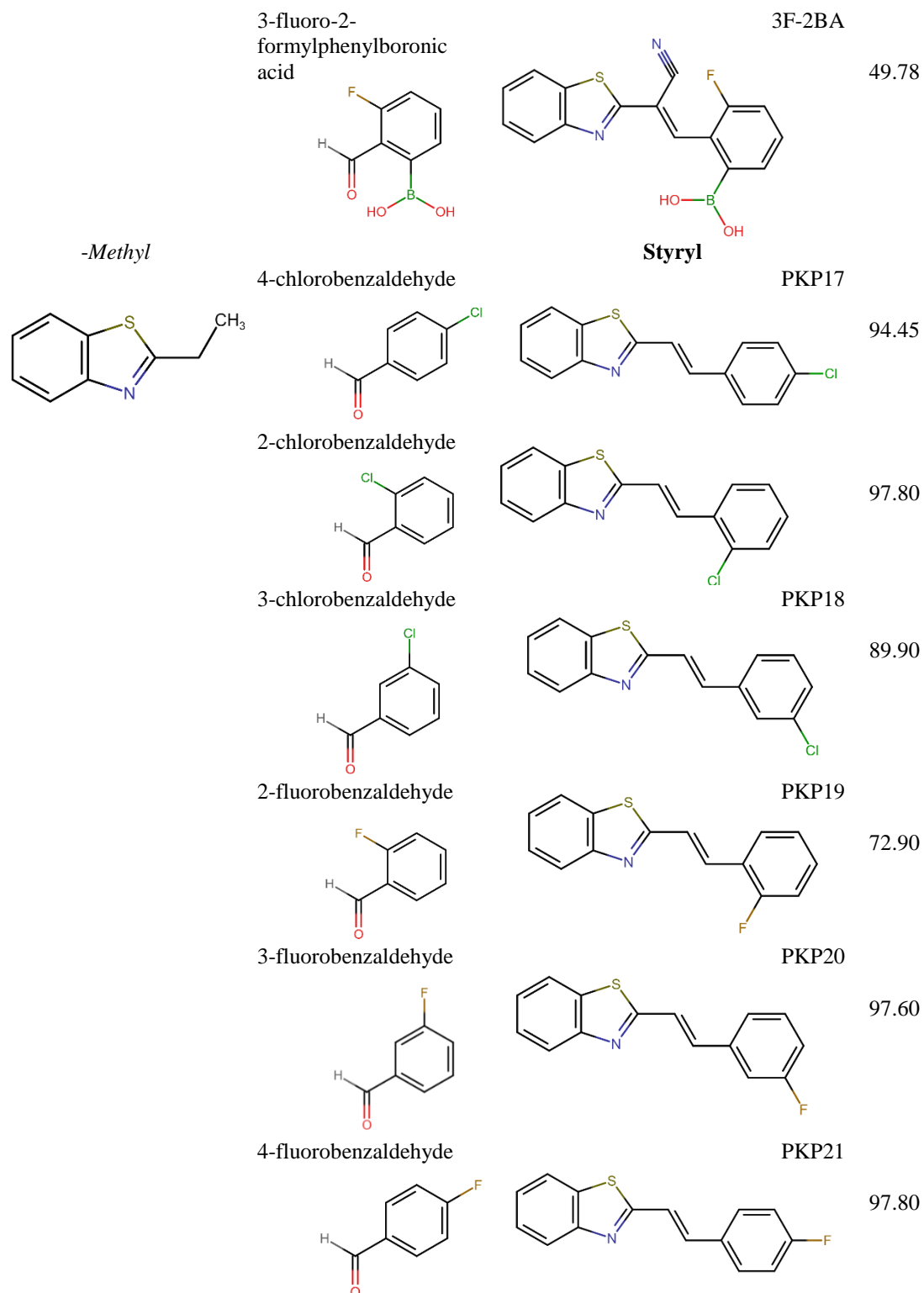
101.94

4-fluoro-3-
formylphenylboronic
acid

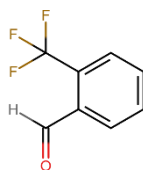
4F-3BA

116.60

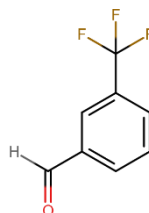




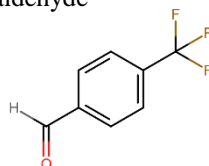
2-(trifluoromethyl)-
benzaldehyde



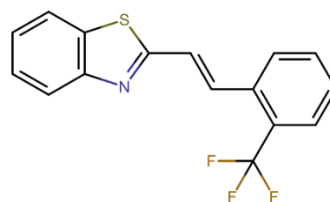
3-(trifluoromethyl)-
benzaldehyde



4-(trifluoromethyl)-
benzaldehyde

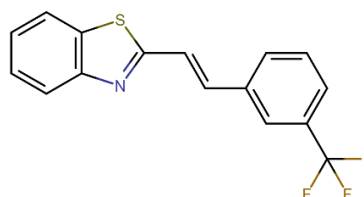


PKP22



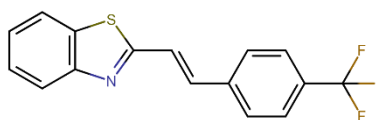
82.77

PKP23



91.1

PKP24



81.00

Biology

Cell Viability Assay

The viability of U-87MG cells was determined after the cells were treated with varying concentrations of the novel hybrid benzothiazoles to establish their LC₅₀ values. The LC₅₀ values of the compounds were converted into μM from mg/ml (Table 4).

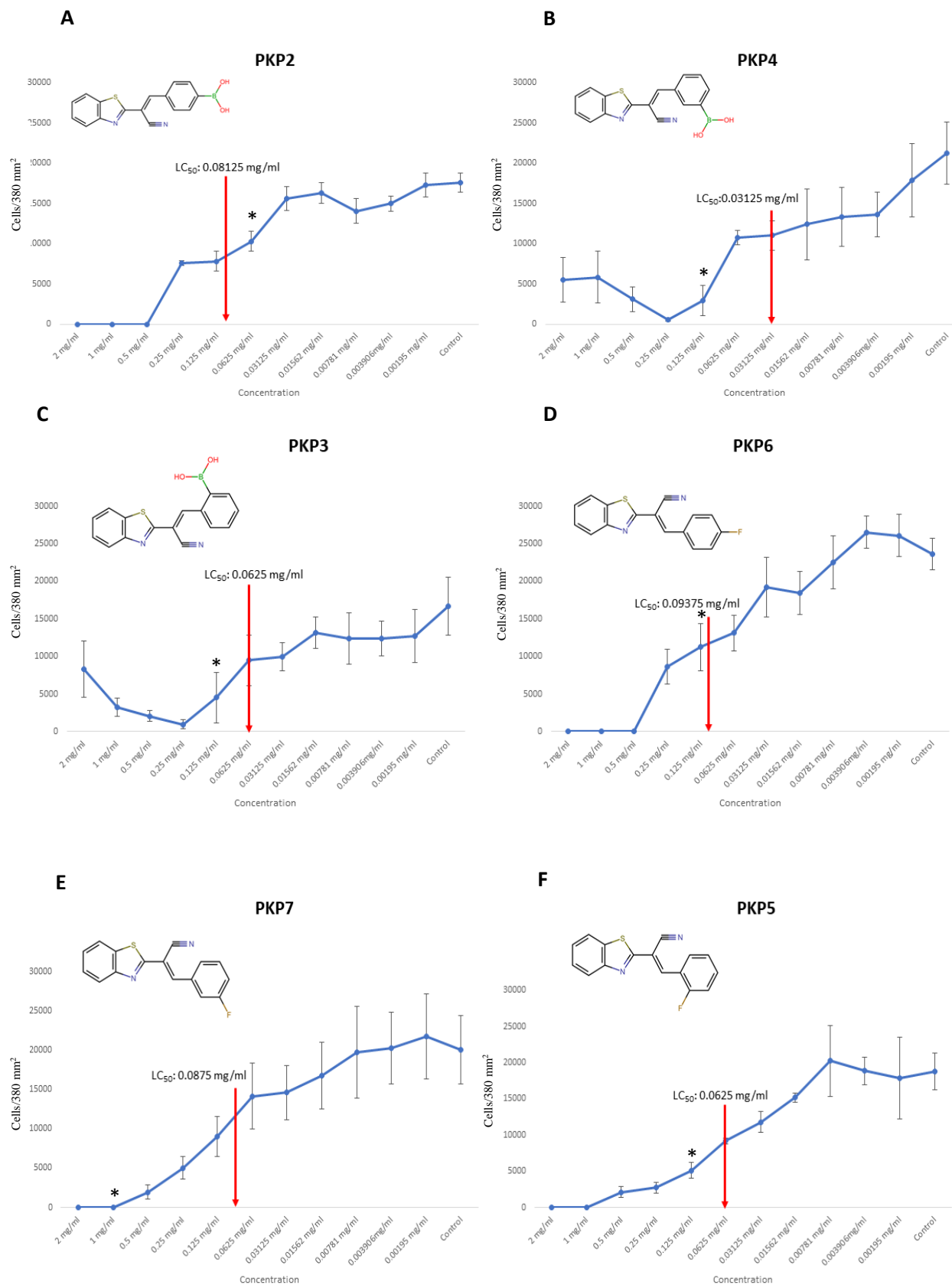
Table 4 Tested compounds represented in μM

TESTED COMPOUND	LC ₅₀ (MG/ML)	LC ₅₀ (μM)
PKP2	0.08125	265.392
PKP3	0.0625	204.14
PKP4	0.03125	102.07
PKP5	0.0625	280.33
PKP6	0.09375	334.42

PKP7	0.0875	312.13
4F-3BA	0.01175	36.25
3F-2BA	0.05625	173.53

Figure 20 shows the cell viability at all eleven concentrations and the red arrow indicates the LC₅₀ of the compounds. Benzothiazoles containing boronic acid substituents at *para*, *meta*, and *ortho* positions are shown in Figure 20, A to C (PKP2, PKP4, PKP3). While all positions showed a reduction in cell viability, *meta* position had the lowest LC₅₀ value (0.03125 mg/ml) and *ortho* position had the highest LC₅₀ value (0.08125 mg/ml).

Figure 20, D to F (PKP6, PKP7, PKP5) shows the effects of benzothiazoles with fluoro substituents on U-87MG cell viability. All three positions showed a reduction in cell viability, with *ortho* position having the lowest LC₅₀ value (0.0625 mg/ml) and *para* position having the highest LC₅₀ value (0.09375 mg/ml). The results showed cell growth at the higher concentration (2 mg/ml to 0.5 mg/ml) PKP4 and PKP3. However, the cells did not look normal; they lacked the shape of glioblastoma cells and were round in shape.



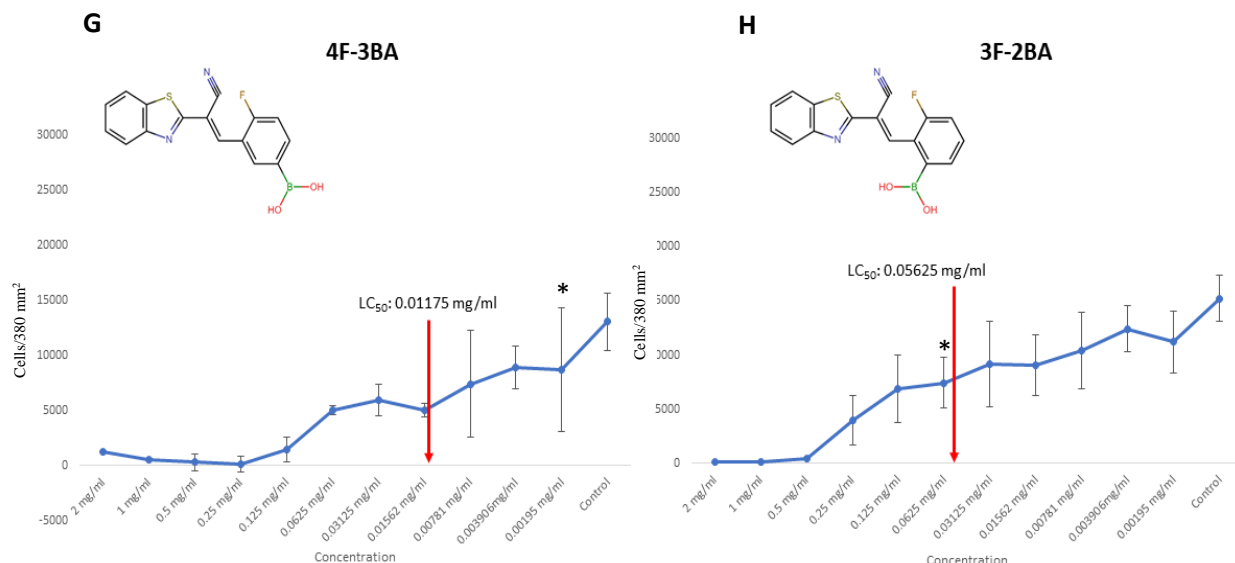


Figure 20 The effect of novel hybrid benzothiazoles on U-87MG glioblastoma cell viability compared to untreated U-87MG cells. Red arrows indicate the LC_{50} values of each compound. A: PKP2-Boronic acid substituent at para position; B: PKP4-Boronic acid substituent at meta position; C: PKP3-Boronic acid substituent at meta position. D: PKP6-Fluoro substituent at para position; E: PKP7-Fluoro substituent at meta position; F: PKP5-Fluoro substituent at ortho position; G: 4F-2BA-Boronic acid substituent at meta position and fluoro substituent at para position to boronic acid substituent; H: 3F-2BA-Boronic acid substituent at ortho position and fluoro substituent at meta position to boronic acid substituent. Asterisks represent the lowest concentration with a statistically significance difference from control $p \leq 0.05$. Error bars indicate standard error, $n = 3$ independent

Treatment with benzothiazoles containing both fluoro and boronic acid substituents are shown in Figure 18, G and H (4F-3BA, 3F-3BA). Both compounds display decreases in cell viability. However, benzothiazole containing boronic acid at *meta* position and fluoro at *para* position of the boronic acid substituent had the lowest LC_{50} among all of the tested compounds.

The results of the novel hybrid compounds were compared with the effect of benzothiazole starting material (benzothiazole-2-acetonitrile) on cell viability. Figure 21 shows the result obtained from the benzothiazole starting material. The LC_{50} value of the starting material (0.2 mg/ml) is approximately two times higher than the LC_{50} value of the tested compound with the highest LC_{50} value (PKP6).

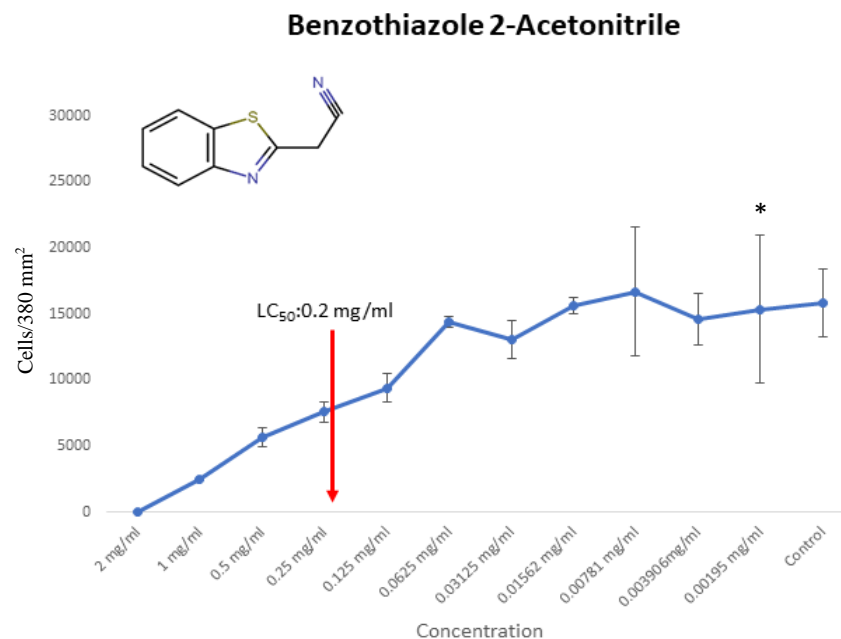


Figure 21 The effects of benzothiazole starting material on U-87MG glioblastoma cells compared to untreated U-87MG cells. Red arrow indicates the LC_{50} value of the starting material. Asterisk represents the lowest concentration with a statistically significant difference from control, $p \leq 0.05$. Error bars indicate standard error, $n=3$ independent experiments in triplicate.

Confirmation of Lethal Concentration (LC_{50})

To ensure that the LC_{50} values obtained from the linear regression using data from the cell viability assay were accurate, concentrations of each compound at the calculated LC_{50} values were verified with nine replicates. Figure 22 shows that while most compounds were within the 50% cell viability range, PKP2 was well below the range (27.7%).

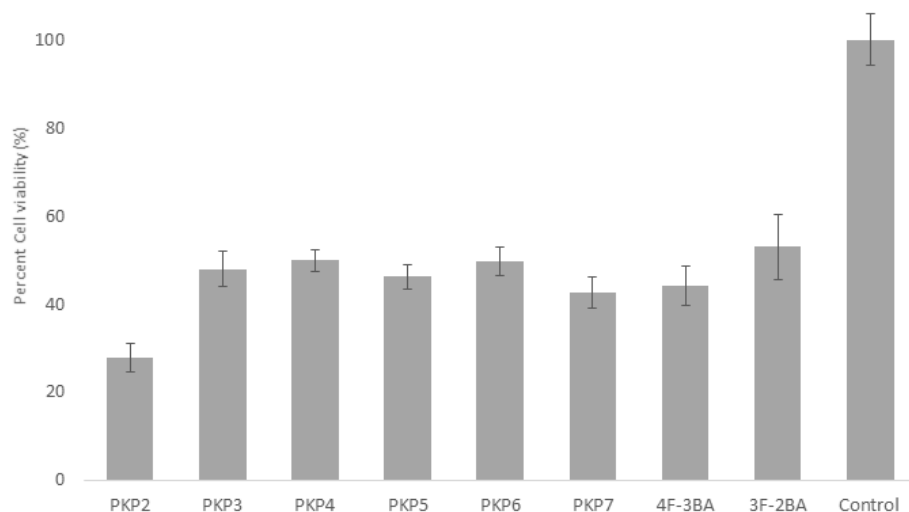


Figure 22 Confirmation of LC_{50} values for eight novel hybrid benzothiazole compounds. Cell viability was measured at the predicted LC_{50} for each of the eight novel hybrid benzothiazoles. Each bar represents the mean and standard error for nine independent replicates.

As seen in Figure 22, the cell viability of PKP2 was much lower when U-87MG glioblastoma cells were treated nine times at the initial LC_{50} value. As a result, PKP2 was tested again using the modified NIH cell viability assay to redefine its LC_{50} value. Figure 23 shows the new LC_{50} value (0.026561 mg/ml) obtained from linear regression.

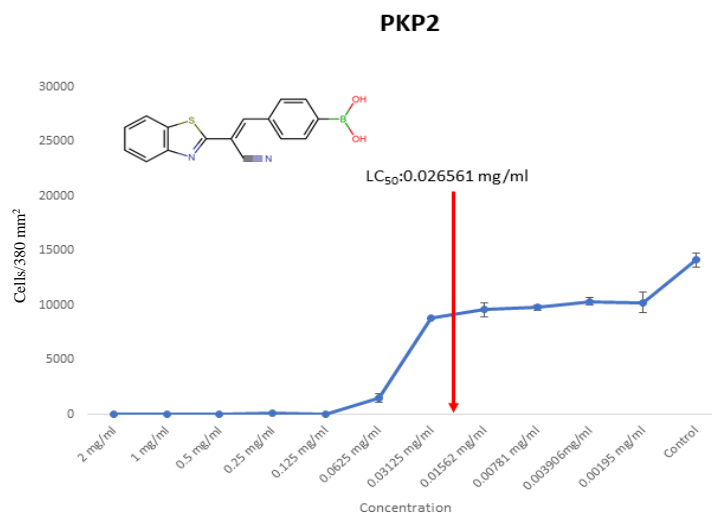
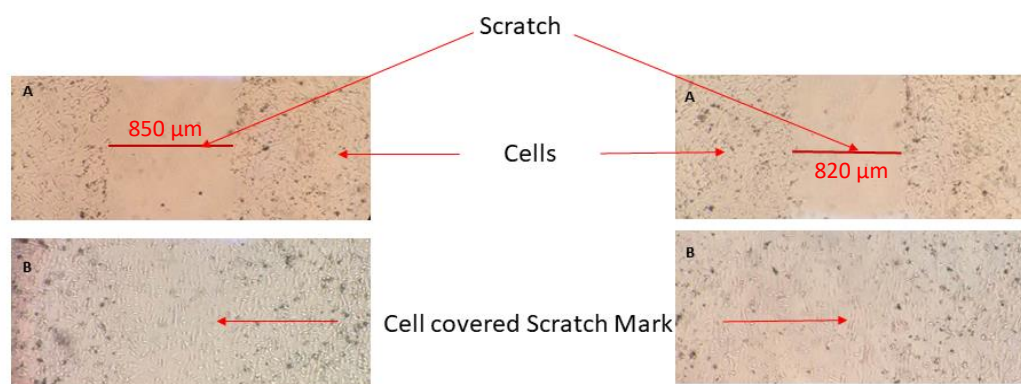


Figure 23 Redefined LC_{50} of PKP2. U-87MG were treated with PKP2 following the modified NIH cell viability assay. Red arrow indicates the LC_{50} value of the compound. Error bars indicate standard error, $n = 3$ independent experiments in triplicate

Wound Healing Scratch Assay

Analysis of cell migration via wound healing scratch assay was used to quantify the alterations in cell migratory capacity in response to treatment with novel hybrid benzothiazoles. The results however showed not migration but rather the present or absence of cells in the scratch. Figure 24 shows the results of untreated cells while Figure 25 shows a representative plate of treated cells. Treated plates filled in the scratch at the same extent as the control plate.



*Figure 24 Scratch Assay – Untreated.
A) Day one B) Day two*

*Figure 25 Scratch Assay - Treated (PKP3)
A) Day one B) Day two*

Neurosphere Assay

To determine the effect of the tested compounds on the formation of neurospheres, U-87MG cells were treated with the LC_{50} and LTC of each novel hybrid benzothiazoles (Table 1). Table 5 shows the neurosphere formation at LTC. While no significant difference between treated and untreated compounds seem to be present, PKP4, PKP5, and PKP6 showed the delay in the formation of neurospheres.

Table 6 shows the neurosphere formation at the LC_{50} . Neurospheres were absent day 1 for all compounds while two small neurospheres were present in the control. There were no neurospheres present at day 3 for all compounds with the exception of PKP4,

PKP5, and PKP6 which had small neurospheres or the initial neurosphere formation (where U-87MG cells are beginning to form a neurosphere can be observed), while two medium neurospheres were present in the control. On day 6, PKP2, PKP5, and PKP7 had neurospheres that were beginning their formation, PKP3 and PKP6 lacked neurospheres, and 4F-3BA, 3F-2BA and PKP4 had one small neurosphere. In contrast, the whole well was covered with neurospheres in the control.

*Table 5 Effect of Novel Hybrid Benzothiazoles on Formation of Neurosphere at **Lowest Tested Concentration***

	DAY 1	DAY 3	DAY 6
PKP2	+, starting	+, medium	+, large
PKP3	+, starting	++ , small	+, large
PKP4	Absent	+, small	+, medium
PKP5	Absent	+, medium	+, large, +, small
PKP6	Absent	+, small-medium	+, medium, ++, small
PKP7	+, starting	+, small	+, large, +, small
4F-3BA	+, small	+, medium	Whole well covered
3F-2BA	+, small	+, medium	+, large
CONTROL	+, small	+, medium	Whole well covered

Table 6 Effect of Novel Hybrid Benzothiazoles on Formation of Neurosphere at LC₅₀

COMPOUND + LC ₅₀	DAY 1	DAY 3	DAY 6
PKP2 (0.02656 MG/ML)	Absent	Absent	+, starting
PKP3 (0.03215 MG/ML)	Absent	Absent	Absent
PKP4 (0.0625 MG/ML)	Absent	+, starting	+, small
PKP5 (0.0625 MG/ML)	Absent	+, small	+, starting
PKP6 (0.09375 MG/ML)	Absent	+, small	Absent
PKP7 (0.0875 MG/ML)	Absent	Absent	+, starting
4F-3BA (0.01171 MG/ML)	Absent	Absent	+, small
3F-2BA (0.05625 MG/ML)	Absent	Absent	+, small
CONTROL	++ , small	++ , medium	Whole well covered

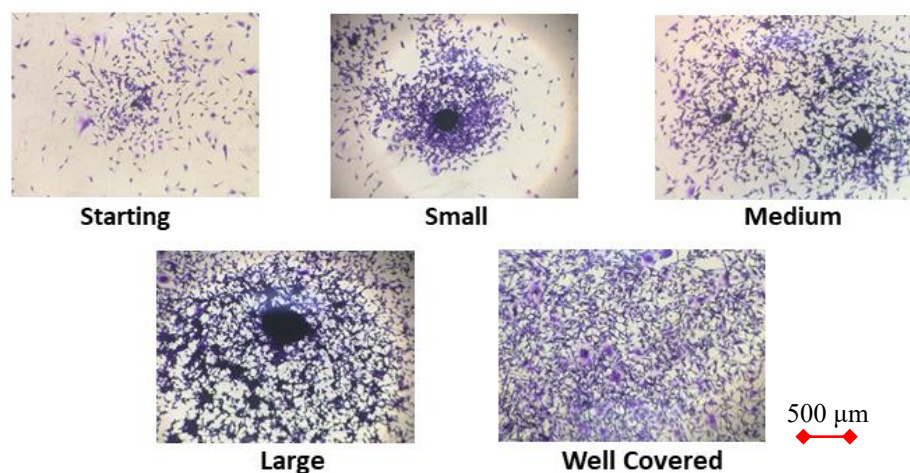


Figure 26 Representation of the sizes and description of neurosphere formation. Red line for scale.

Invasion Assay

To determine the anti-invasive properties of the tested compounds, U-87MG cells were treated with HCRC (Table 2). Figure 24 shows the effect of the tested compounds on the cell's invasive properties. PKP2 and PKP3 both possessing boronic acid substituents at the *para* or *meta* positions and PKP5 which contain fluoro substituent at *ortho* position display a statistically significant decrease in the percentage of invasive cells. While PKP4, PKP6, and PKP7 display a decrease in the number of invasive cells, the differences are not statistically significant.

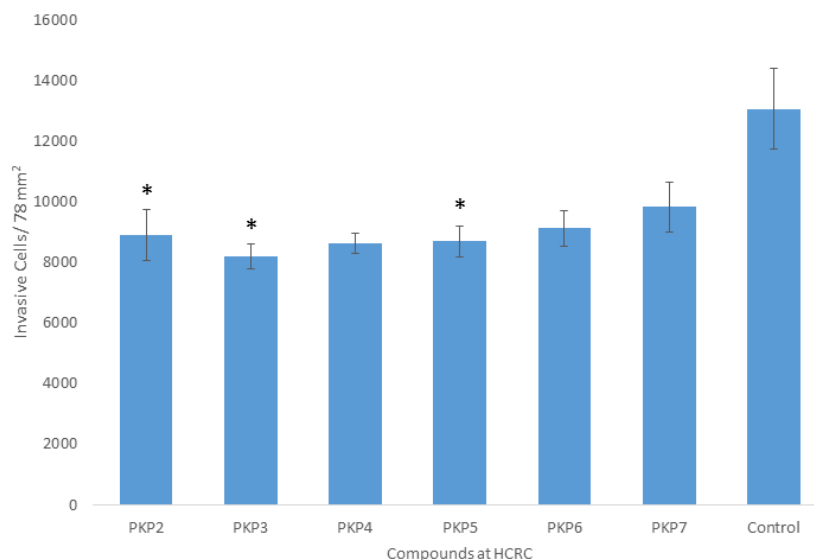


Figure 27 Anti-invasive property of tested compounds. U-87MG cells were treated with six compounds at their HCRC values. Statistically significant difference ($P \leq 0.05$ for one-way ANOVA) between untreated cells and tested compounds are indicated by an asterisk. Error bars indicate standard error, $n = 3$ individual experiments done in duplicate wells for each experiment.

CHAPTER 4

DISCUSSION

Predicted Bioavailability and Blood-brain barrier Permeability of Novel Hybrid

Benzothiazoles

Lipophilicity

As discussed, lipophilicity of a compound plays an important role in the bioavailability and blood-brain barrier permeability. Higher lipophilicity has been shown to allow higher permeability in the gastrointestinal tract and across the blood-brain barrier (Winiwarter et al., 2007). However, if the lipophilicity is too high ($\text{LogP} > 5$), this could result in high metabolic turnover, low solubility, and poor oral absorption as well as toxicity from inappropriate target interactions. Low lipophilicity, on the other hand, could also affect negatively on potency and permeability of a compound which results in reduced/poor bioavailability and efficacy. Compounds with LogP less than 4 and greater than 1 has been shown to have optimal physicochemical properties for oral drugs (Gao et al., 2016). As shown in Table 1, novel hybrid benzothiazoles are all highly lipophilic. However, while most compounds fall within the range of LogP value with the optimal physicochemical properties, PKP6 and PKP7 are slightly above the optimal range. Therefore I believe all tested compounds, with the exception of PKP6 and PKP7, will most likely have the optimal physicochemical properties for oral drugs.

Oral Bioavailability

The number of hydrogen-bond donor (nOHNH) for all novel hybrid benzothiazoles are well below 5 and are in accordance with Lipinski's rule. All novel hybrid benzothiazoles have molecular weight of less than 500 which would allow them to be easily transported, diffused and absorbed as compared to those that are greater 500. LogP, as mentioned previously, determines the lipophilicity of novel hybrid benzothiazoles. All novel hybrid benzothiazoles have been shown to have LogP values that are less than 5, in accordance with Lipinski's rule. The number of hydrogen-bond acceptors for all novel hybrid benzothiazoles is less than 10. None of the novel hybrid benzothiazoles violated Lipinski's rule.

Moreover, novel hybrid benzothiazoles meet the two additional extensions of Lipinski's rules. All three types have less than 10 rotatable bonds and their topological polar surface area (TPSA) values range from 53-77 Å. TPSA has been correlated with hydrogen bonding of the molecules and is a reliable indicator of the bioavailability, gastrointestinal absorption, and blood-brain barrier penetration of a compound. Using the TPSA I calculated the percent absorption using the equation provided by Zhao et al. (2002). The calculated percent absorption for novel hybrid benzothiazoles ranged between 82.38-96.34%, indicating good oral bioavailability.

Blood-brain Barrier Penetration

Blood-brain barrier penetration properties of a compound can be predicted using the quantitative structure-activity relationship (QSAR). Hansch and Fujita (1964) have shown that the critical components for the blood-brain barrier penetration include

lipophilicity, hydrogen bonding, and molecular weight. Generally, compounds that are moderately lipophilic can cross the blood-brain barrier through passive diffusion. As mentioned above, lipophilicity of a compound can be determined by LogP. Pike (2009) has shown that the blood-brain barrier penetration is optimal when the LogP values are within the threshold of 2-3.5.

Molecular weight is another critical component for blood-brain barrier (BBB) penetration. Compounds with a molecular weight less than 450 is needed to facilitate BBB penetration and lower for better oral absorption (Atkinson et al., 2002). Hydrogen bonding properties of a compound can also play a significant role in the CNS uptake profile. Polar molecules are often poor CNS agents, unless they are transported across the CNS by active transport (Pajouhesh and Lenz, 2005). Polar surface area (PSA) has also been used to predict BBB penetration. Generally, compounds with lower PSA have been shown to be more effective at penetration of the BBB. The optimal PSA for BBB penetration has been estimated at 60-70 Å through 90 Å (Mouritsen and Jorgensen, 1998).

Based on the LogP values, all novel hybrid benzothiazoles, except for those with just fluoro substituents (PKP5-7) fall within the optimal blood-brain barrier penetration threshold. According to the previous studies, the BBB penetration is optimal within the LogP value range of 2-3.5. The LogP values of novel hybrid benzothiazoles ranges between 2.77-4.11. PSA values of all tested novel hybrid benzothiazoles, except for those with only fluoro substituent (PKP5-7), fall within the estimated optimal PSA range. In terms of molecular weight, all of novel hybrid benzothiazoles meet the condition to facilitate the BBB penetration; they are all less than 450.

Chemistry

Benzothiazole α -cyanostilbenes synthesis was achieved via base-catalyzed Knoevenagel condensation reaction. Knoevenagel condensation reaction is a nucleophilic addition of an active hydrogen atom to a carbonyl group, aldehyde in this specific reaction, with a base catalyst (Jones, 2011). This addition is then followed by elimination of a water molecule through the dehydration reaction (Fig 27).

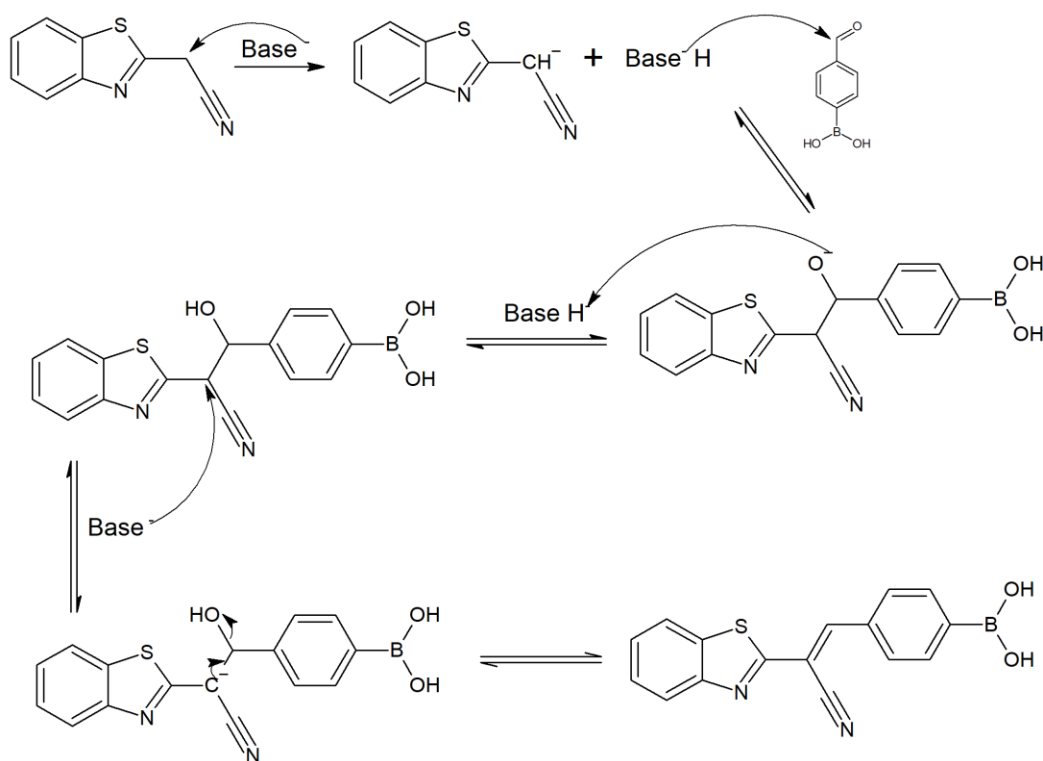


Figure 27 Mechanism of Knoevenagel Condensation reaction which occurs in the synthesis of hybrid benzothiazole α -cyanostilbene. Boronic acid substituent is used as an example.

The design and synthesis of benzothiazole α -cyanostilbenes were focused on covalently linking benzothiazole-2-acetonitrile and an aromatic aldehyde with or without boronic acid substituents to produce novel hybrid molecules. Various functional groups such as boronic acid, fluoro, chloro at *ortho*, *meta*, or *para* positions were synthesized for

comparison. Such comparisons are noted between PKP2, PKP3, PKP4, PKP5, PKP6, PKP7, 4F-3BA, and 3F-2BA. All of these compounds had a merged benzothiazole-stilbene scaffold. However, PKP2, PKP3, and PKP4 have boronic acid substituent, whereas PKP5, PKP6, and PKP7 have fluoro substituent. 4F-3BA and 3F-2BA contain both boronic acid and fluoro substituents. Boronic acid was chosen as a substituent because of their success as FDA approved anti-cancer drugs (i.e. Ixazomib and Bortezomib). Fluoro substituents were chosen because of their ability to enhance a number of pharmacokinetic and physiochemical properties including enhanced membrane permeation and improved metabolic stability (Shah and Westwell, 2007).

Catalyst and solvent used in the process of Knoevenagel condensation reaction plays an important role in the percentage yield of the products. Evidences of the importance of the base catalyst can be seen in multiple studies with modified Knoevenagel reaction. For example, Rao and Venkataratnam (1991), utilized zinc chloride as a catalyst for their modified Knoevenagel condensation reaction and obtained products of good purity and high in yield. Schenider et al. (2015) reported the use of copper metal surfaces as their catalyst in their modified Knoevenagel reactions. Their study tested pure copper metal powder and compared it against carbon coated-copper nanoparticles (C/Cu) which has been shown to produce the highest activity in the Knoevenagel reaction (Koehler et al., 2009). Reactions catalyzed by pure metal powder showed higher yield and time efficiency. Panja et al. (2015) compared several different solvents for their Knoevenagel reactions such as the use of water, acetonitrile, dichloromethane, ethanol and solvent-free conditions. Their report indicated that the

solvent which optimized the reaction best was ethanol with the reaction time of 3 *mins* at room temperature and 98% yield.

In this project, calcium oxide was used as the base catalyst and ethanol and water were used as the solvents. The percentage yields obtained from the synthesis of the benzothiazole α -cyanostilbenes ranged from 49.78% to 116.60%. All benzothiazole α -cyanostilbenes were synthesized under the same conditions (catalyst, solvent, and time). Based on the literature for optimizing percentage yields, it is possible to increase the compound with 49% yield. Varying reaction conditions such as reaction time, catalyst, and/or solvent could have resulted in increased percent yield of the product.

4F-3BA, with the highest percent yield of 116.60% and other compounds with percent yield over 100% could have produced higher yields due to the presence of impurities. The impurities in the product could have been the calcium oxide catalyst. These compounds were further purified by utilizing separation techniques and washing techniques in ethyl acetate as a solvent. All compounds that were purified had a decrease in percent yield by half of the initial percent yield. This may be the result of product loss during the purification process. Purification techniques which optimize product retention should be explored in future studies. Furthermore, changing the catalyst to calcium hydride or calcium hydroxide can decrease the presence of the catalyst in the product.

Styrylbenzothiazole were synthesized using the aldol-type condensation reaction. Aldol-type condensation is the reaction of a stabilized carbanion ion and a carbonyl group which forms a β -hydroxyl (ketone/aldehyde) and water (Jones and Fleming, 2010). Figure 28 shows the general mechanism of Aldol-type condensation reaction which occurs in the synthesis of hybrid styrylbenzothiazoles.

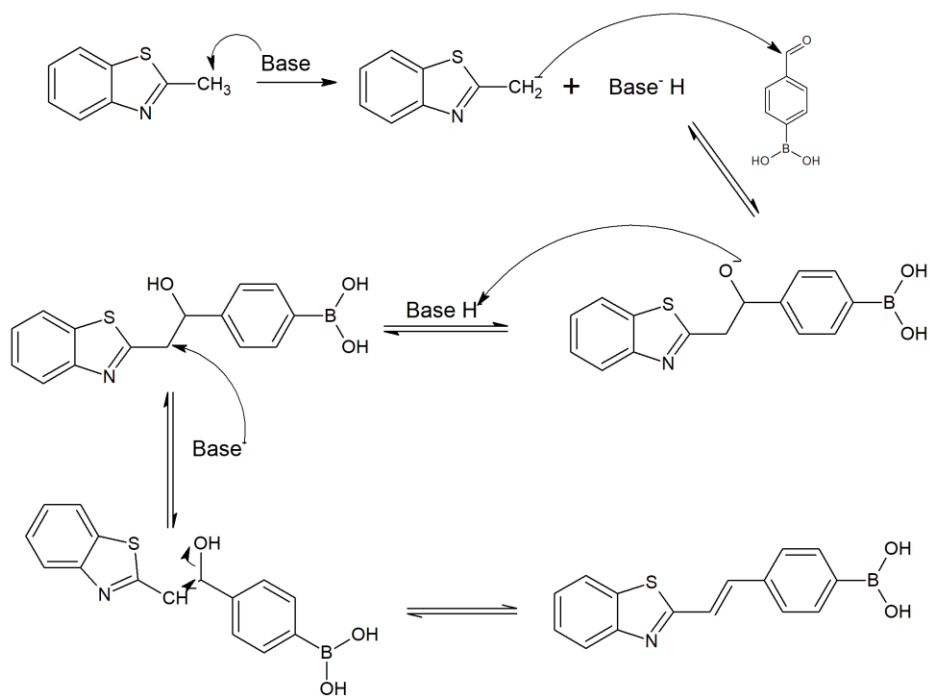


Figure 28 Mechanism of Aldol-type condensation reaction which occurs in the synthesis of hybrid styrylbenzothiazole. Boronic acid substituent is used as an example.

In the synthesis of styrylbenzothiazoles, no catalyst was used, and the reaction occurred at room temperature in four hours. While I was able to obtain products for chloro, fluoro, and trifluoromethyl substituents, I was unable to successfully produce products containing boronic acid substituents. In the initial experiment in the synthesis of styrylbenzothiazoles, I used dimethylformamide (DMF) as the solvent and potassium *t*-butoxide (KTB) and lithium hydride (LiH) to deprotonate and to produce enolate ions. However, I obtained low percent yield for all the products and they were sticky in texture. To optimize the percent yield and to solve the texture problem, I opted for using just LiH without KTB. This produced better results. The percent yield obtained from the modified method ranged from 72% to 97%. However, I was not able to successfully synthesize styrylbenzothiazole containing boronic acid substituent. When analyzed under

NMR and IR, the absence of boronic acid was noted. The cause of deboronation is still unknown and needs further exploration.

Biological Evaluation

In recent years, benzothiazole derivatives have been explored as potential new therapies with various biological activities against infection, osteoarthritis, and cancer (Bondock et al., 2010; Brantley et al., 2006; Vicini et al., 2011). Benzothiazole analogues, such as tetrahydrobenzothiazoles have been tested as potential anti-tumor drugs via inhibition of mutated p53 activity to enhance paclitaxel-induced apoptosis (Christodoulou et al., 2011). In addition, benzothiazole derivatives have been shown to produce cytotoxicity in human cancer cell lines *in vitro* (Kok et al., 2008) and act as potent growth inhibitors in a number of human-derived cancer cell lines (Hu et al., 2010; Tzanopoulou et al., 2010).

The results from this study confirm the biological activity of the novel hybrid benzothiazole structure. I have shown the potential anti-cancer effect of a new series of hybrid benzothiazoles in U-87MG glioblastoma cells. All tested compounds showed a decrease in cell viability. Based on the modified NIH cell viability assay, 4F-3BA, benzothiazole α -cyanostilbenes, containing both fluoro and boronic acid substituent on the aromatic ring, was the most effective compound tested (LC₅₀: 36.25 μ M), immediately followed by PKP2 which contains boronic acid substituent at *para* position (LC₅₀:86.76 μ M). This outcome could imply that fluoro-containing compounds had enhanced pharmacokinetic and physiochemical properties. Fluorines have been shown to

influence permeability and potency of compounds due to its high electronegativity and high lipophilicity (Gillis et al., 2015).

Overall, there was no clear correlation between the potency of the compound and the substituent's position on the aromatic ring. However, in compounds with boronic acid substituent, *para* position has the highest potency (LC_{50} : 86.76 μM) while *ortho* position had the lowest potency (LC_{50} : 280.33 μM). In compounds with fluoro substituent, *ortho* position had the highest potency (LC_{50} : 280.33 μM) and *para* position has the lowest potency (LC_{50} : 334.42 μM). In general, compounds containing boronic acid substituents seem to favor the cytotoxic activity more than compounds containing fluoro substituents, since PKP2, PKp3, and PKP4 were more active than PKP5, PKP6, and PKP7.

Neurospheres play an important role in multilineage differentiation in neural cells (Ishiguro et al., 2017). They are highly heterogeneous entities which produce the same cellular components of neural stem cells. Due to their abilities that mimic that of neural stem cells, they have been highly exploited in drug screening (Galli, 2013).

In this project, U-87MG glioblastoma cells were treated with LC_{50} and LTC of the tested compounds to determine their effects on the formation of neurospheres. At the LTC, there appears to be no significant difference between treated and untreated compounds. However, PKP4, PKP5, and PKP6 seems to slightly decrease the formation of neurospheres compared to the other three tested compounds. Regardless, it does not take away from the fact that none of the compounds were able to significantly reduce neurosphere formation. At the LC_{50} , there is a significant reduction of neurosphere formation in treated compounds. All tested compounds appear to inhibit the formation of neurospheres at the same rate. This may be the result of 50% cell viability which prevents

the formation of neurospheres or the reduced number of neurospheres could be the cause of the reduced cell numbers and should be investigated further.

As discussed in Chapter 1, one of the hallmarks of cancer is invasion and metastasis. Invasion and metastasis, in the context of GBM, plays a vital role in cancer progression and recurrence. None of novel hybrid benzothiazoles seems to inhibit or prevent cell migration as seen in the wound healing scratch assay. However, it is possible that the assay was not measuring the motility of the cells but instead their proliferation. Further modification of the assay is needed to be explored to accurately measure the migration of the cells. One area of modification could be the media used. By using serum free medium instead of serum containing fetal bovine serum, the assay could be made to measure only the migration of the cell.

Three of the novel hybrid benzothiazoles (PKP2, PKP3, and PKP5) seem to decrease the number of invasive cells, as shown in the invasion assay. These three promising compounds warrant further detailed analyses to elucidate the underlying molecular mechanism of action. Moreover, due to the literature reports of benzothiazoles analogs with the abilities to induce apoptosis, novel hybrid benzothiazoles should be tested for the underlying mechanism of the cause of cell death.

CHAPTER 5

CONCLUSION

As disclosed in Chapter 1, glioblastoma multiforme is highly lethal due to its aggressive and invasive proliferation. A major factor shaping the high mortality lies in cancer cells' ability to migrate and to proliferate. Therefore, development of cancer therapies targeting invasion and induction of apoptosis is necessary.

In this study, 19 novel hybrid benzothiazole α -cyanostilbenes with or without boronic acid substituents and 7 novel hybrid styrylbenzothiazoles without boronic acid substituents were synthesized and described. Out of the total synthesized compounds, 8 novel hybrid benzothiazole α -cyanostilbenes were screened for their anti-cancer activities. The result of the project demonstrated the anti-cancer activity of novel hybrid benzothiazole derivatives, particularly compound 4F-3BA, which had the highest potency *in vitro*.

Based on the neurosphere assay, at LTC (0.00195 mg/ml) PKP4 (boronic acid at *meta* position), PKP5 (fluoro at *ortho* position), and PKP6 (fluoro at *para* position) were the most successful compounds in delaying the formation of the neurospheres. At LC₅₀ all tested compounds were effective at preventing the formation of the neurospheres, with PKP4 (boronic acid at *meta* position) and PKP5 (fluoro at *ortho* position) being the least effective compounds.

The result of the invasion assay showed that three compounds, PKP2 (boronic acid at *para* position), PKP3 (boronic acid at *ortho* position) and PKP5 (display some anti-invasive properties). The anti-invasive properties of these three compounds should be

further evaluated by a more reliable invasion assay which utilizes Calcein fluorescence to quantify the number of invasive cells. All 8 tested compounds should be further tested to determine their effect on caspases to explore their potential as apoptotic inducing agents. In addition, all novel hybrid benzothiazoles should be further studied for their anti-cancer properties and verify the underlying mechanism of action.

REFERENCES

- Ali R & Siddiqui N. 2013. Biological aspects of emerging benzothiazoles: a short review. J. Chem. 2013:345198
- American Cancer Association. 2016. Types of brain and spinal cord tumors in adults. Atlanta: American Cancer Association.
- American Cancer Association. 2019. Cancer facts & figures 2019. Atlanta: American Cancer Society.
- Atkinson F, Cole S, Green C, & van de Waterbeemd H. 2002. Lipophilicity and other parameters affecting brain penetration. Curr Med Chem. 2(3): 229-240
- Barbour B, Brew H, & Attwell D. 1988. Electrogenic glutamate uptake in glial cells is activated by intracellular potassium. Nature. 335: 433-43
- Blackburn D, Sargsyan S, Monk PN, & Shaw PJ. 2009. Astrocyte function and role in motor neuron disease: a future therapeutic target? Glia. 57(12): 1251-64
- Bolognesi ML and Cavalli A. 2016. Multitarget drug discovery and polypharmacology. Chem Med Chem. 11:1190-1192
- Bondock S, Fadaly W, & Metwally MA. 2010. Synthesis and antimicrobial activity of some new thiazole, thiophene and pyrazole derivatives containing benzothiazole moiety. Eur J Med Chem. 45: 3692–3701.
- Brantley E, Antony S, Kohlhagen G, Meng L, Agama K, Stinson SF, Sausville E, & Pommier Y. 2006. Anti-tumor drug candidate 2-(4-amino-3-methylphenyl)- 5-fluorobenzothiazole induces singlestrand breaks and DNA-protein crosslinks in sensitive MCF-7 breast cancer cells. Cancer Chemother Pharmacol. 58: 62–72
- Cavalli A & Bolognesi ML. 2009. Neglected tropical diseases: multi-target-directed ligands in search for novel lead candidates against *Trypanosoma* and *Leishmania*. J Med Chem. 52: 7339-7359.
- Chan DA & Giaccia AJ. 2007. Hypoxia, gene expression, and metastasis. Cancer Metastasis Rev. 26(2): 333-339
- Christodoulou MS, Colombo F, Passarella D, Ireonimo G, Zuco V, De Cesare M, & Zunino F. 2011. Synthesis and biological evaluation of imidazolo [2,1-

- b]benzothiazole derivatives, as potential p53 inhibitors. *Bioorg Med Chem.* 19: 1649–1657.
- Dechy-Cabaret O, Benoit-Vical F, Robert A, & Meunier B. 2000. Preparation and antimalarial activities of “Trioxaquinines”, new modular molecules with a trioxane skeleton linked to a 4-aminoquinoline. *ChemBioChem.* 1(4): 281-283
- Ehrlich P. 1909.Ueber den jetzigen Stand der Chemotherapie. *Ber Dtsch Chem Ges.* 42:17-47
- Galli R. 2013. The neurosphere assay applied to neural stem cells and cancer stem cells. *Methods Mol Biol.* 986: 267–77.
- Gao Y, Gesenberg C, & Zheng W. 2017. Oral formulations for preclinical studies: principle, design, and development considerations. In: Qiu Y, Chen Y, Zhang GGZ, Yu L, Mantri RV. *Developing Solid Oral Dosage Forms: Pharmaceutical Theory and Practice* (2nd ed.). Cambridge (Massachusetts): Academic Press. pp. 455-495
- Garwood J, Rigato F, Heck N, Faissner A. 2001. Tenascin glycoproteins and the complementary ligand DSD-1-PG/ phosphacan-Structuring the neural extracellular matrix during development and repair. *Restor Neurol Neurosci.* 19:51-64
- Gaspar LE, Fisher BJ, Macdonald DR, Leber DV, Halperin EC, Schold Jr. SC, & Cairncross JG. 1992. Supratentorial malignant glioma: patterns of recurrence and implications for external beam local treatment. *Int. J. Radiat. Oncol.* 24:55-57
- Gautam CS, Saha L. 2008. Fixed dose drug combinations (FDCs): rational or irrational: aview point. *Br J Clin Pharmacol.* 65(5): 795-796
- Gendiya LK, Njar VCO. 2009. Promise and challenges in drug discovery and development of hybrid anticancer drugs. *Expert Opin Drug Discov.* 4(11): 1099-1111
- Giese A, Bjerkvig R, Berens ME, & Westphal M. 2003. Cost of migration: invasion of malignant gliomas and implications for treatment. *J. Clin. Oncol.* 21(8):1624-1636
- Gillis EP, Eastman KJ, Hill MD, Donnelly DJ, and Meanwell NA. 2015. Applications of fluorine in medicinal chemistry. *J. Med. Chem.* 58: 8315-8359

- Hanahan D & Weinberg RA. 2000. The hallmarks of cancer. *Cell*. 100(1): 57-70
- Hansch C & Fujita T. 1964. p - σ - π Analysis. A method for the correlation of biological activity and chemical structure. *J. Am. Chem. Soc.* 86(8): 1616-1626
- Hiyoshi H, Goto N, Tsuchiya M, Iida K, Nakajima Y, Hirata N, Kanda Y, Nagasawa K, & Yanagisawa J. 2014. 2-(4-Hydroxy-3-methoxyphenyl)-benzothiazole suppresses tumor progression and metastatic potential of breast cancer cells by inducing ubiquitin ligase CHIP. *Scientific Reports*. 7:7095
- Hu WP, Chen YK, Liao CC, Yu HS, Tsai YM, Huang SM, Tsai FY, Shen HC, Chang LS, & Wang JJ. 2010. Synthesis, and biological evaluation of 2-(4-aminophenyl) benzothiazole derivatives as photosensitizing agents. *Bioorg Med Chem*. 18: 6197–6207.
- Ishiguro T, Ohata H, Sato A, Yamawaki K, Enomoto T, & Okamoto K. 2017. Tumor-derived spheroids: Relevance to cancer stem cells and clinical applications. *Cancer science*, 108(3), 283–289. doi:10.1111/cas.13155
- Jones G. 2011. The Knoevenagel condensation. *Organic Reactions*, 1. doi: 10.1002/0471264180.02
- Jones Jr. M & Fleming SA. 2010. *Organic chemistry*. 4th ed. New York
- Jonsson G, Hogberg G, & Nilsson T. 1977. Treatment of advanced prostatic carcinoma with estramustine phosphate (Estracyt®). *Scandinavian Journal of Urology and Nephrology*. 11(3): 231-238
- Kodama T, Ikeda E, Okada A, Ohtsuka T, Shimoda M, Shiomi T, Yoshida K, Nakada M, Ohuchi E, & Okada Y. 2004. ADAM12 is selectively overexpressed in human glioblastomas and is associated with glioblastoma cell proliferation and shedding of heparin-binding epidermal growth factor. 165(5):1743-1753
- Koehler FM, Luechinger NA, Ziegler D, Athanassiou EK, Grass RN, Rossi A, Hierold C, Stemmer A, & Stark WJ. 2009. Permanent pattern-resolved adjustment of the surface potential of graphene-like carbon through chemical functionalization. *Angew Chem Int. Ed.* 48:224
- Kok SH, Gambari R, Chui CH, Yuen MC, Lin E, Wong RS, Lau FY, Cheng GY, Lam WS, Chan SH, Lam KH, Cheng CH, Lai PB, Yu MW, Cheung F, Tang JC, Chan AS. Kok SH et al. 2008. Synthesis and anticancer activity of benzothiazole

- containing phthalimide on human carcinoma cell lines. *Bioorg Med Chem.* 16: 3626–3631.
- Langer T & Hoffmann RD. 2006. *Pharmacophores and pharmacophore searches.* John Wiley & Sons
- Mortimer CG, Wells G, Crochard J, Stone EL, Bradshaw TD, Stevens MFG, & Westwell AD. 2005. Antitumor benzothiazoles. 26. 2-(3,4-dimethoxyphenyl)-5-fluorobenzothiazole (GW 610, NSC 721648), a simple fluorinated 2-arylbenzothiazole, shows potent and selective inhibitory activity against lung, colon, and breast cancer cell lines. *J. Med. Chem.* 49(1):179-185
- Mouritsen OG, Jorgensen K. 1998. A new look at lipid membrane structure in relation to drug research. *Pharm Res.* 15:1507-1519
- Nakada M, Nakada S, Demuth T, Tran NL, Hoelzinger DB, & Berens ME. 2007. Molecular targets of glioma invasion. *Cell Mol Life Sci.* 64:458-478
- Nakada M, Okada Y, & Yamashita J. 2003. The role of matrix metalloproteinase in glioma invasion. *Front. Biosci.* 8:e261-e269
- Novak U. 2004. ADAM proteins in the brain. *J Clin Neurosci.* 11(3): 227-35
- Ogier C, Bernard A, Chollet AM, LE Diguardher T, Hanessian S, Charton G, Khrestchatisky M, & Rivera S. 2006. Matrix metalloproteinase-2 (MMP-2) regulates astrocyte motility in connection with the actin cytoskeleton and integrins. *Glia.* 54(4): 272-84
- Pajouhesh H & Lenz GR. 2005. Medicinal chemical properties of successful central nervous system drugs. *NeuroRx.* 2(4): 541-553
- Panja SK, Dwivedi N, & Saha S. 2015. First report of the application of simple molecular complexes as organo-catalysts for Knoevenagel condensation. *Royal Society of Chemistry.* 5:65526-65531
- Piepmeier JM, Keefe DL, Weinstein MA, Yoshida D, Zielinski J, Lin TT, Chen Z, & Naftolin F. 1993. Estramustine and estrone analogs rapidly and reversibly inhibits deoxyribonucleic acid synthesis and alter morphology in cultured human glioblastoma cells. *Neurosurgery.* 32(3): 422-431
- Pike VW. 2009. PET radiotracers: crossing the blood-brain barrier and surviving metabolism. *Trends Pharmacol Sci.* 30:431-40

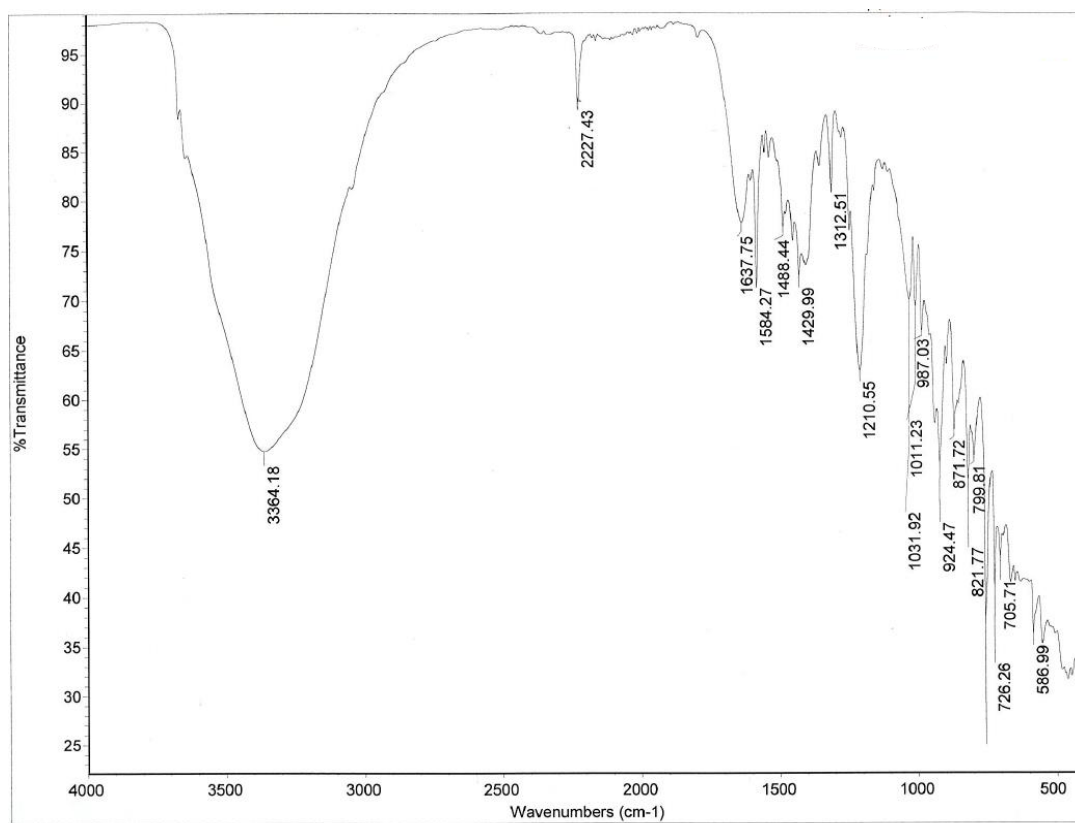
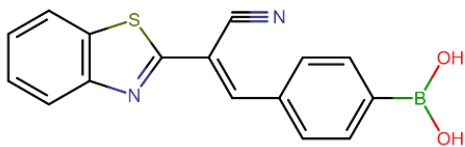
- Ponta H, Sherman L, & Herrlich PA. 2003. CD44: from adhesion molecules to signaling regulators. *Nature Rev. Mol. Cell. Biol.* 4:33-45
- Rao PS & Venkataratnam RV. 1991. Chloride as a new catalyst for knoevenagel condensation. *Tetrahedron Letters.* 32(41): 5821-5822
- Rao JS, Yamamoto M, Mohaman S, Gokslan ZL, Fuller GN, Stetler-Stevenson WG, Rao VH, Liotta LA, Nicolson GL, & Sawaya RE. 1996. Expression and localization of 92 kDa type IV collagenase/gelatinase B (MMP-9) in human gliomas. *Clin. Exp. Metastasis.* 14(1):12-8
- Saini MS, Kumar A, Dwivedi J, & Singh R. 2013. A review: biological significances of the heterocyclic compounds. *Int J Pharma Sci Res.* 4(3): 66-77
- Sawaya RE, Yamamoto M, Gokaslan ZL, Wang SW, Mohanam S, Fuller GN, McCutcheon IE, Stetler-Stevenson WG, Nicolson GL, & Rao JS. 1996. Expression and localization of 72 kDa type IV collagenase (MMP-2) in human malignant gliomas in vivo. *Clin. Exp. Metastasis.* 14(1):35-42
- Schneider EM, Zeltner M, Kranzlin N, Grass RN, & Stark WJ. 2015. Base-free Knoevenagel condensation catalyzed by copper metal surfaces. *Chem Commun.* 51:10695-10698
- Shah P & Westwell AD. 2007. The role of fluorine in medicinal chemistry. *Journal of Enzyme Inhibition and Medicinal Chemistry.* 22(5): 527-540
- Simard M & Nedergaard M. 2004. The neurobiology of glia in the context of water and ion homeostasis. *Neuroscience.* 129(4): 877-96
- Singh M & Singh SK. 2014. Benzothiazoles: how relevant in cancer drug design strategy? *Anticancer Agents Med Chem.* 14(1): 127-46
- Takamune Y, Ikebe T, Nagano O, Nakayama H, Ota K, Obayashi T, Saya H, & Shinohara M. 2007. ADAM-17 associated with CD44 cleavage and metastasis in oral squamous cell carcinoma. *Virchows. Arch.* 450:169-177
- Trippier PC & McGuigan C. 2010. Boronic acids in medicinal chemistry: anticancer, antibacterial and antiviral applications. *Med Chem Comm.* 1:183-198
- Tzanopoulou SL, Sagnou M, Paravatou-Petsotas M, Gourni E, Loudos G, Xanthopoulos S, Lafkas D, Kiaris H, Varvarigou A, Pirmettis IC, Papadopoulos M, & Pelecanou M. 2010. Evaluation of Re and (99m)Tc complexes of 2-(4'-

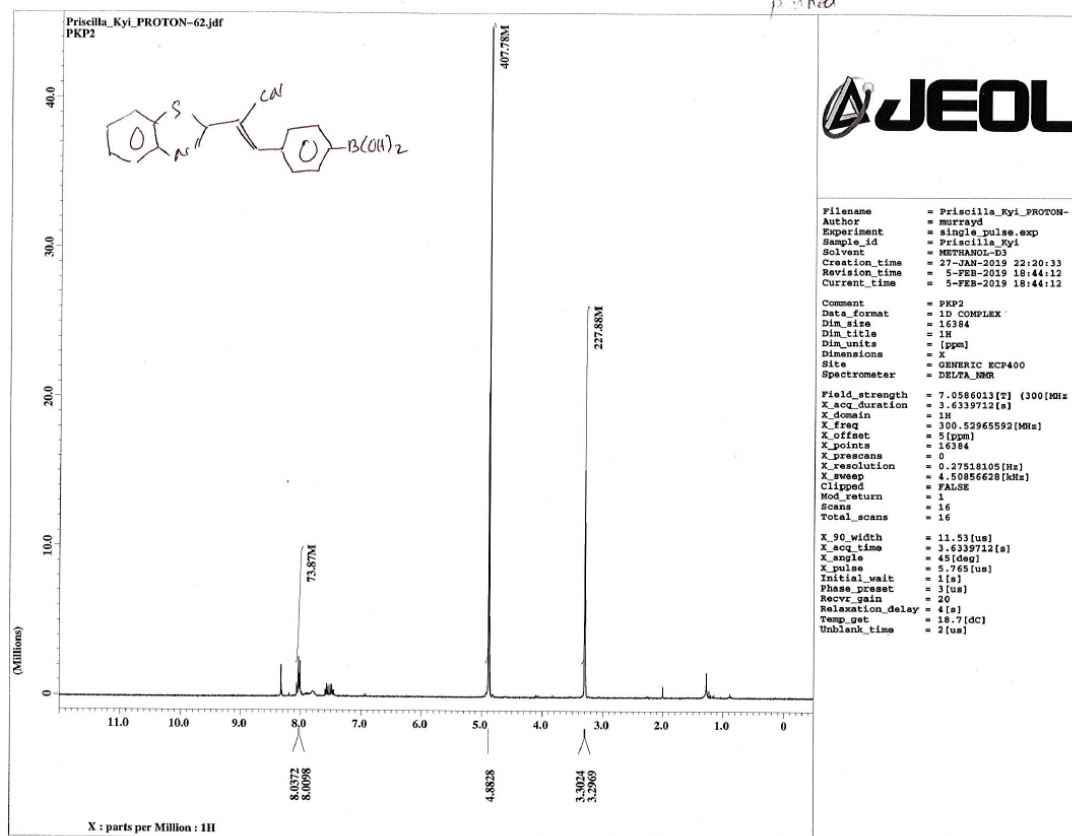
- aminophenyl)benzothiazole as potential breast cancer radiopharmaceuticals. *J Med Chem.* 53: 4633– 4641.
- Upadhyay RK. 2014. Drug delivery systems, CNS protection, and the blood-brain barrier. *BioMed Res Int.* 2014:e869269
- Veber DF, Johnson SR, Cheng HY, Smith BR, Ward KW, & Kopple KD. 2002. Molecular properties that influence the oral bioavailability of drug candidates. *J Med Chem.* 45(12): 2615-2623
- Verhoeff JJC, van Tellingen O, Claes A, Stapler LJA, van Linde ME, Richel DJ, Leeders WPJ, & van Furth WR. 2009. Concerns about anti-angiogenic treatment in patients with glioblastoma multiforme. *BMC Cancer.* 9:444
- Vicini P, Crasci L, Incerti M, Ronsisvalle S, Venera C, & Panico AM. 2011. Benzisothiazolyiminothiazolidin-4-ones with chondroprotective properties: searching for potent and selective inhibitors of MMP-13. *ChemMedChem.* 6: 1199–1202.
- Wang Z, Shi XH, Wang J, Zhou T, Xu YZ, Huang TT, Li YF, Zhao YL, Yang L, Yang SY, Yu LT, & Wei YQ. 2011. Synthesis, structure-activity relationships and preliminary antitumor evaluation of benzothiazole-2-thiol derivatives as novel apoptosis inducers. *Bioorg. Med. Chem. Lett.* 21(4):1097-101
- Wen PY & Kesari S. 2008. Malignant glioma in adults. *N. Engl. J. Med.* 359:492-507
- Winiwarter S, Ridderstorm M, Ungell AL, Andersson TB, & Zamora I. 2007. Use of Molecular Descriptors for Absorption, Distribution, Metabolism, and Excretion Predictions. In: *comprehensive medicinal chemistry II* (anonymous), Tayler JB, Triggler DJ. London: Elsevier Ltd. pp. 531-554
- Yang W, Gao X, & Wang B. 2003. Boronic acid compounds as potential pharmaceutical agents. *Med Res Rev.* 23(3): 36-68
- Zhao YH, Abraham MH, Le J, Hersey H, Luscombe CN, Beck G, Sherborne B, & Cooper I. 2002. Rate-Limited Steps of Human Oral Absorption and QSAR Studies. *Pharm Res.* 19(10): 1446-1457
- Zimmermann GR, Lehar J, & Keith CT. 2007. Multi-target therapeutics: when the whole is greater than the sum of the parts. *Drug Discovery Today.* 12(1-2): 34-42

APPENDIX I

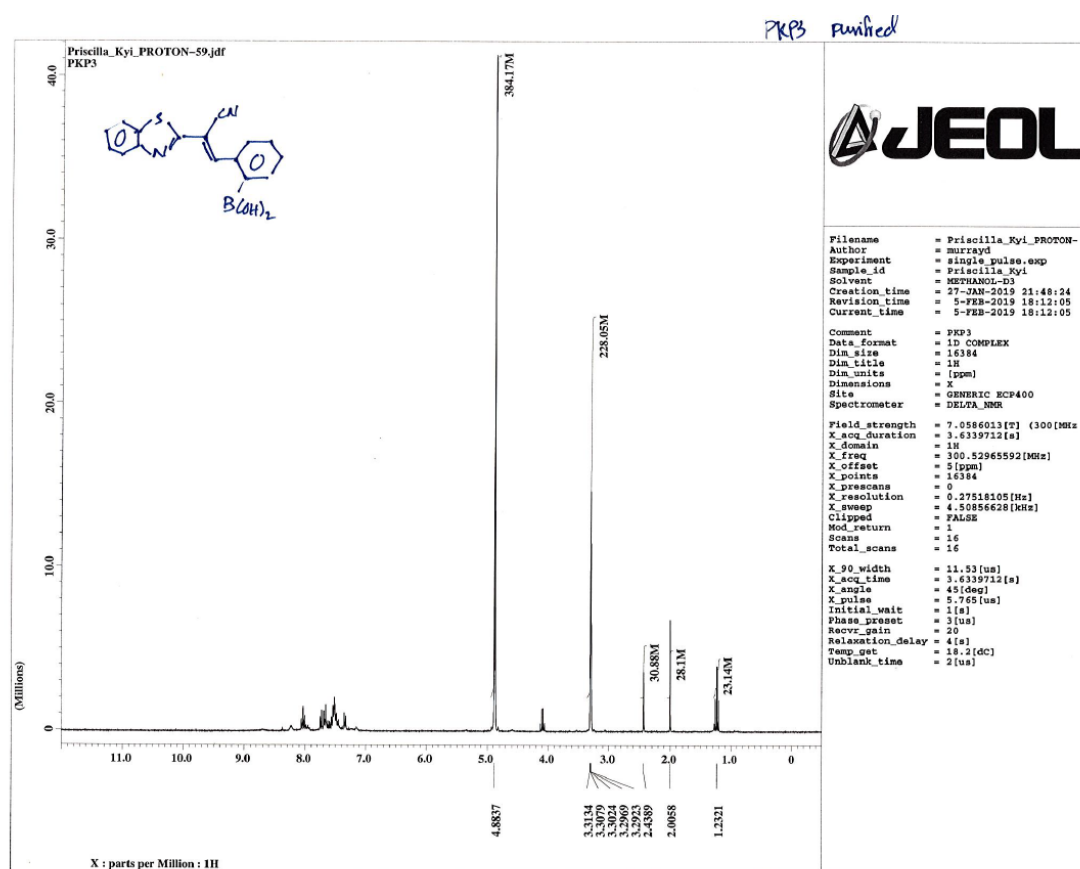
SPECTRAL DATA OF SYNTHESIZED COMPOUNDS

PKP2

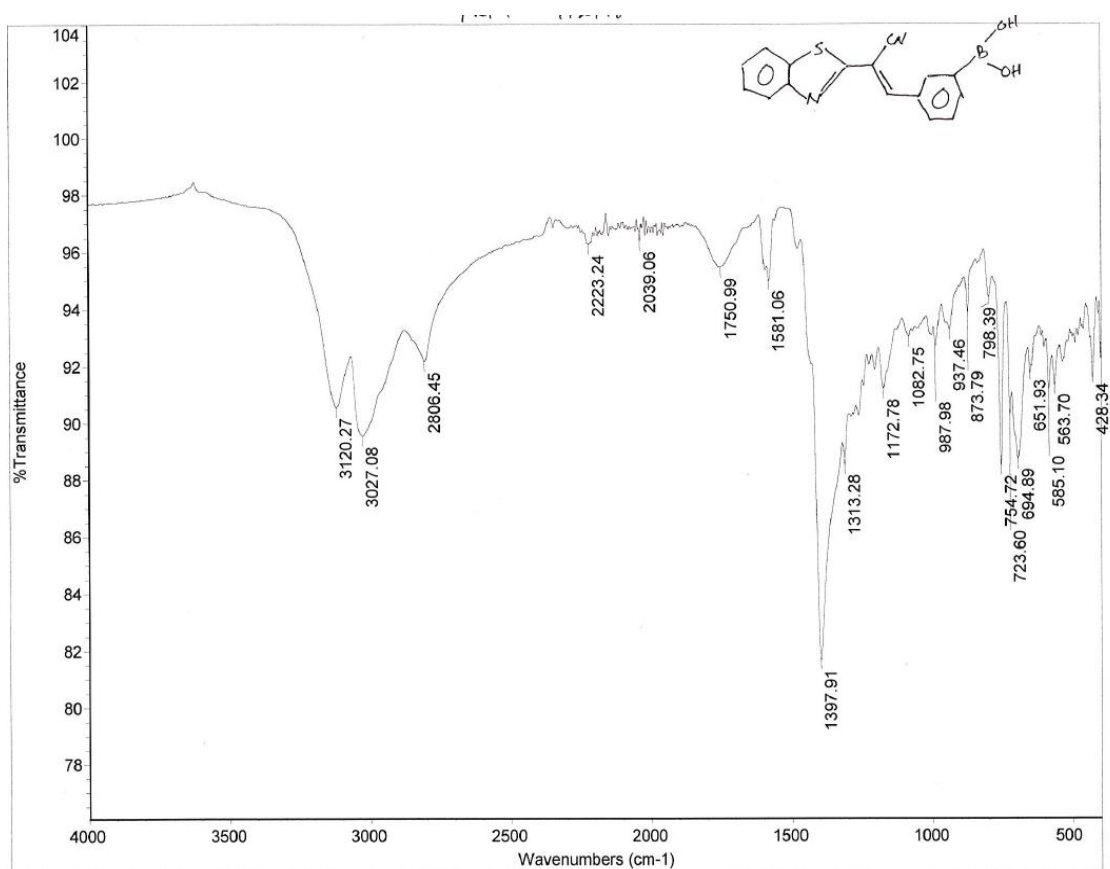
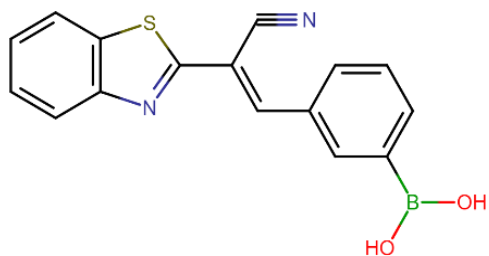


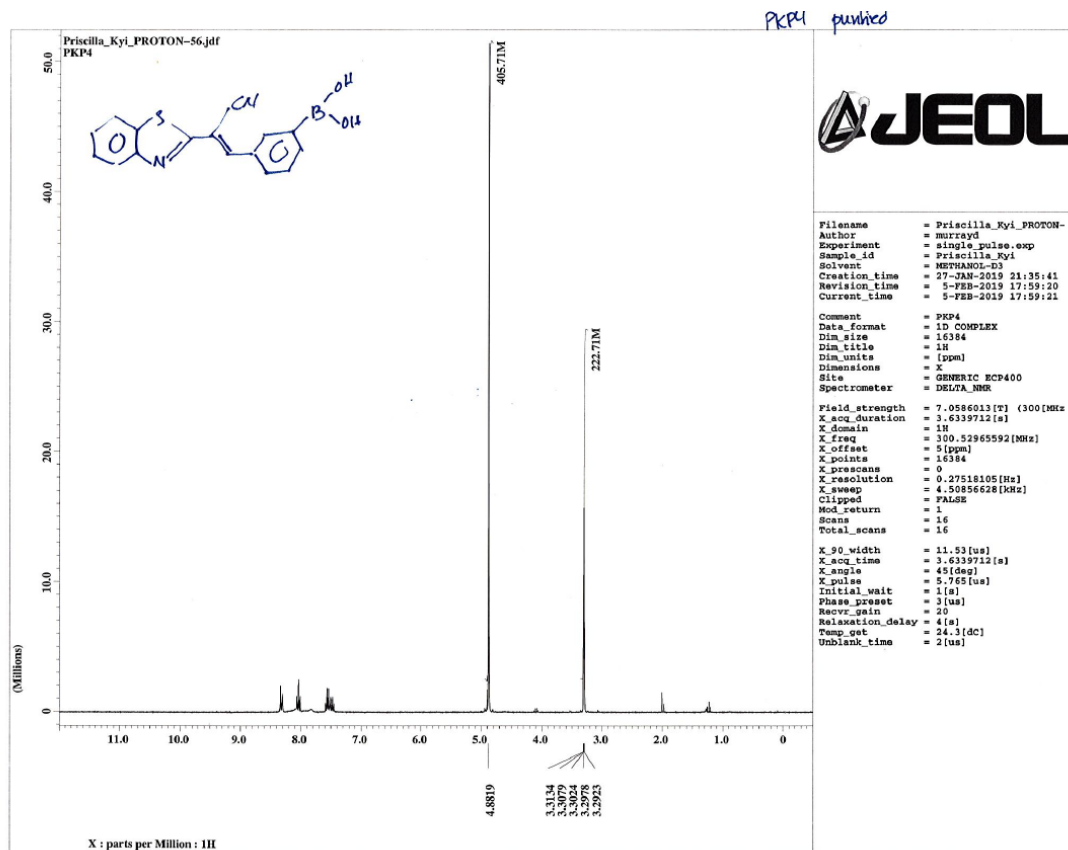


N#CC=C(c1ccc(cc1)C(=O)O)C2=NC3=CC=CC=C3S2

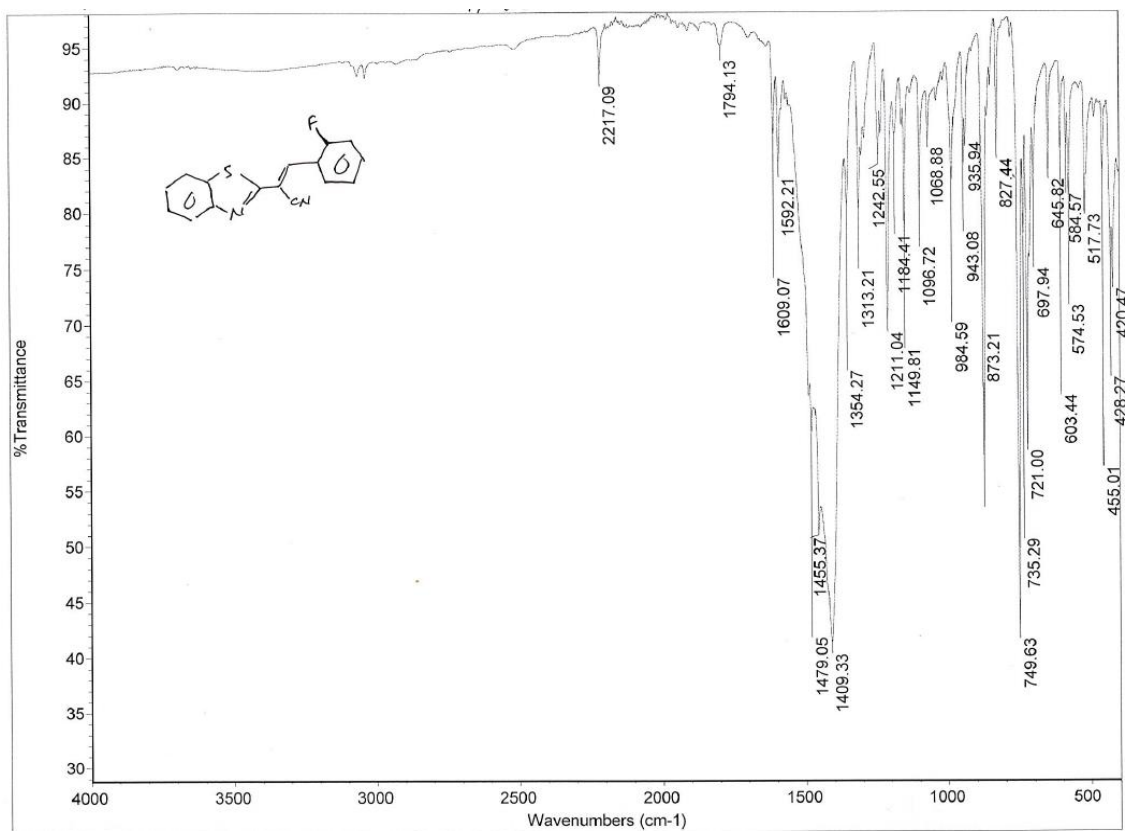
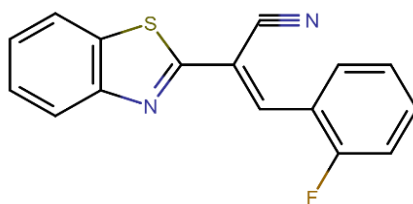


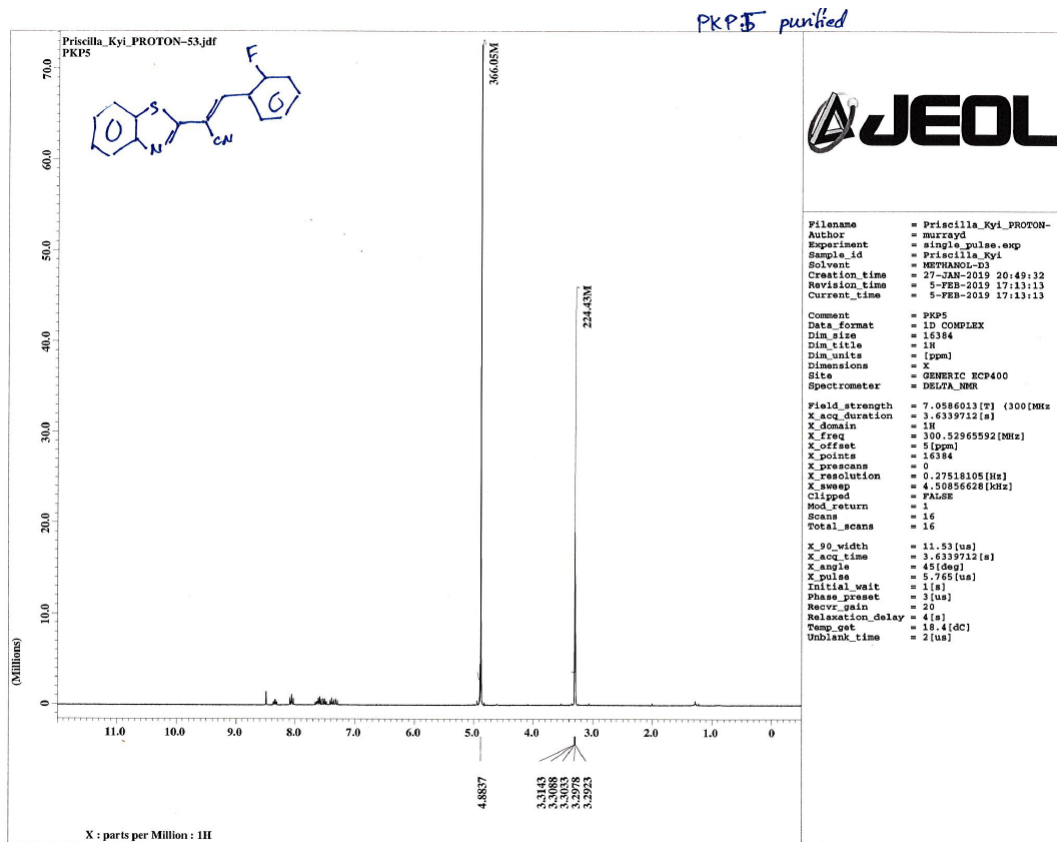
PKP4



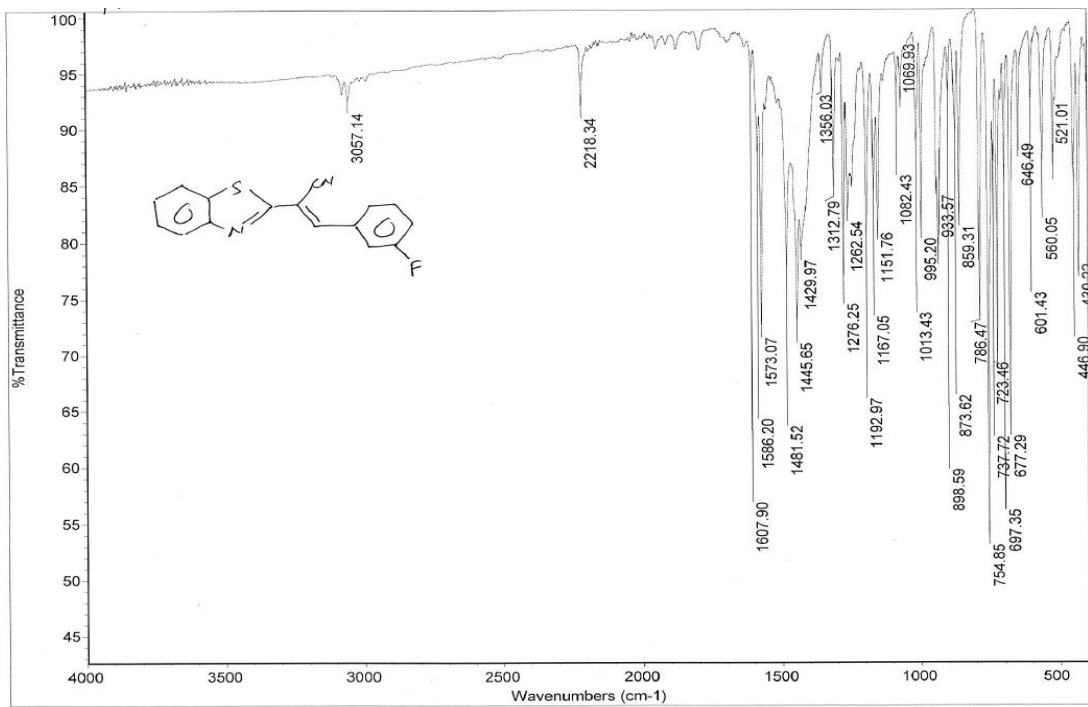
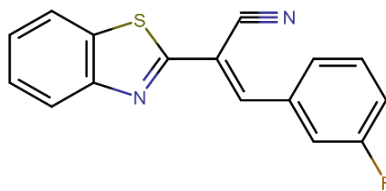


PKP5

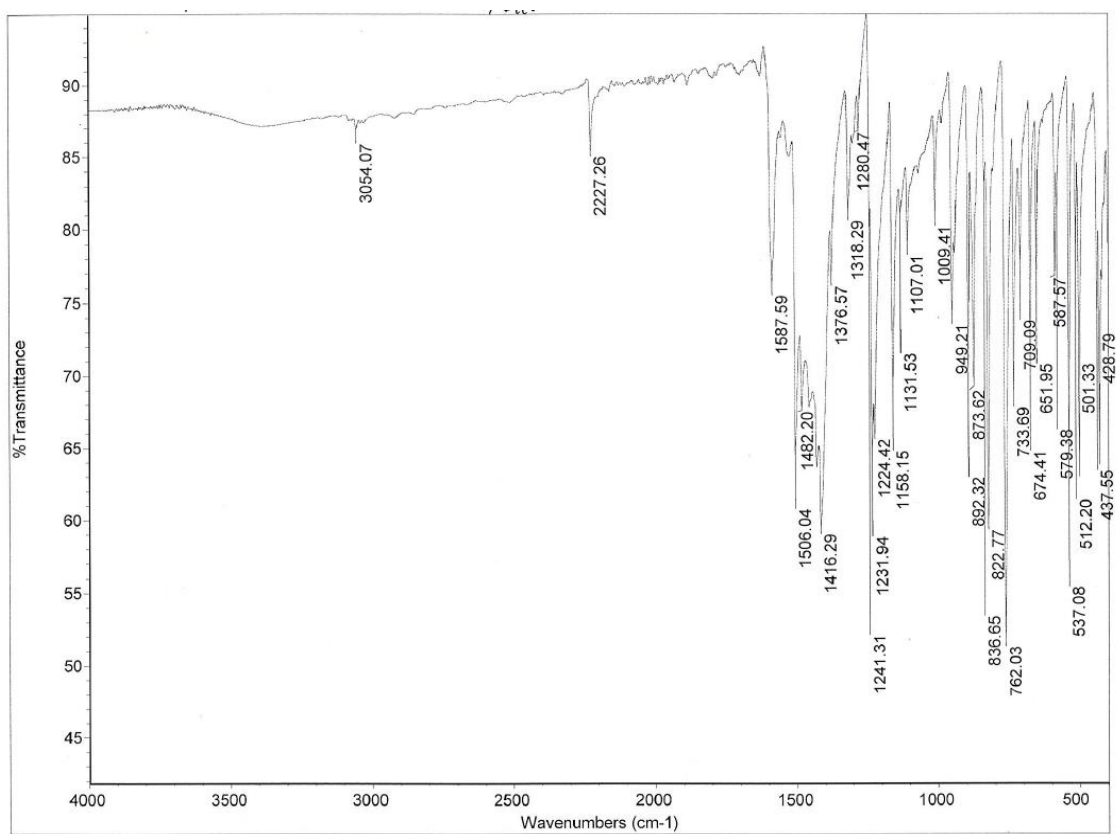
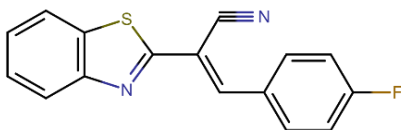


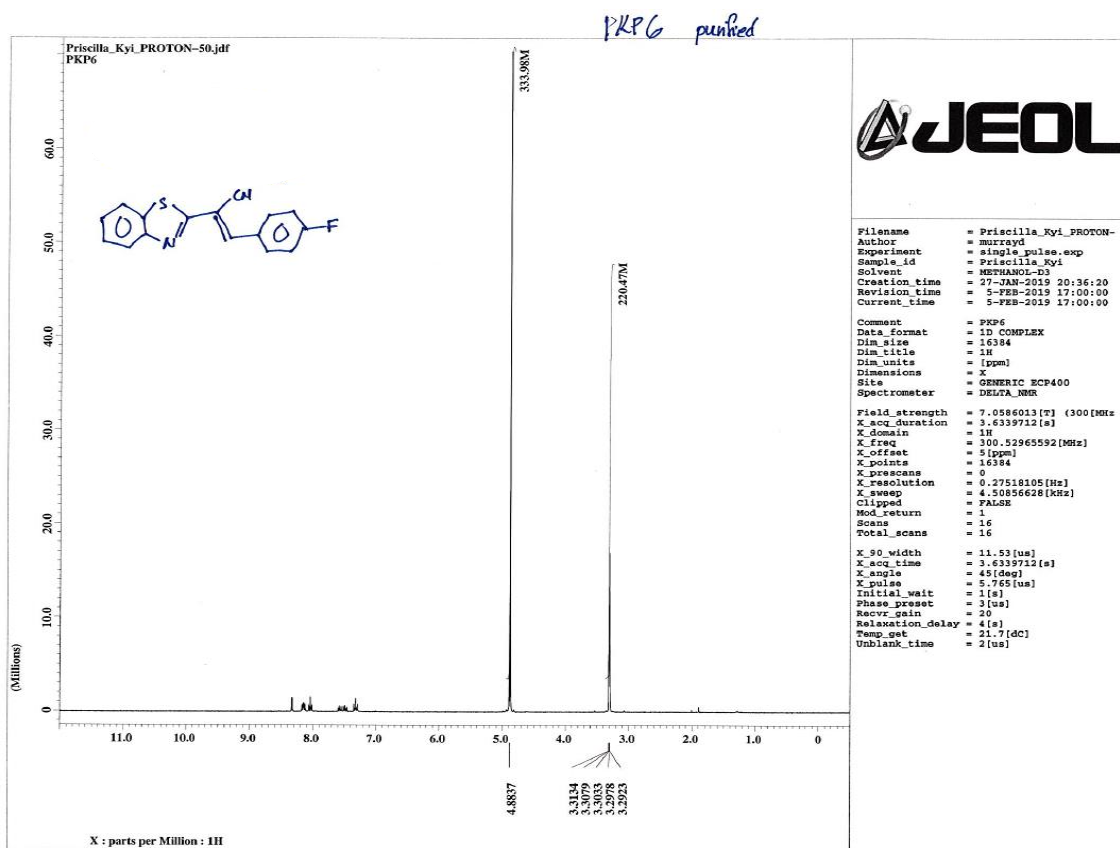


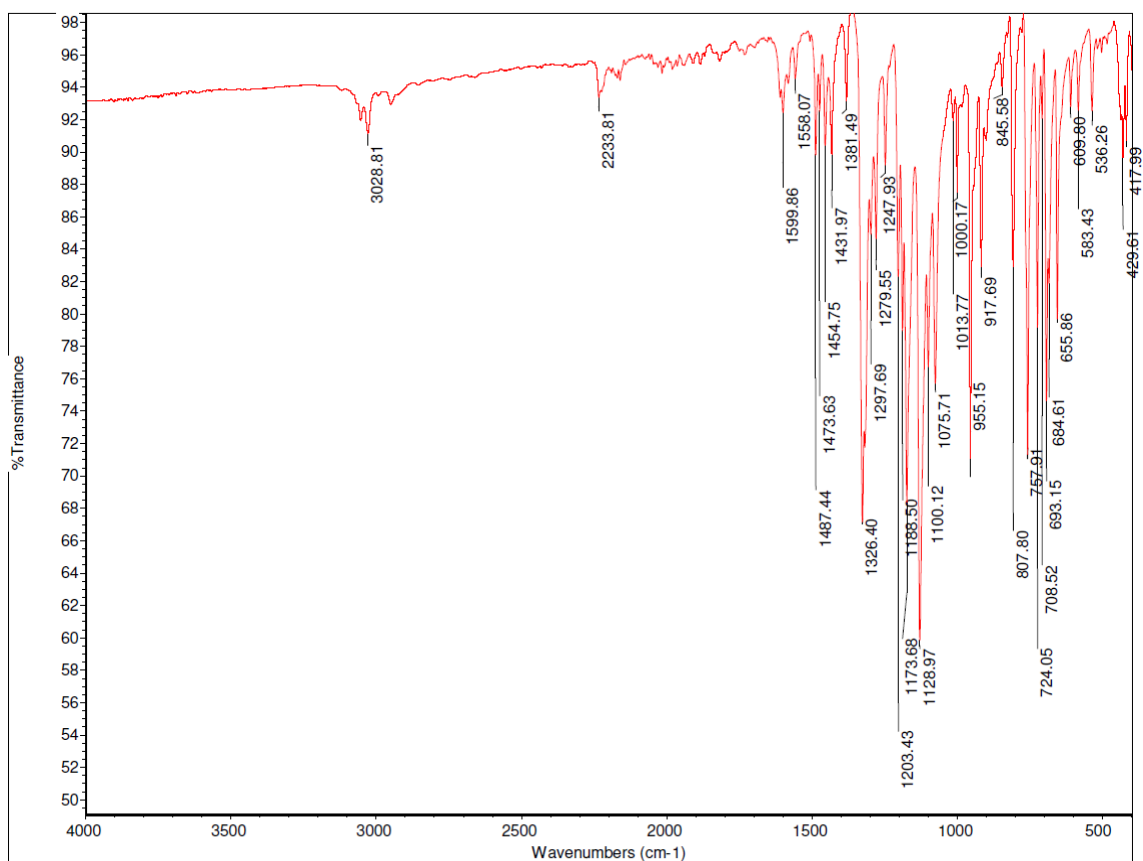
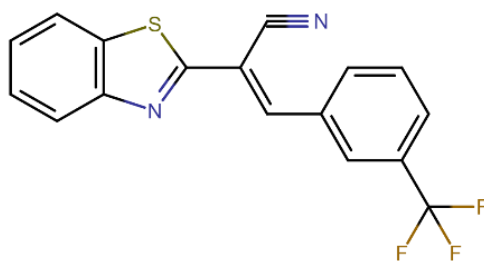
PKP7

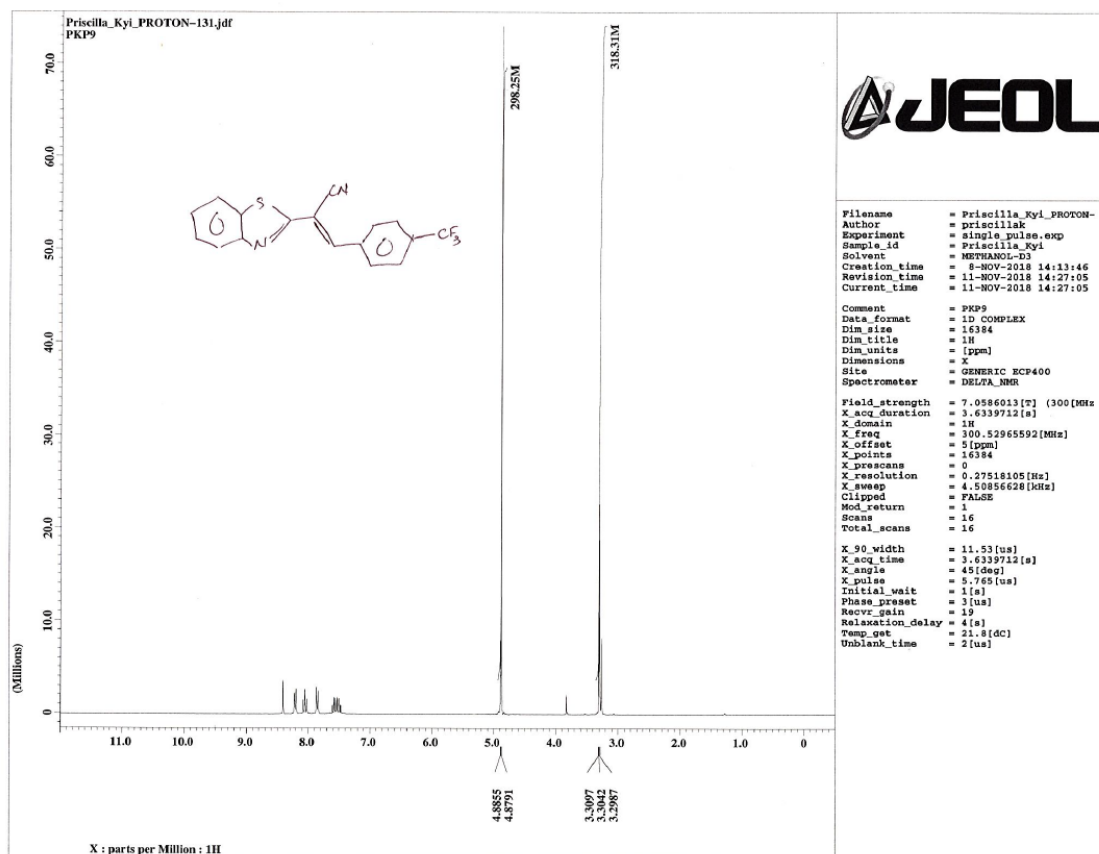


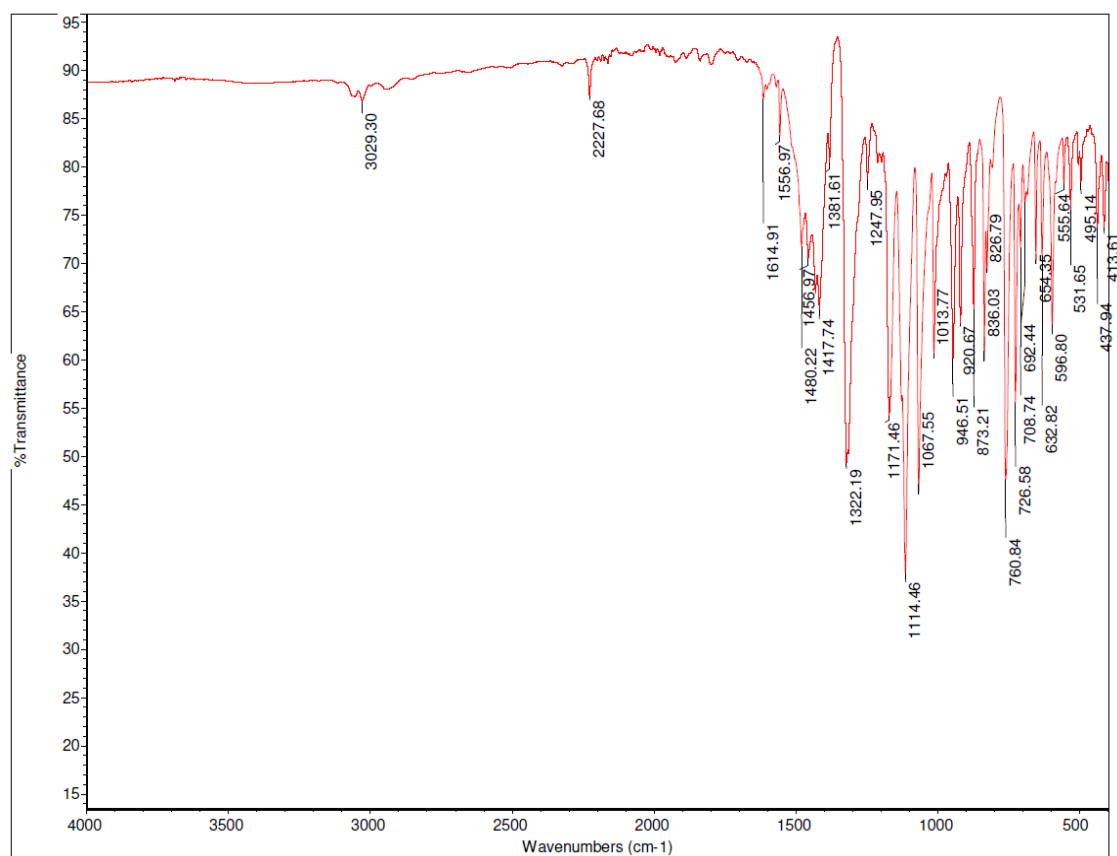
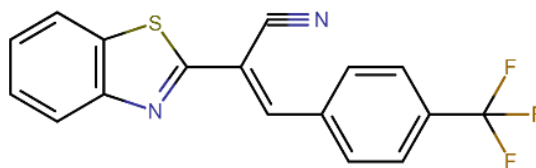
PKP6

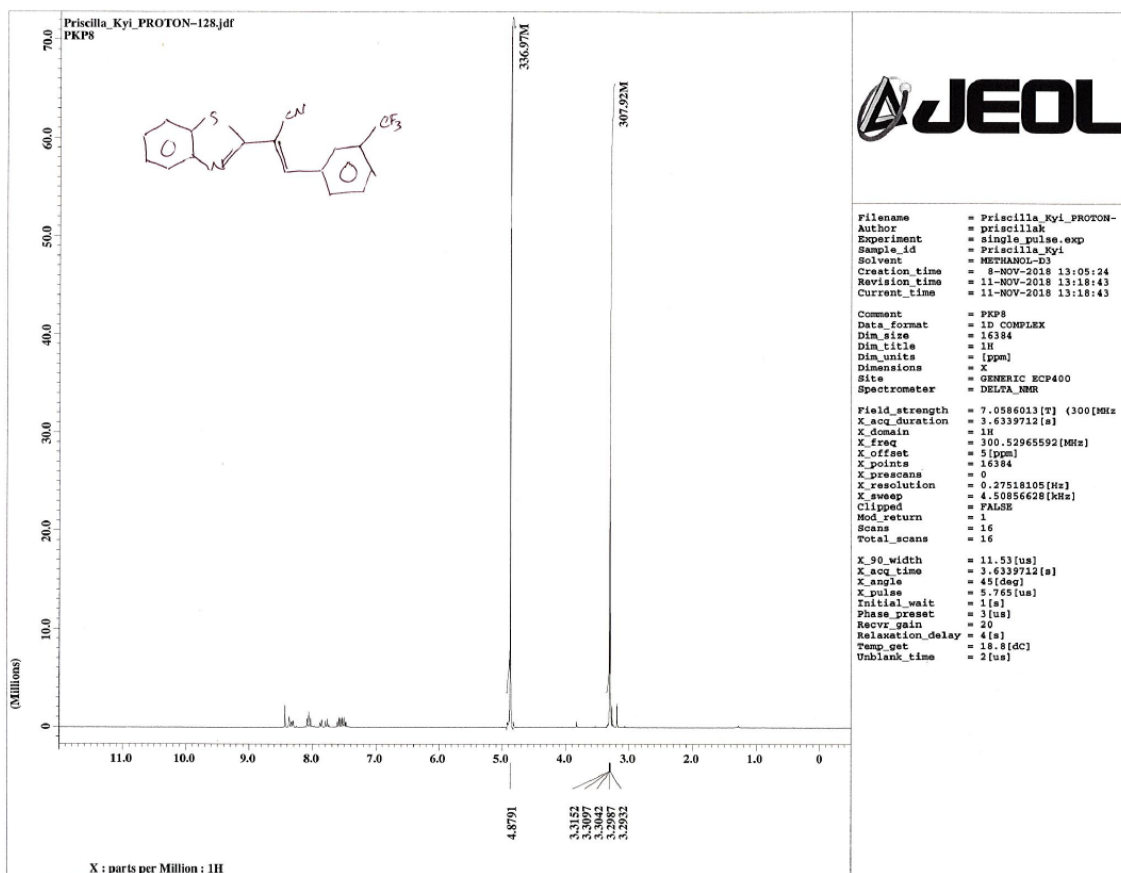


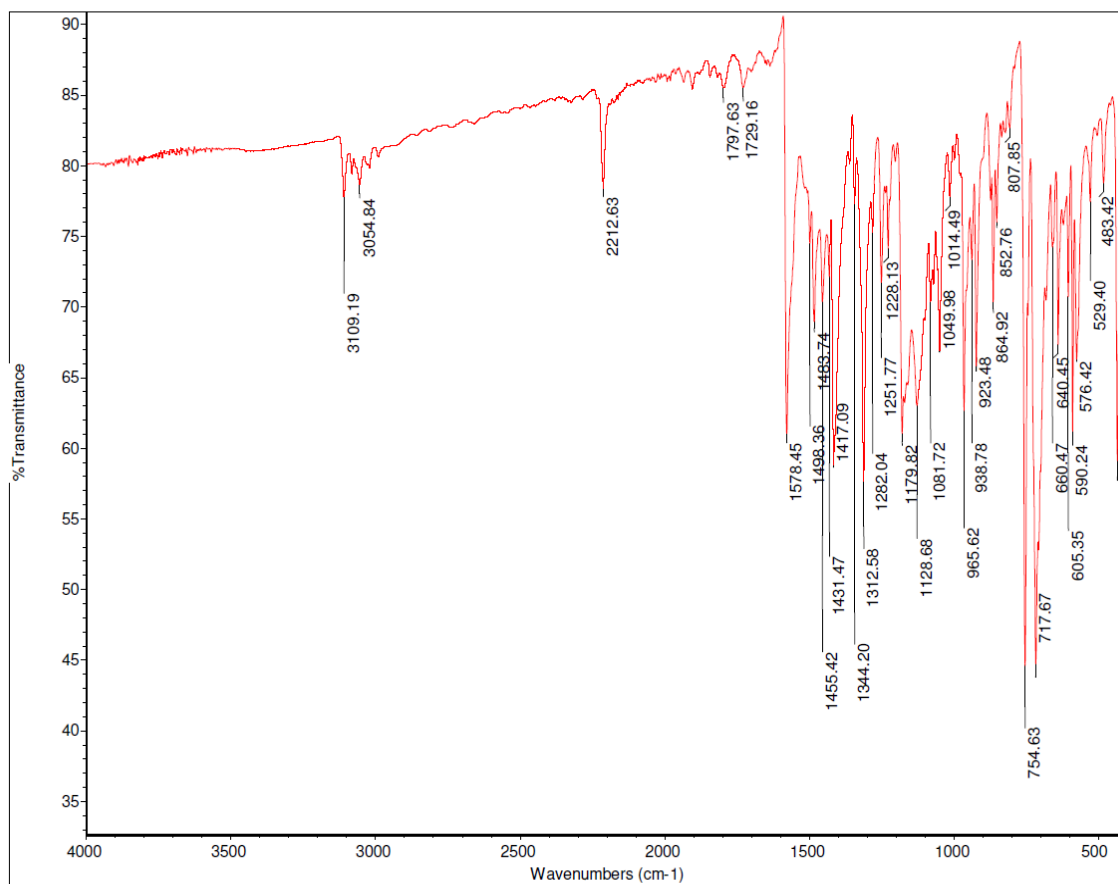
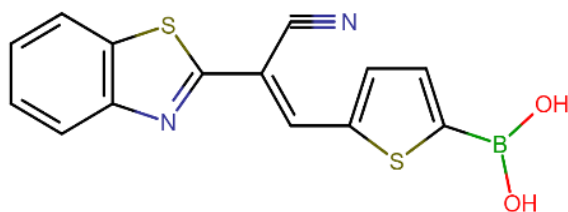


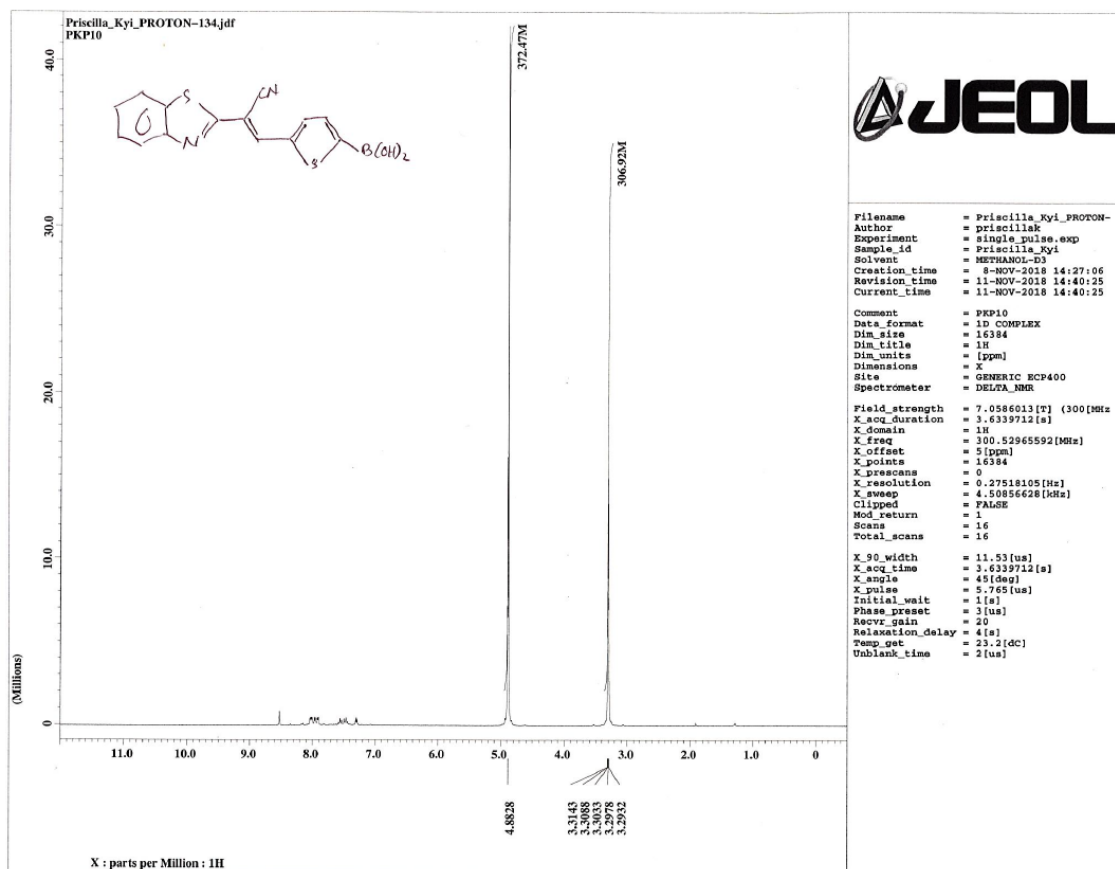


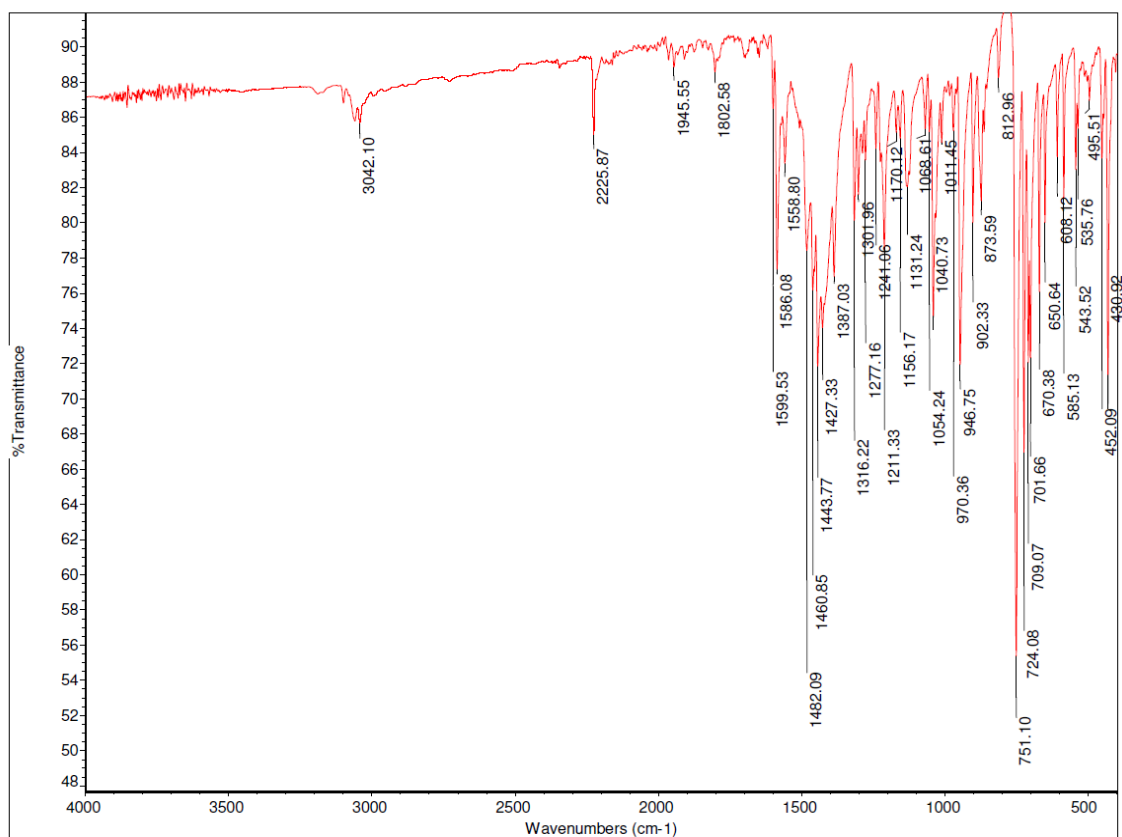
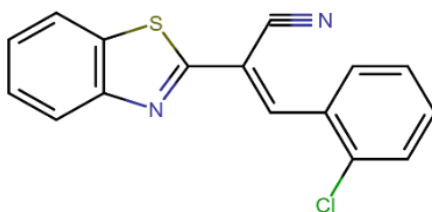


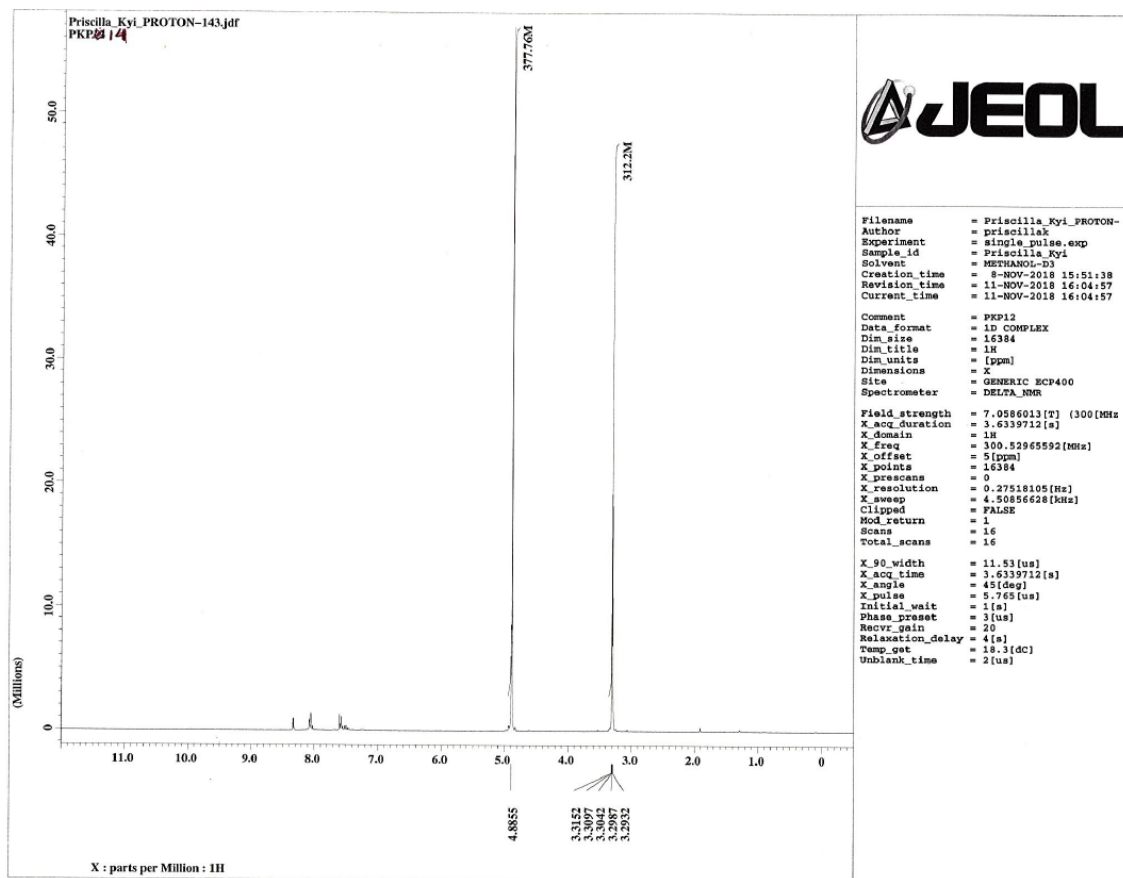


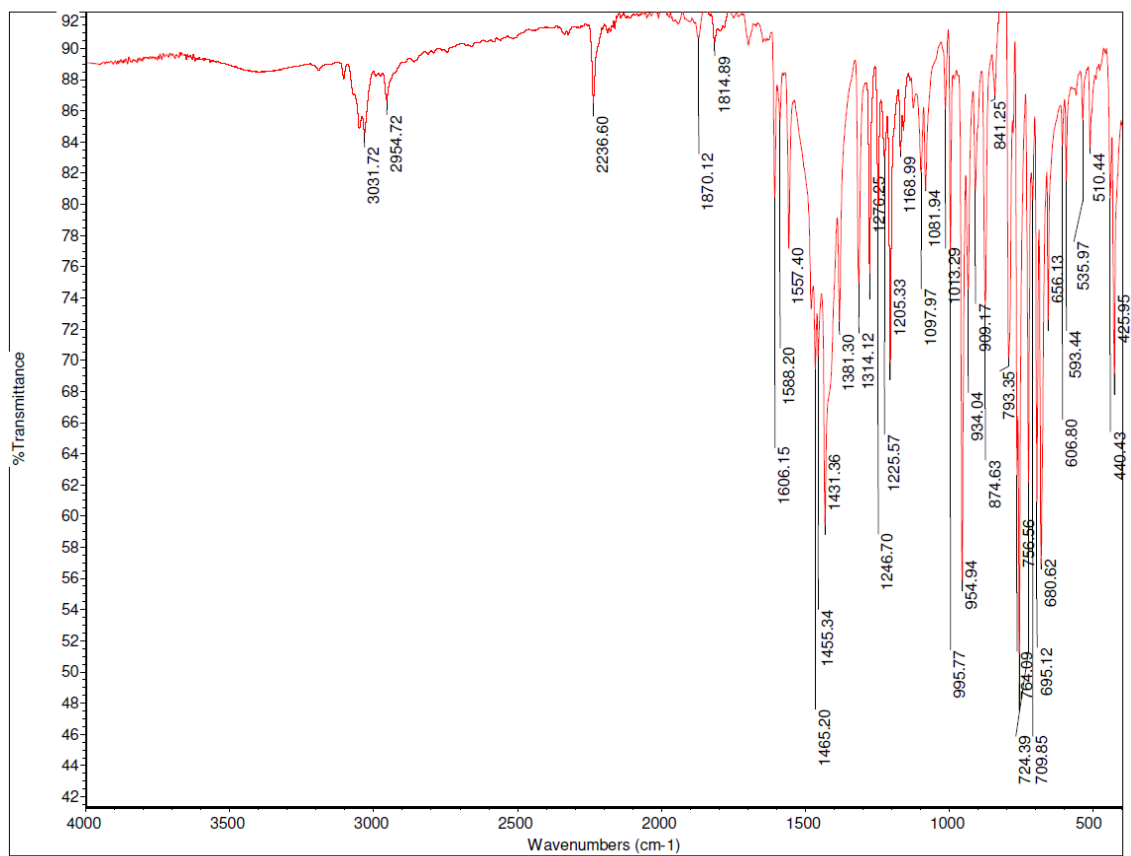
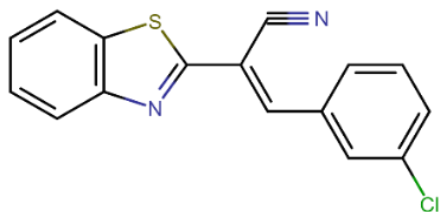


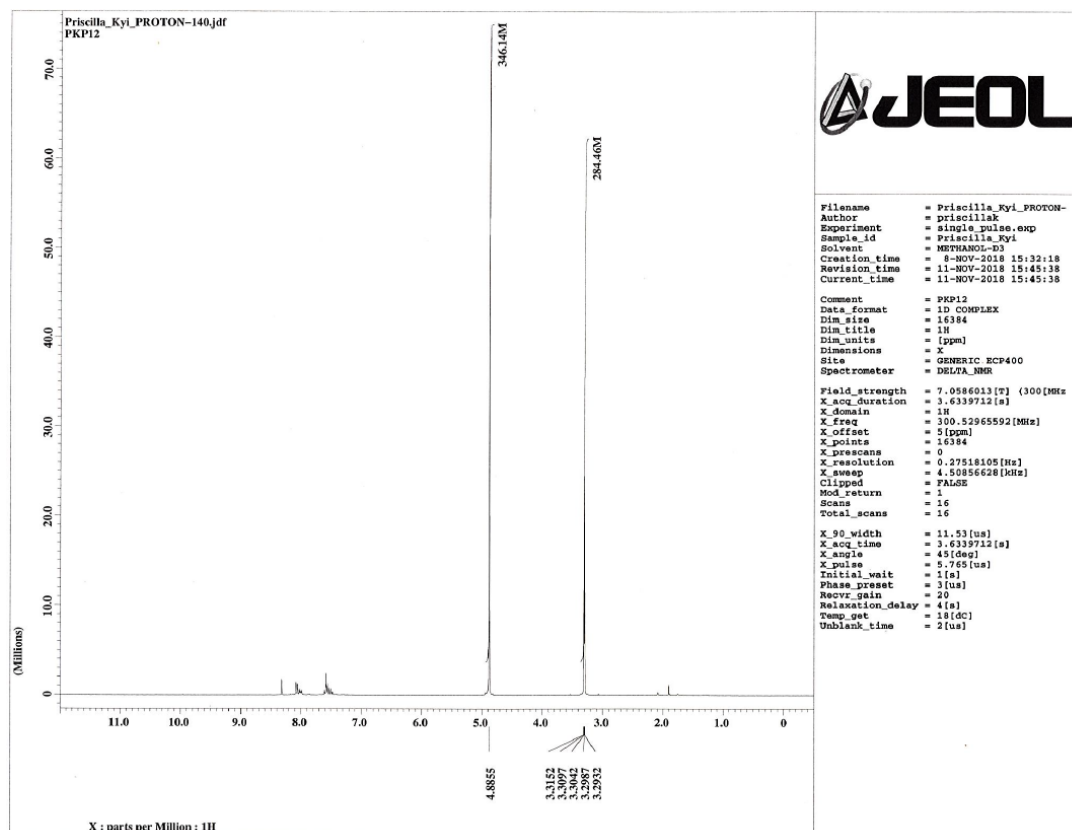


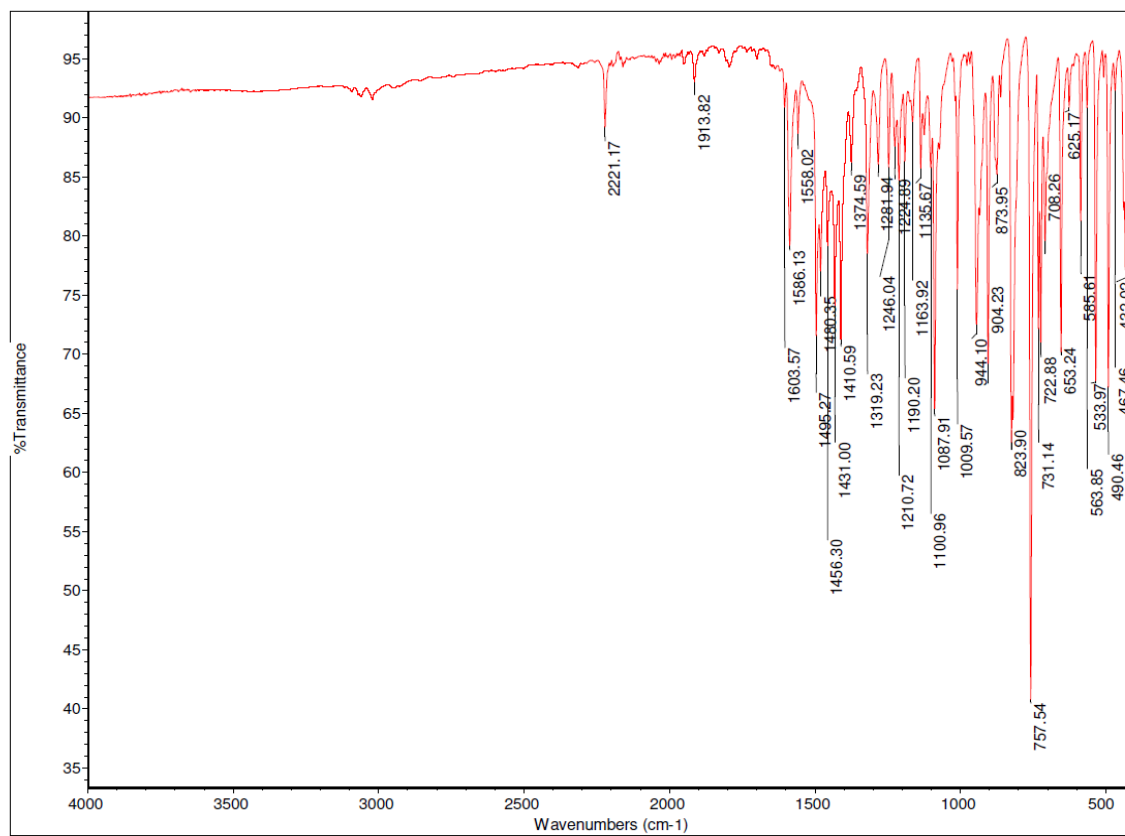
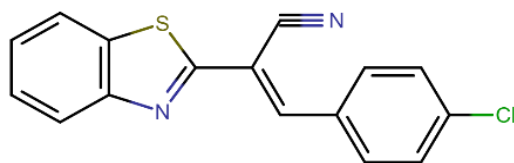


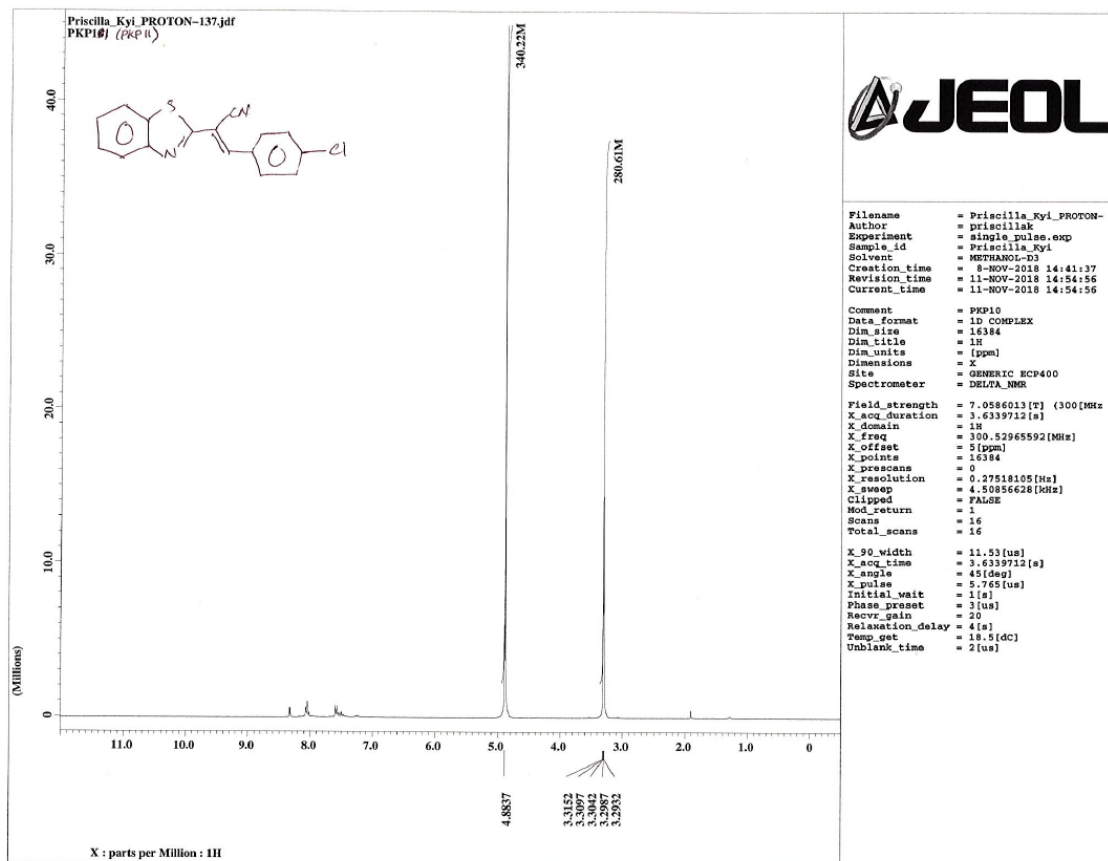


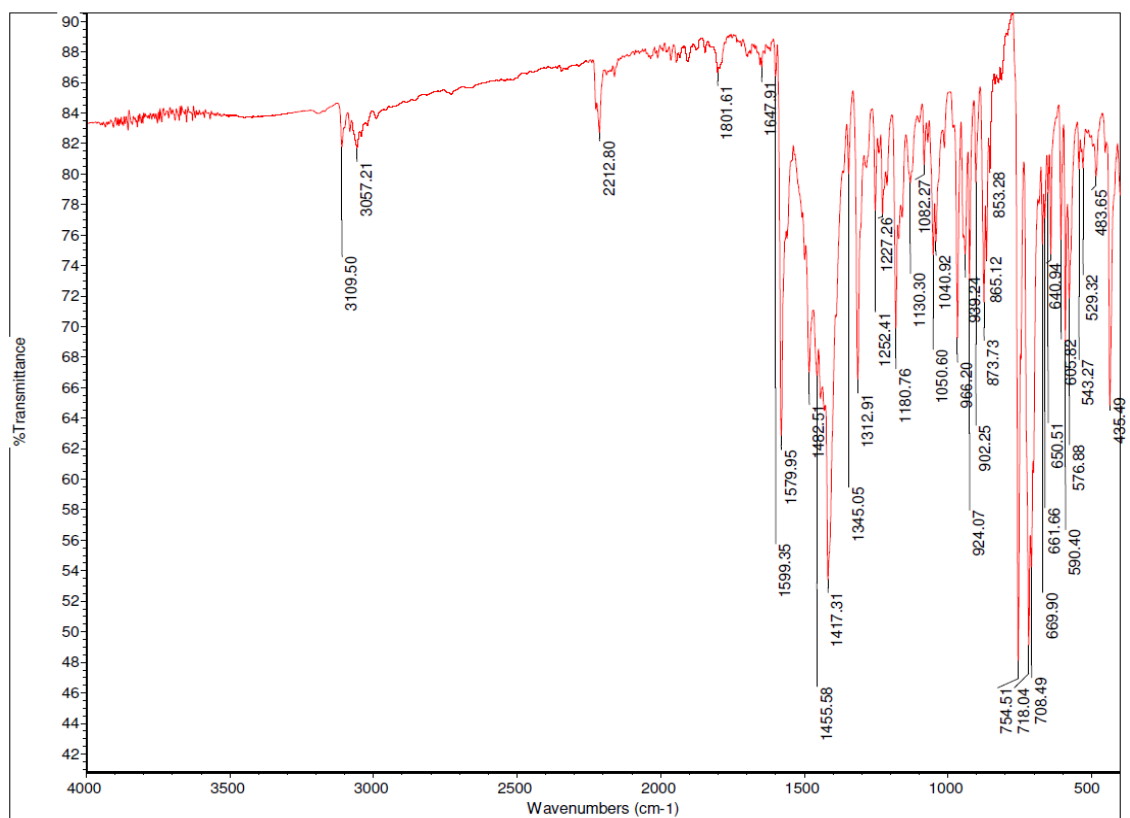
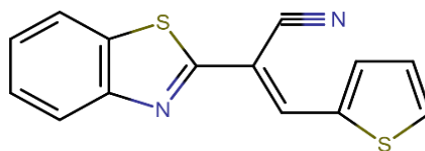


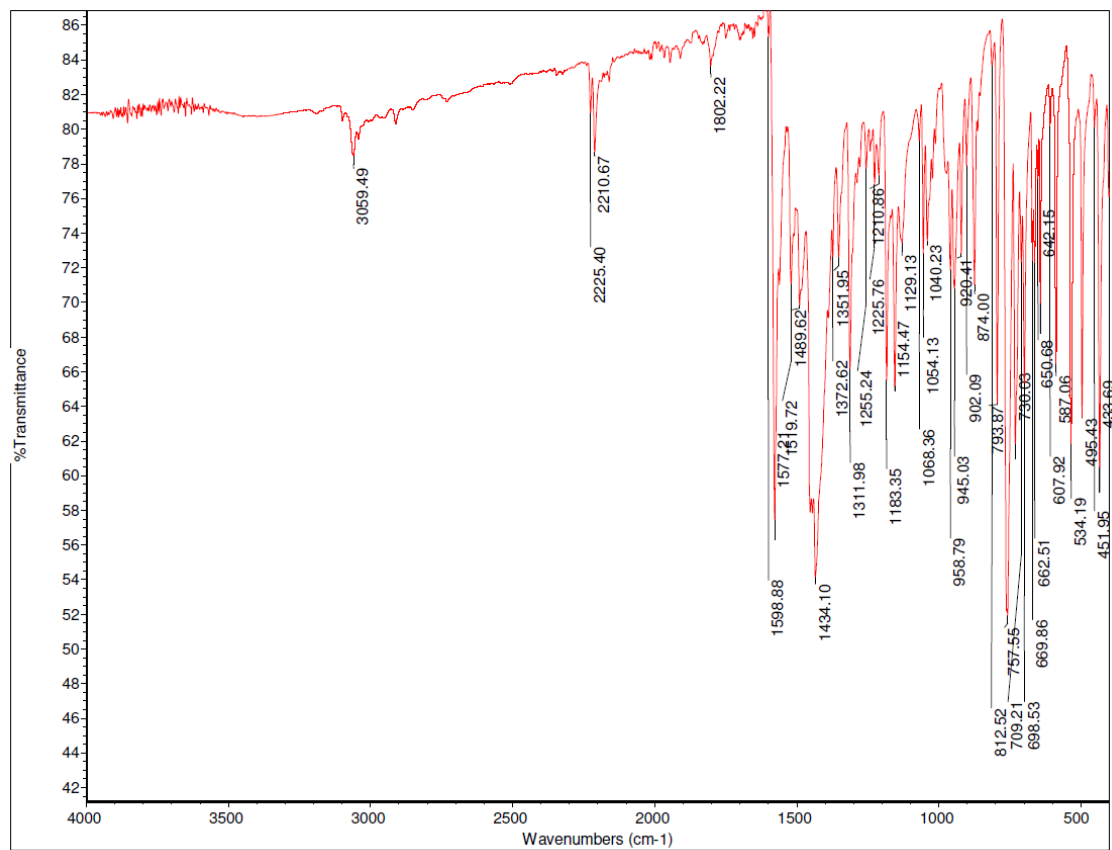
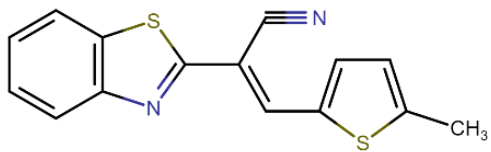


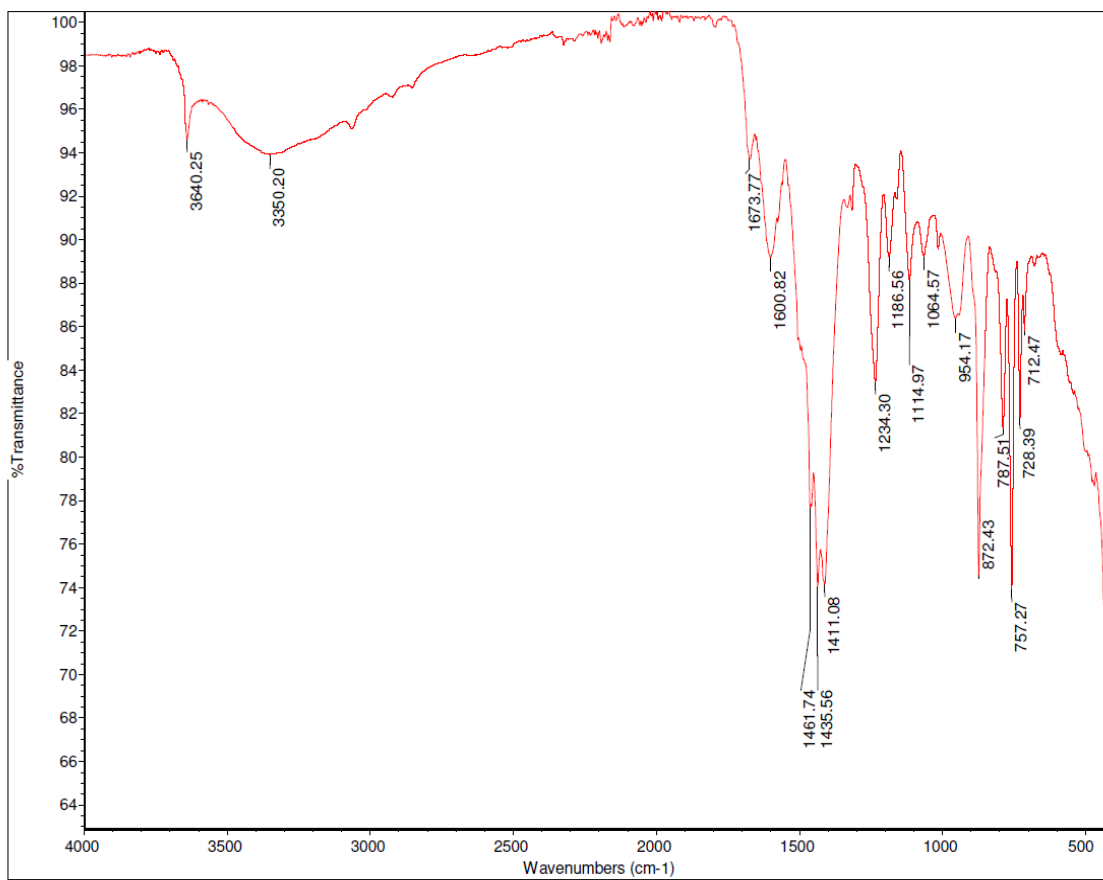
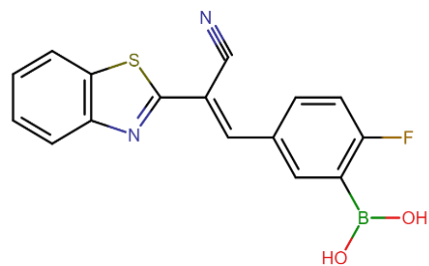


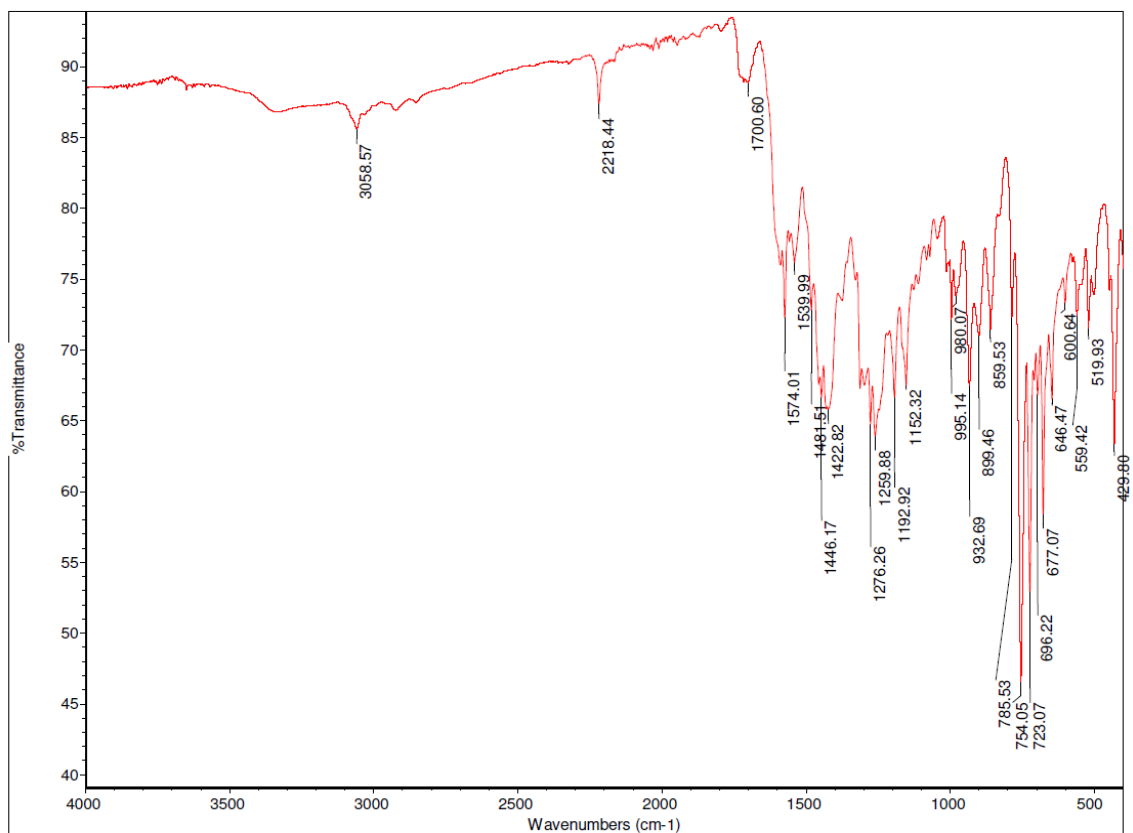
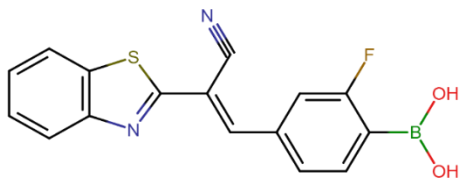


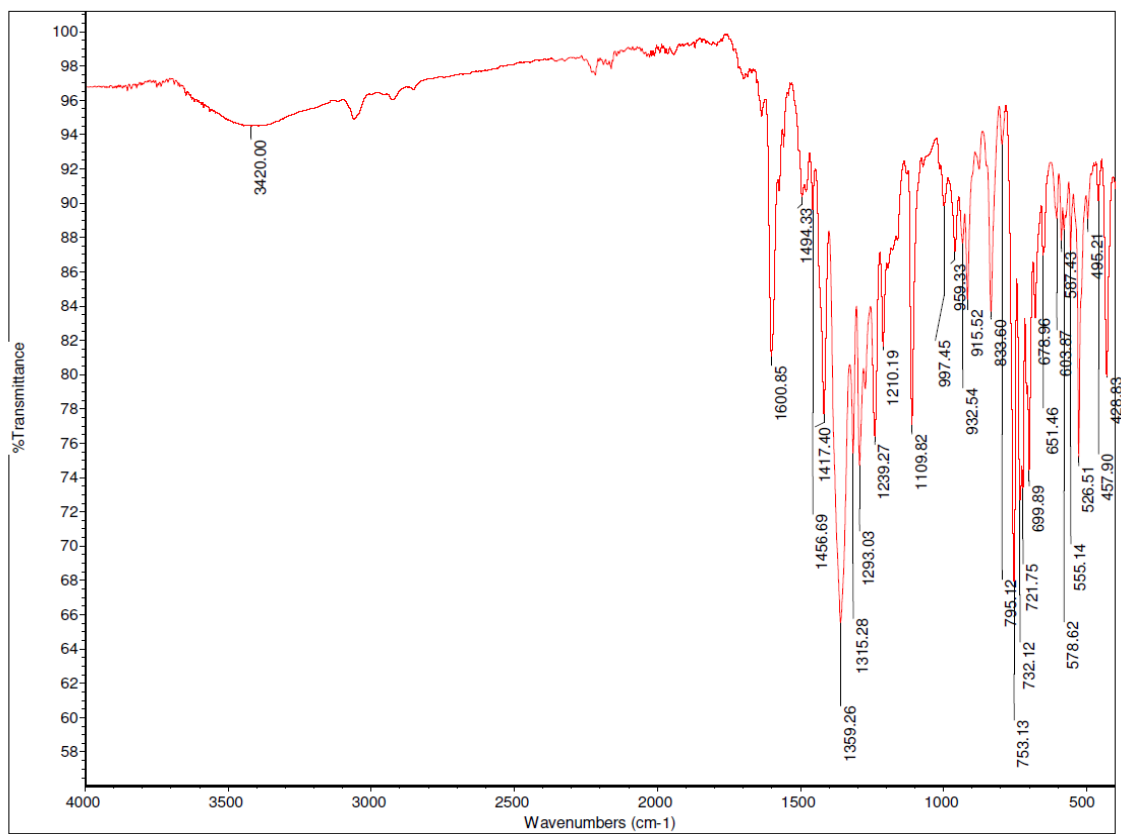
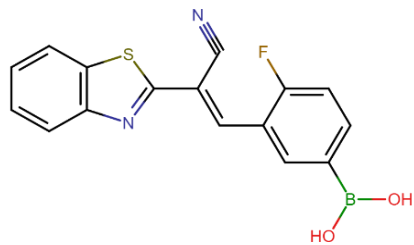


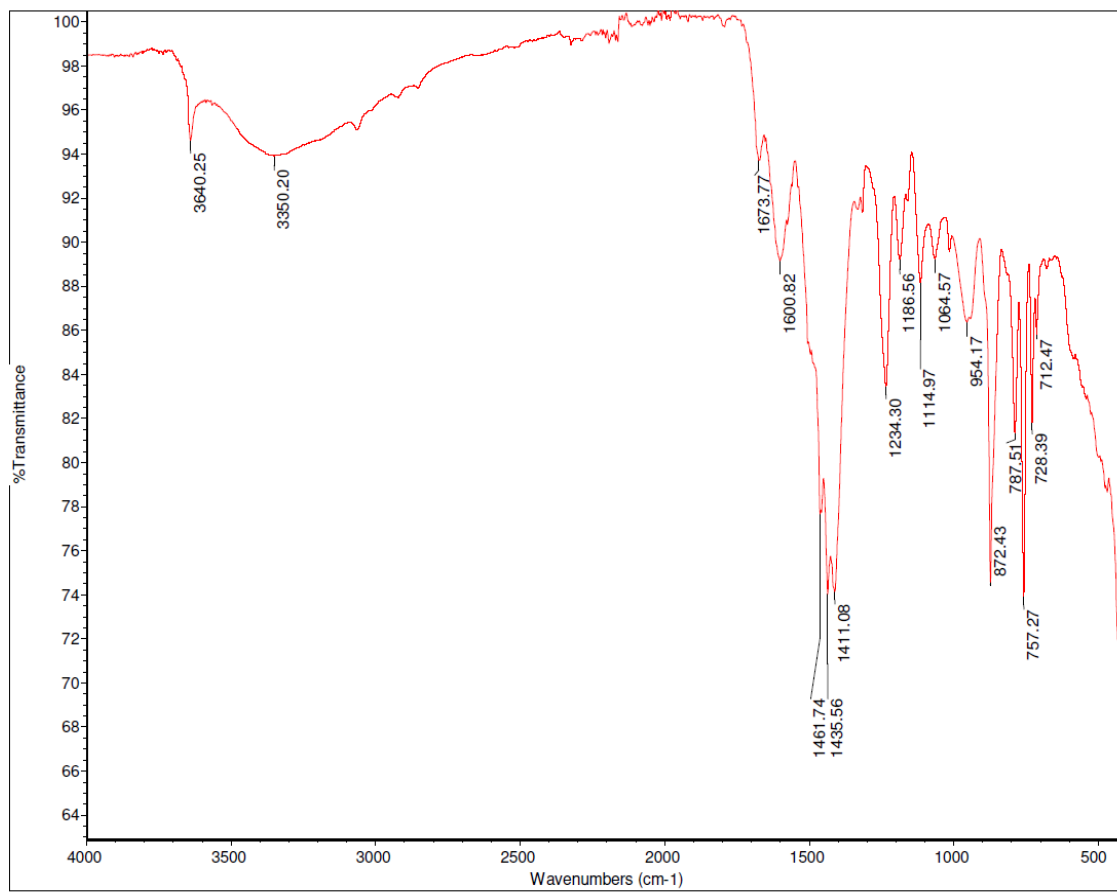
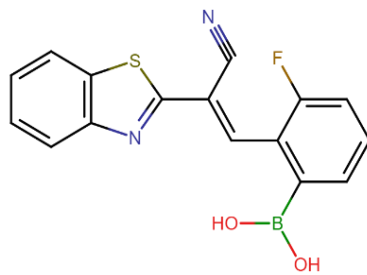


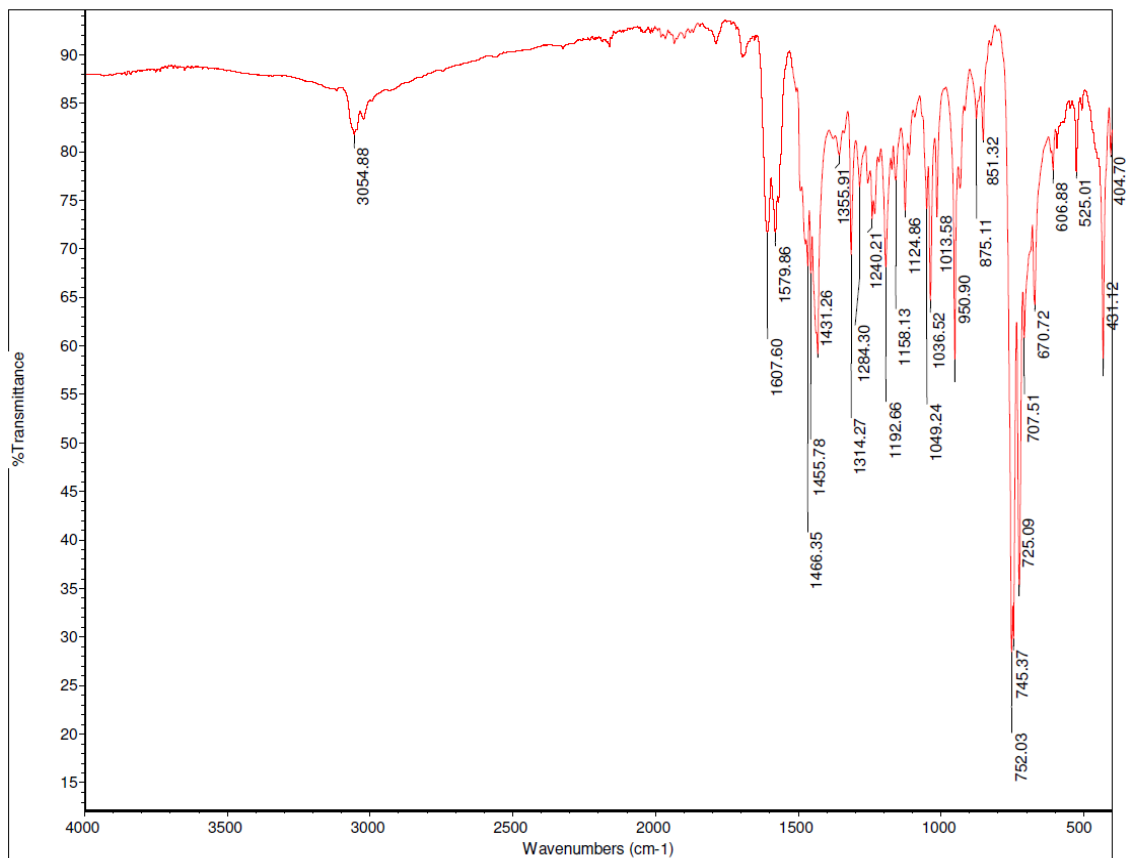


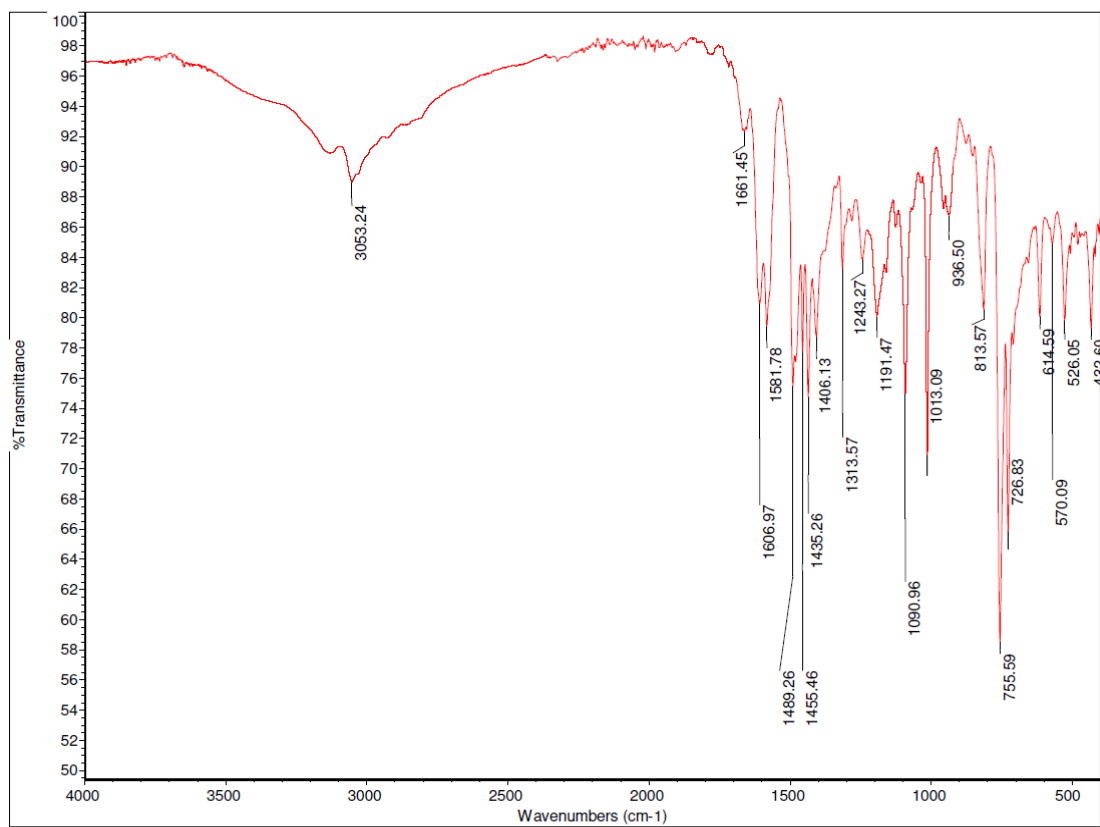
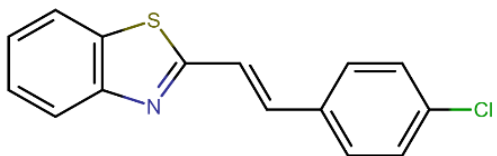


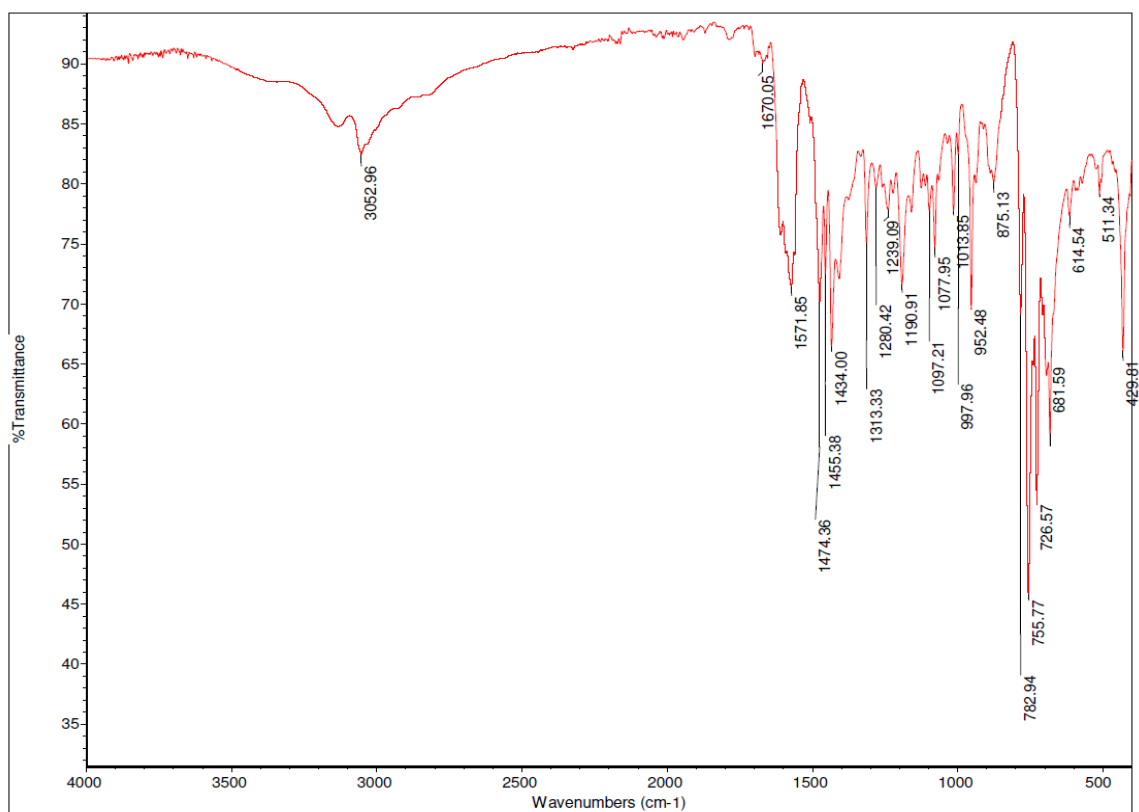
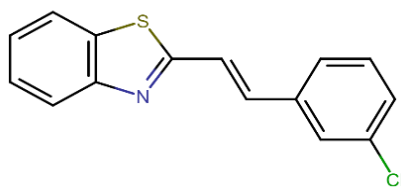


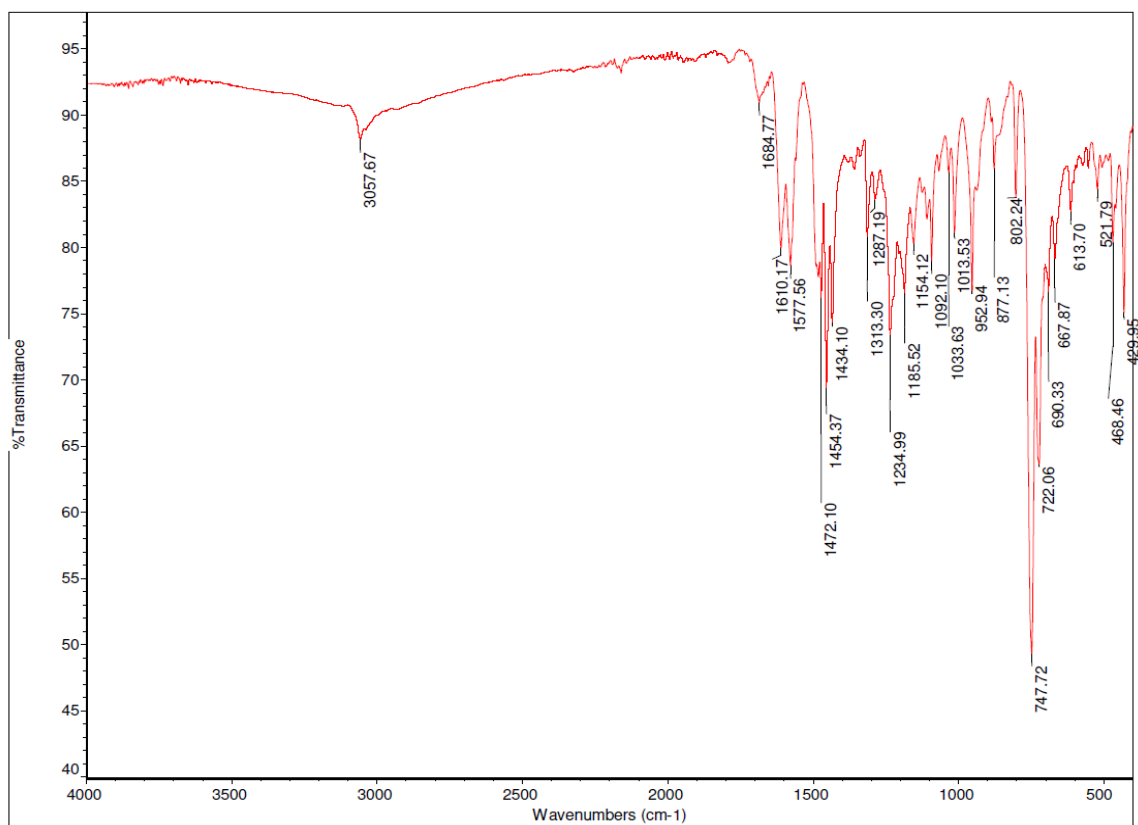
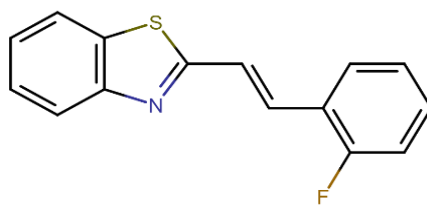


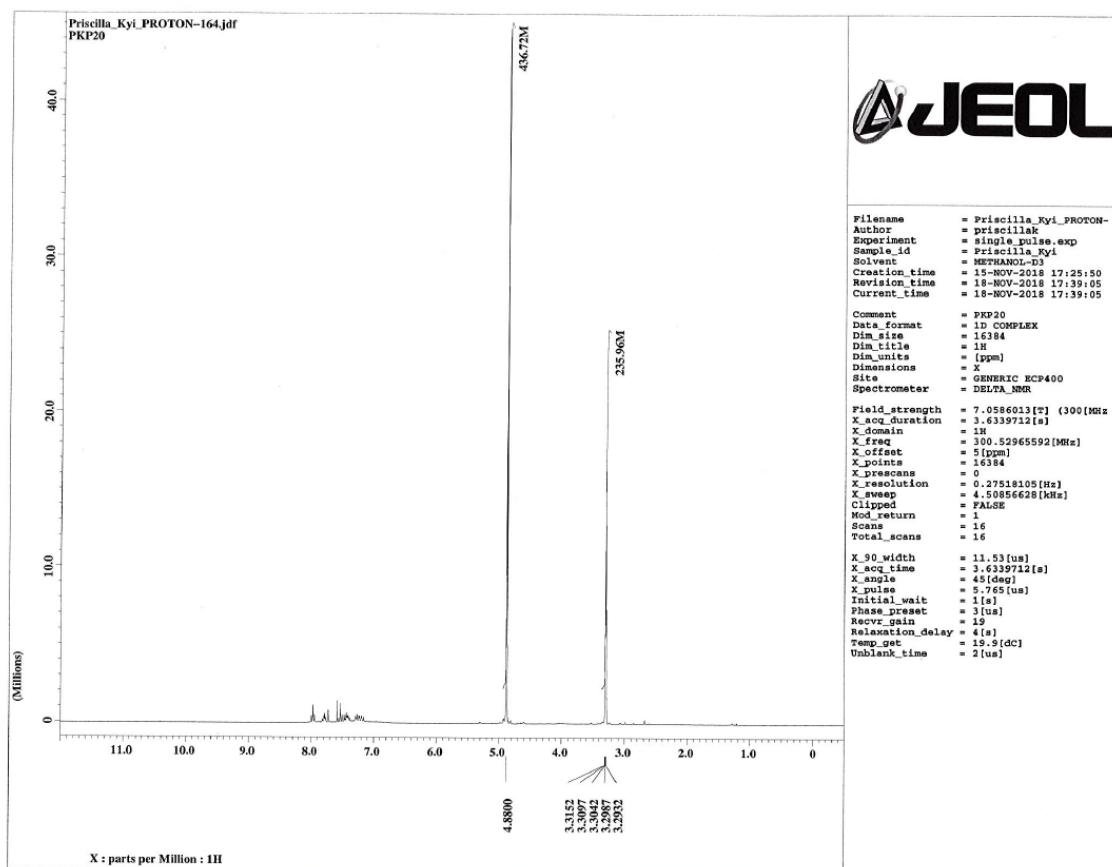


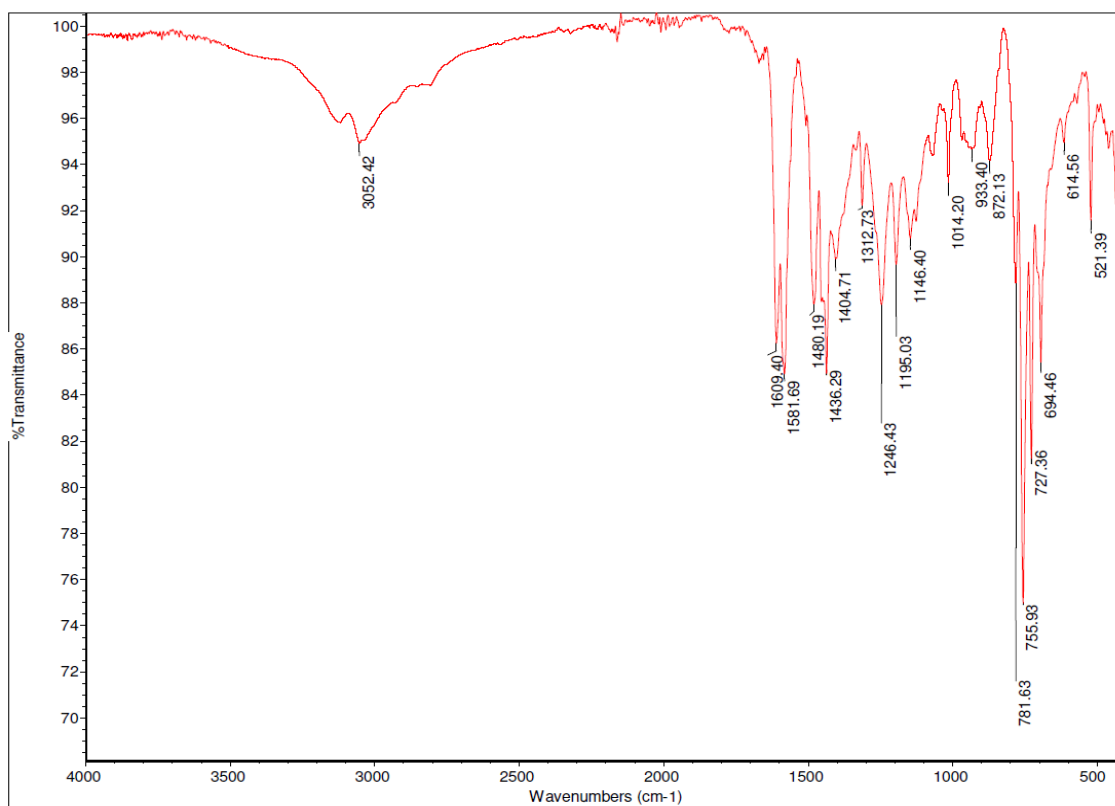
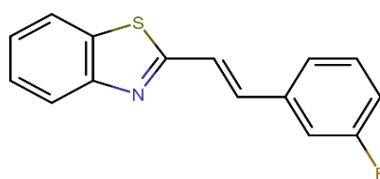


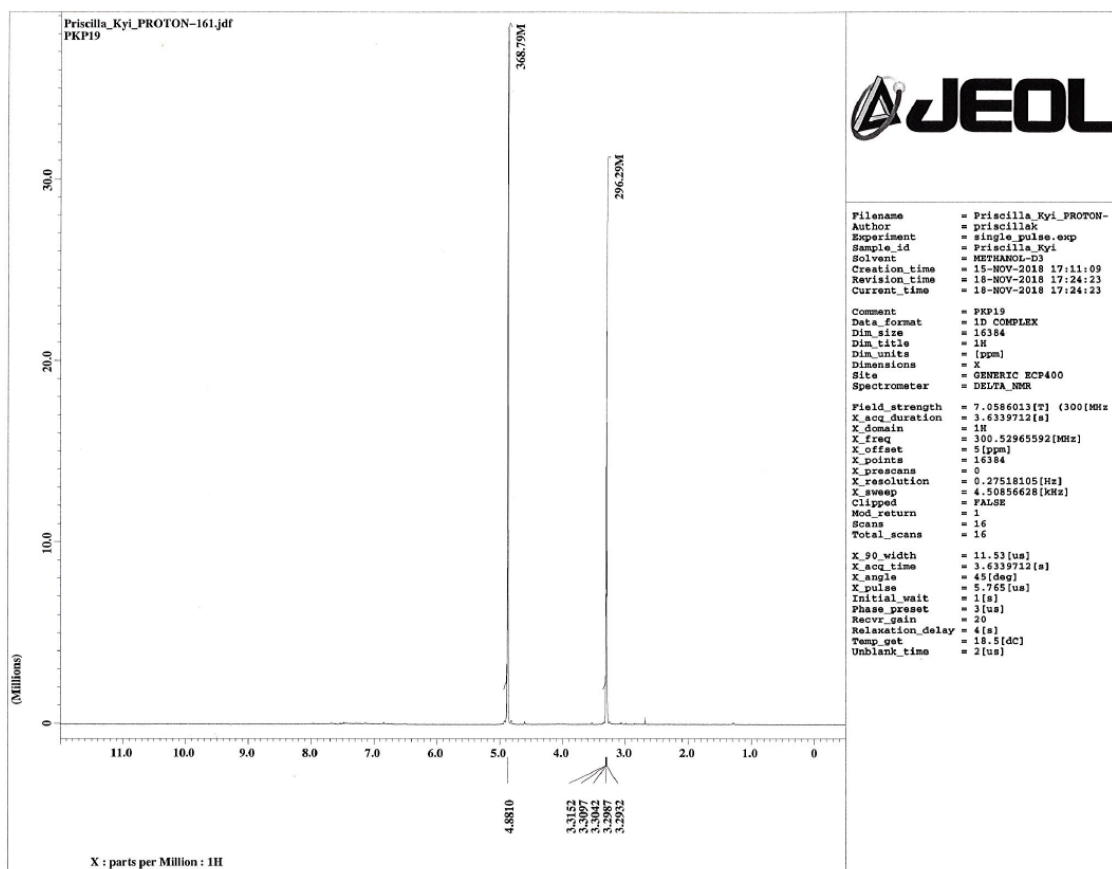


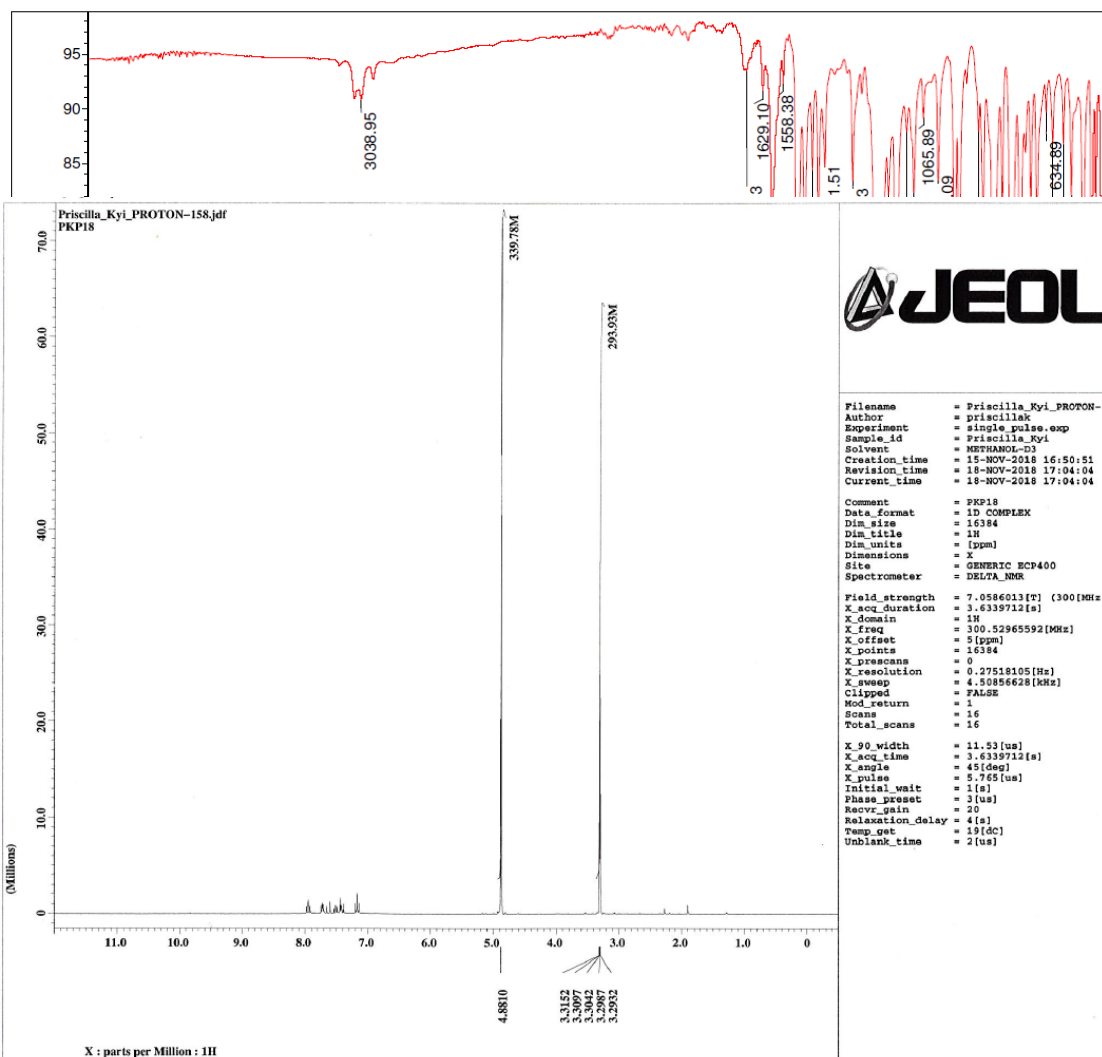
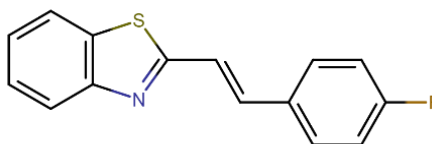


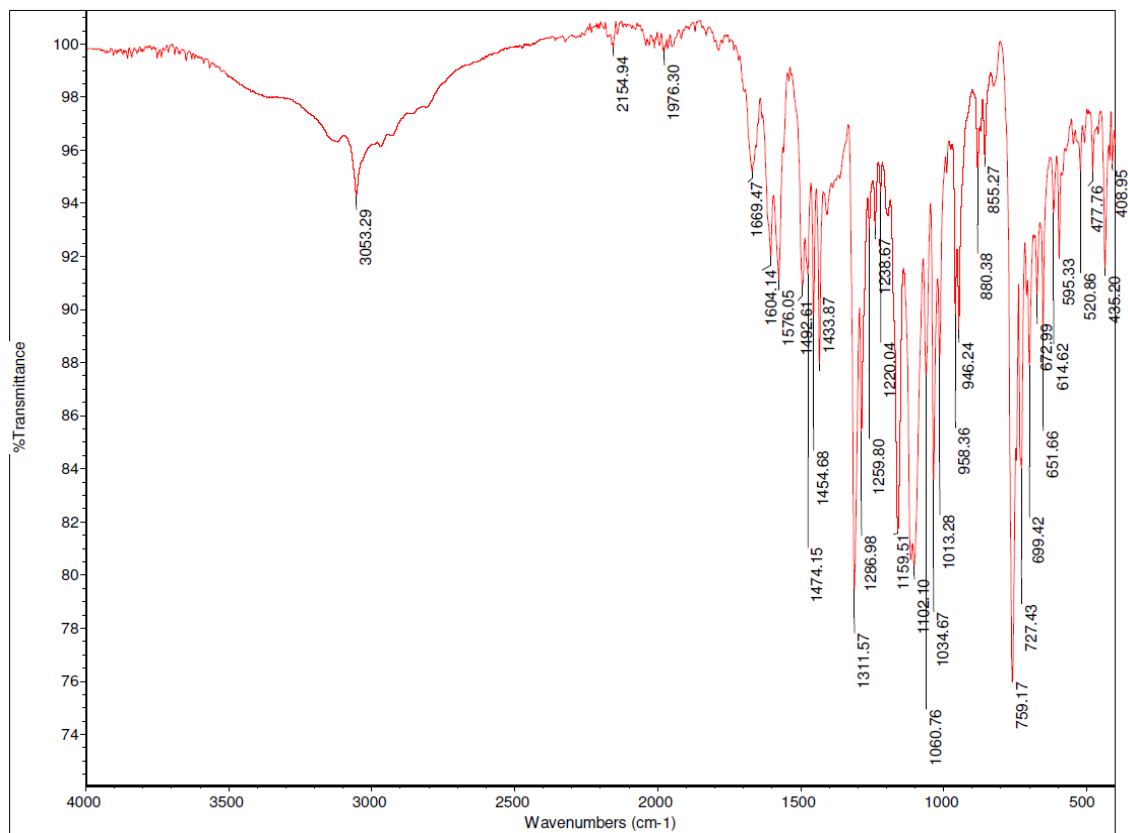
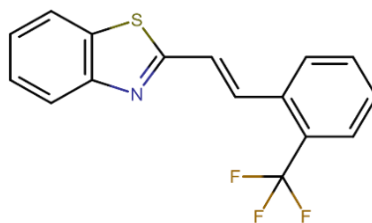


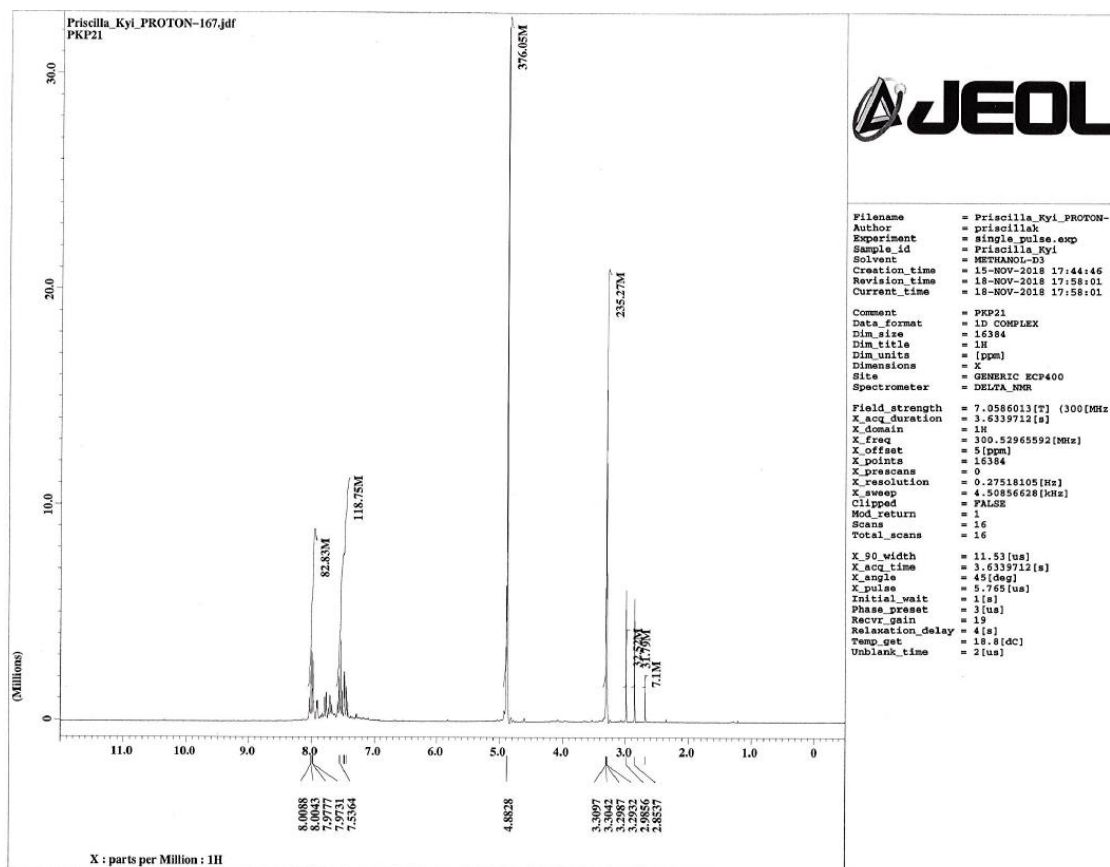


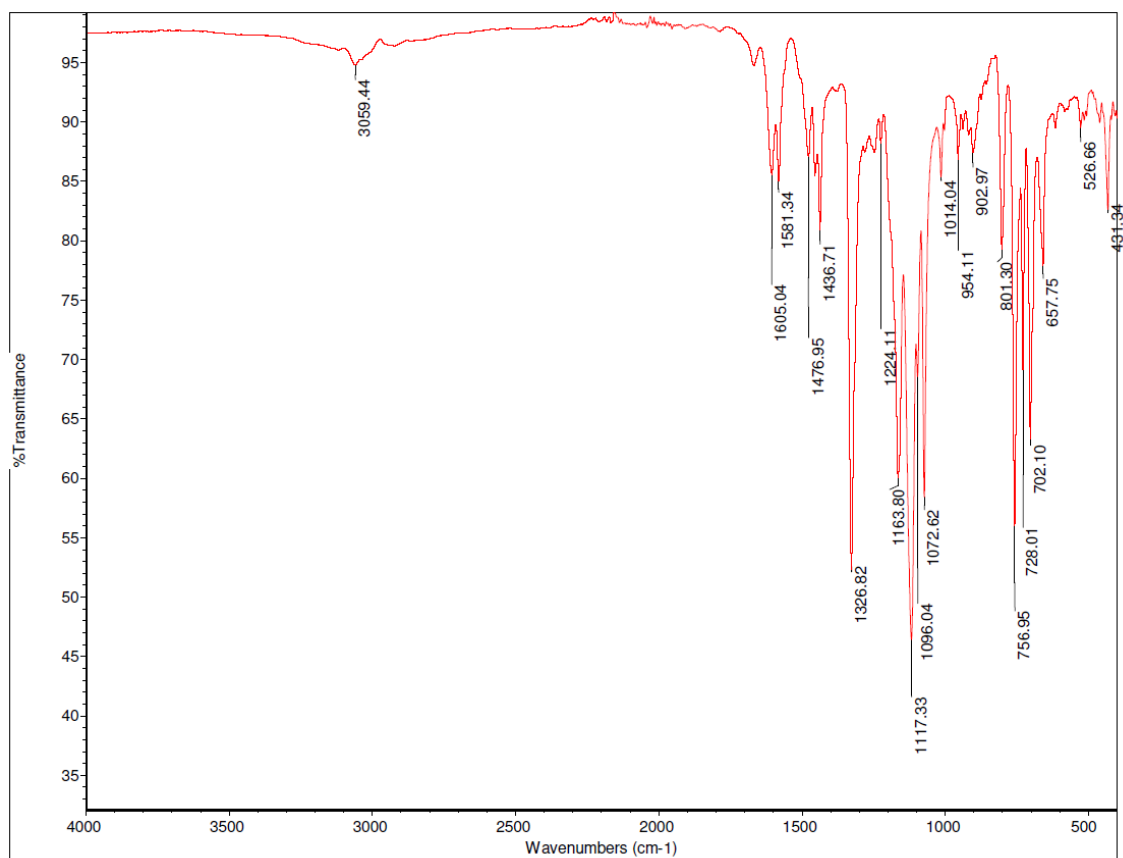
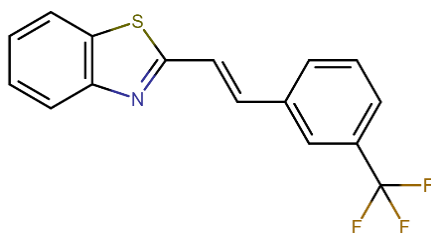


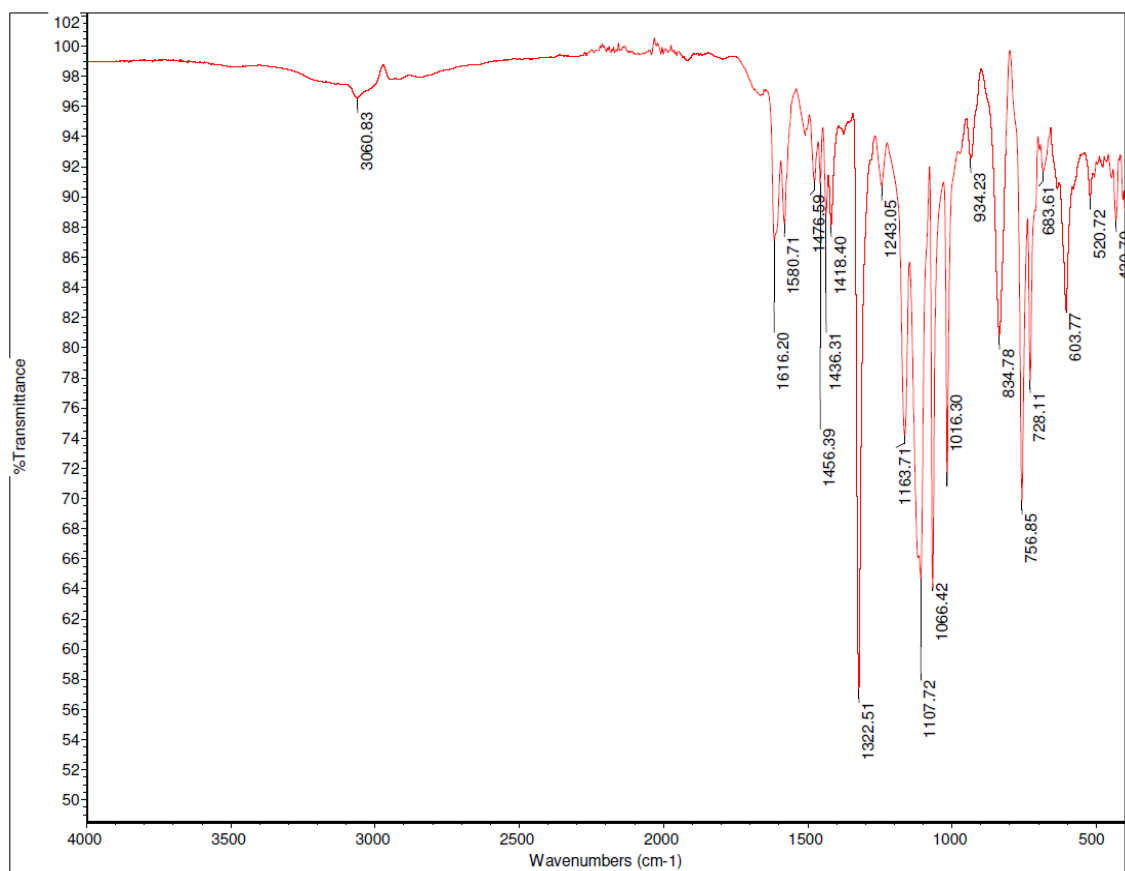
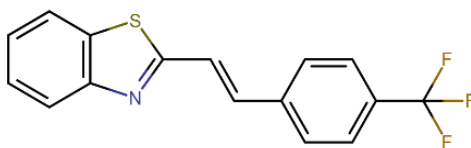












APPENDIX II
P-VALUES OF TEST COMPOUNDS

Multiple Comparisons (PKP2)

Dependent Variable: Cells

Dunnett t (2-sided)^a

(I) Concentration	(J) Concentration	Mean Difference (I- J)	Std. Error	Sig.	95% Confidence Interval	
					Lower Bound	Upper Bound
2 mg/ml	Control	-176.00000*	15.18273	.000	-221.0579	-130.9421
1 mg/ml	Control	-176.00000*	15.18273	.000	-221.0579	-130.9421
0.5 mg/ml	Control	-176.00000*	15.18273	.000	-221.0579	-130.9421
0.25	Control	-100.00000*	15.18273	.000	-145.0579	-54.9421
0.125 mg/ml	Control	-97.89000*	15.18273	.000	-142.9479	-52.8321
0.0625	Control	-73.00000*	15.18273	.001	-118.0579	-27.9421
0.03125	Control	-19.89000	15.18273	.765	-64.9479	25.1679
0.01562	Control	-13.00000	15.18273	.972	-58.0579	32.0579
0.00781	Control	-35.66667	15.18273	.174	-80.7246	9.3912
0.003906	Control	-26.11000	15.18273	.483	-71.1679	18.9479
0.00195	Control	-3.44333	15.18273	1.000	-48.5012	41.6146

*. The mean difference is significant at the 0.05 level.

a. Dunnett t-tests treat one group as a control, and compare all other groups against it.

Multiple Comparisons (PKP3)

Dependent Variable: Cells

Dunnett t (2-sided)^a

(I) Concentration	(J) Concentration	Mean Difference (I- J)	Std. Error	Sig.	95% Confidence Interval	
					Lower Bound	Upper Bound
2 mg/ml	Control	-83.66767	38.93939	.249	-199.2284	31.8930
1 mg/ml	Control	-133.77667*	38.93939	.018	-249.3374	-18.2160
0.5 mg/ml	Control	-145.77667*	38.93939	.008	-261.3374	-30.2160
0.25	Control	-156.77767*	38.93939	.004	-272.3384	-41.2170
0.125 mg/ml	Control	-121.33333*	38.93939	.036	-236.8940	-5.7726
0.0625	Control	-71.89000	38.93939	.404	-187.4507	43.6707
0.03125	Control	-66.44333	38.93939	.492	-182.0040	49.1174
0.01562	Control	-34.89000	38.93939	.963	-150.4507	80.6707
0.00781	Control	-42.78000	38.93939	.888	-158.3407	72.7807

0.003906	Control	-42.44333	38.93939	.893	-158.0040	73.1174
0.00195	Control	-39.11333	38.93939	.929	-154.6740	76.4474

*. The mean difference is significant at the 0.05 level.

a. Dunnett t-tests treat one group as a control, and compare all other groups against it.

Multiple Comparisons (PKP4)

Dependent Variable: Cells

Dunnett t (2-sided)^a

(I) Concentration	(J) Concentration	Mean Difference (I- J)	Std. Error	Sig.	95% Confidence Interval	
					Lower Bound	Upper Bound
2 mg/ml	Control	-157.55333*	41.65868	.008	-281.1841	-33.9226
1 mg/ml	Control	-154.11000*	41.65868	.009	-277.7407	-30.4793
0.5 mg/ml	Control	-181.33333*	41.65868	.002	-304.9641	-57.7026
0.25	Control	-207.11000*	41.65868	.000	-330.7407	-83.4793
0.125 mg/ml	Control	-182.77667*	41.65868	.002	-306.4074	-59.1459
0.0625	Control	-105.00000	41.65868	.126	-228.6307	18.6307
0.03125	Control	-102.11333	41.65868	.144	-225.7441	21.5174
0.01562	Control	-88.66667	41.65868	.257	-212.2974	34.9641
0.00781	Control	-79.11333	41.65868	.373	-202.7441	44.5174
0.003906	Control	-76.22000	41.65868	.413	-199.8507	47.4107
0.00195	Control	-33.77667	41.65868	.980	-157.4074	89.8541

*. The mean difference is significant at the 0.05 level.

a. Dunnett t-tests treat one group as a control, and compare all other groups against it.

Multiple Comparisons (PKP5)

Dependent Variable: Cells

Dunnett t (2-sided)^a

(I) Concentration	(J) Concentration	Mean Difference (I- J)	Std. Error	Sig.	95% Confidence Interval	
					Lower Bound	Upper Bound
2 mg/ml	Control	-187.66667*	34.29165	.000	-289.4342	-85.8991
1 mg/ml	Control	-187.66667*	34.29165	.000	-289.4342	-85.8991
0.5 mg/ml	Control	-166.77778*	34.29165	.001	-268.5453	-65.0102
0.25	Control	-160.33333*	34.29165	.001	-262.1009	-58.5658
0.125 mg/ml	Control	-136.88889*	34.29165	.005	-238.6564	-35.1213
0.0625	Control	-95.77778	34.29165	.072	-197.5453	5.9898
0.03125	Control	-69.88890	34.29165	.299	-171.6565	31.8787

0.01562	Control	-35.77777	34.29165	.914	-137.5453	65.9898
0.00781	Control	14.55557	34.29165	1.000	-87.2120	116.3231
0.003906	Control	.88890	34.29165	1.000	-100.8787	102.6565
0.00195	Control	-9.22223	34.29165	1.000	-110.9898	92.5453

*. The mean difference is significant at the 0.05 level.

a. Dunnett t-tests treat one group as a control, and compare all other groups against it.

Multiple Comparisons (PKP6)

Dependent Variable: Cells

Dunnett t (2-sided)^a

(I) Concentration	(J) Concentration	Mean Difference (I- J)	Std. Error	Sig.	95% Confidence Interval	
					Lower Bound	Upper Bound
2 mg/ml	Control	-236.11000*	37.02171	.000	-345.9796	-126.2404
1 mg/ml	Control	-235.00000*	37.02171	.000	-344.8696	-125.1304
0.5 mg/ml	Control	-219.00000*	37.02171	.000	-328.8696	-109.1304
0.25	Control	-150.22333*	37.02171	.004	-260.0929	-40.3538
0.125 mg/ml	Control	-124.22000*	37.02171	.021	-234.0896	-14.3504
0.0625	Control	-105.44667	37.02171	.065	-215.3162	4.4229
0.03125	Control	-44.11000	37.02171	.839	-153.9796	65.7596
0.01562	Control	-52.44333	37.02171	.693	-162.3129	57.4262
0.00781	Control	-11.44333	37.02171	1.000	-121.3129	98.4262
0.003906	Control	28.55333	37.02171	.986	-81.3162	138.4229
0.00195	Control	24.33333	37.02171	.996	-85.5362	134.2029

*. The mean difference is significant at the 0.05 level.

a. Dunnett t-tests treat one group as a control, and compare all other groups against it.

Multiple Comparisons (PKP7)

Dependent Variable: Cells

Dunnett t (2-sided)^a

(I) Concentration	(J) Concentration	Mean Difference (I- J)	Std. Error	Sig.	95% Confidence Interval	
					Lower Bound	Upper Bound
2 mg/ml	Control	-193.66667*	54.44449	.013	-355.2419	-32.0914
1 mg/ml	Control	-192.89000*	54.44449	.014	-354.4653	-31.3147
0.5 mg/ml	Control	-180.33333*	54.44449	.023	-341.9086	-18.7581
0.25	Control	-149.78000	54.44449	.079	-311.3553	11.7953
0.125 mg/ml	Control	-109.88667	54.44449	.309	-271.4619	51.6886

0.0625	Control	-58.44333	54.44449	.900	-220.0186	103.1319
0.03125	Control	-53.99667	54.44449	.934	-215.5719	107.5786
0.01562	Control	-32.33333	54.44449	.998	-193.9086	129.2419
0.00781	Control	-2.55433	54.44449	1.000	-164.1296	159.0209
0.003906	Control	2.55667	54.44449	1.000	-159.0186	164.1319
0.00195	Control	-66.44333	54.44449	.822	-228.0186	95.1319

*. The mean difference is significant at the 0.05 level.

a. Dunnett t-tests treat one group as a control, and compare all other groups against it.

Multiple Comparisons (4F-3BA)

Dependent Variable: Cells

Dunnett t (2-sided)^a

(I) Concentration	(J) Concentration	Mean Difference (I- J)	Std. Error	Sig.	95% Confidence Interval	
					Lower Bound	Upper Bound
2 mg/ml	Control	-117.77778*	17.11267	.000	-168.5632	-66.9924
1 mg/ml	Control	-125.44445*	17.11267	.000	-176.2298	-74.6591
0.5 mg/ml	Control	-127.44444*	17.11267	.000	-178.2298	-76.6591
0.25	Control	-129.11111*	17.11267	.000	-179.8965	-78.3257
0.125 mg/ml	Control	-116.11111*	17.11267	.000	-166.8965	-65.3257
0.0625	Control	-80.44444*	17.11267	.001	-131.2298	-29.6591
0.03125	Control	-71.44444*	17.11267	.003	-122.2298	-20.6591
0.01562	Control	-80.33333*	17.11267	.001	-131.1187	-29.5479
0.00781	Control	-56.33334*	17.11267	.024	-107.1187	-5.5480
0.003906	Control	-41.66667	17.11267	.148	-92.4521	9.1187
0.00195	Control	-43.11110	17.11267	.126	-93.8965	7.6743

*. The mean difference is significant at the 0.05 level.

a. Dunnett t-tests treat one group as a control, and compare all other groups against it.

Multiple Comparisons (3F-2BA)

Dependent Variable: Cells

Dunnett t (2-sided)^a

(I) Concentration	(J) Concentration	Mean Difference (I- J)	Std. Error	Sig.	95% Confidence Interval	
					Lower Bound	Upper Bound
2 mg/ml	Control	-151.55556*	25.28414	.000	-226.5915	-76.5196
1 mg/ml	Control	-150.66667*	25.28414	.000	-225.7026	-75.6308
0.5 mg/ml	Control	-147.66667*	25.28414	.000	-222.7026	-72.6308

0.25	Control	-112.44444*	25.28414	.002	-187.4804	-37.4085
0.125 mg/ml	Control	-83.55556*	25.28414	.024	-158.5915	-8.5196
0.0625	Control	-77.88889*	25.28414	.039	-152.9248	-2.8530
0.03125	Control	-60.44445	25.28414	.161	-135.4804	14.5915
0.01562	Control	-61.88890	25.28414	.145	-136.9248	13.1470
0.00781	Control	-48.44446	25.28414	.363	-123.4804	26.5915
0.003906	Control	-28.33334	25.28414	.878	-103.3693	46.7026
0.00195	Control	-40.11111	25.28414	.573	-115.1470	34.9248

*. The mean difference is significant at the 0.05 level.

a. Dunnett t-tests treat one group as a control, and compare all other groups against it.

Multiple Comparisons (PKP2 revised)

Dependent Variable: Cells

Dunnett t (2-sided)^a

(I) Concentration	(J) Concentration	Mean Difference (I- J)	Std. Error	Sig.	95% Confidence Interval	
					Lower Bound	Upper Bound
2 mg/ml	Control	-141.50000*	5.76749	.000	-160.0670	-122.9330
1 mg/ml	Control	-141.33333*	5.76749	.000	-159.9003	-122.7664
0.5 mg/ml	Control	-141.16667*	5.76749	.000	-159.7336	-122.5997
0.25	Control	-140.66667*	5.76749	.000	-159.2336	-122.0997
0.125 mg/ml	Control	-141.00000*	5.76749	.000	-159.5670	-122.4330
0.0625	Control	-126.50000*	5.76749	.000	-145.0670	-107.9330
0.03125	Control	-53.50000*	5.76749	.000	-72.0670	-34.9330
0.01562	Control	-45.50002*	5.76749	.000	-64.0670	-26.9331
0.00781	Control	-43.49998*	5.76749	.000	-62.0669	-24.9330
0.003906	Control	-38.00000*	5.76749	.000	-56.5670	-19.4330
0.00195	Control	-39.16665*	5.76749	.000	-57.7336	-20.5997

*. The mean difference is significant at the 0.05 level.

a. Dunnett t-tests treat one group as a control, and compare all other groups against it.